Speed Control of BLDC Motor Using Neural Network Based Model Reference Adaptive Control (MRAC) For Electric Vehicle Drive (In the Case of Yaris Car)

Taddese Bekele Tariku

A Thesis Submitted to
The Department of Electrical Power and Control Engineering
School of Electrical Engineering and Computing

Presented in Partial Fulfillment of the Requirement for the Degree of Master's in Electrical Power and Control Engineering

(Control Engineering)

Office of Graduate Studies
Adama Science and Technology University

March, 2023.
Adama, Ethiopia

Speed Control of BLDC Motor Using Neural Network Based Model Reference Adaptive Control (MRAC) For Electric Vehicle Drive

(In the Case of Yaris Car)

Taddese Bekele Tariku

Advisor:

Dr. Prathibha. E.

A Thesis Submitted to

The Department of Electrical Power and Control Engineering

School of Electrical Engineering and Computing

Presented in Partial Fulfillment of the Requirement for the Degree of Master's in Electrical Power and Control Engineering

(Control Engineering)

Office of Graduate Studies

Adama Science and Technology University

March, 2023.

Adama, Ethiopia

DECLARATION

I hereby declare that this Master Thesis entitled "Speed Control of BLDC Motor Using Neural Network Based Model Reference Adaptive Control (MRAC) For Electric Vehicle Drive :(In the Case of Yaris Car)" is my original work. That is, it has not been submitted for the award of any academic degree, diploma or certificate in any other university. All sources of materials that are used for this thesis have been duly acknowledged through citation.

________________________ ______________________ _______________

Name of the student Signature Date

RECOMENDATION

We, the advisors of this thesis, hereby certify that we have read the revised version of the thesis entitled “Speed Control of BLDC Motor Using Neural Network Based Model Reference Adaptive Control (MRAC) For Electric Vehicle Drive: (In the Case of Yaris Car)” prepared under our guidance by Taddese Bekele submitted in partial fulfillment of the requirements for the degree of Mater’s of Science in Electrical Power and Control Engineering (Control). Therefore, we recommend the submission of revised version of the thesis to the department following the applicable procedures.

________________________	______________________	_______________
Major Advisor	Signature	Date
________________________	______________________	_______________
Co-advisor	Signature	Date

ACKNOWLEDGMENT

I would like to thank my Adivsor **Dr. Prathibha. E.** for she supervision, friendly attitude, and sharing of many good ideas. Regardless of she's often high work load, she always makes time to answer questions as well as giving encouraging advice. You are highly appreciated! I am also very grateful to **Associative Prof. Dereje Tekilu Aseffa** for lots of advice and helping in preparing the thesis documentation, but also for good ideas and discussions regarding everything from implementations of the system in Simulink in general. I would moreover like to thank **Mr. Minyamer Gelawe Wase (MSc.)** for his patience, helpful attitude, and sharing of his work regarding the implementation of the nonlinear Simulink modeling.

Further,more I would like to thank you **Dr. Damise Jobir** ,**Tamiru Takele Mola(MSc.)**,**Lema Degefa Suyume** for their valuable advise willingness to share their knowledge,and numerous suggestion throughout doing this work.

Finally, my deep and sincere gratitude to my father Ato **Bekele Tariku Aseffa** for he continuous and unparalleled love, help and support. I am grateful to my lovely wife **Maria Niguse Haile** for always being there for me as a friend. I am forever indebted to my parents for giving me the opportunities and experiences that have made me who I am. They selflessly encouraged me to explore new directions in life and seek my own destiny. This thesis would not have been possible if not for them, and I dedicate this milestone to them.

APPROVAL SHEET

We, the advisors of the thesis entitled "Speed Control of BLDC Motor Using Neural Network Based Model Reference Adaptive Control (MRAC) For Electric Vehicle Drive: (In the case of Yaris Car)" and developed by Taddese Bekele, hereby certify that the recommendation and suggestions made by the board of examiners are appropriately incorporated into the final version of the thesis.

Major Advisor	Signature	Date
Co-advisor	Signature	Date

APPROVAL BOARD OF EXAMINERS

We, the undersigned, members of the Board of Examiners of the thesis by Taddese Bekele have read and evaluated the thesis entitled "Speed Control of BLDC Motor Using Neural Network Based Model Reference Adaptive Control (MRAC) For Electric Vehicle Drive :(In the Case of Yaris Car)" and examined the candidate during open defense. This is, therefore, to certify that the thesis is accepted for partial fulfillment of the requirement of the degree of Master of Science in Electrical Power and Control Engineering (Control).

Chairperson	Signature	Date
Internal Examiner	Signature	Date
External Examiner	Signature	Date

Finally, approval and acceptance of the thesis is contingent upon submission of its final copy to the Office of Postgraduate Studies (OPGS) through the Department Graduate Council (DGC) and School Graduate Committee (SGC).

Department Head	Signature	Date
School Dean	Signature	Date
Office of Postgraduate Studies, Dean	Signature	Date

ABSTRACT

Electric vehicles are widely considered a viable solution to reduce fossil oil dependence and environmental footprints in the ground transportation sector. Electric vehicle reduce oil consumption and air pollutant emission where concerns about oil security and availability and the negative environmental impact of petroleum-based transportation systems. Different Motors are being used in Electric Vehicles. Brushless DC motors showed best performance as compared to other motors like(brushed DC motor, Induction motor, Brushless AC motor and other motor), because of its great efficiency, high energy density, Less maintenance, Long operating life, Low electric noise, Better speed versus torque characteristics and etc. *Different researchers have proposed different controller model in order to control speed of Brushless DC Motors. Among these controllers, Model reference adaptive controller is the one which is a component controller that emulates the reference model behavior efficiently. Conventional MRAC scheme is used for linear systems. However, since BLDC is nonlinear system by nature using conventional MRAC is very difficult. Hence in this thesis it proposed Neural Network based MRAC to control the speed of BLDC motors to compensate its nonlinearity which is not considered in conventional MRAC. The proposed neural network-based model reference adaptive controller can significantly improve the system behavior and force the system to follow the reference model and minimize the error between the model and the plant output. Adaptive law using Lyapunov stability criteria for updating the controller parameters online have been formulated. The simulation results show that the proposed neural network-based MRAC has 0.0236 sec rise time, 0.0450 sec settling time and overshoot 0.0736 percent .This performance is closely the same with model reference performance which has 0.0257sec rise time, 0.0438sec settling time and overshoot 0.0363 percent The performance of the neural network based MRAC have been compared with conventional MRAC and MRAC-PID. The neural network based MRAC was selected for speed control of BLDC motor drive system. Because of in the case of NN based MRAC the output speed is closely the same with model reference output and the difference between them is very small when it compared with other controller which is listed in this thesis. The result have been using MATLAB/ SIMULINK.*

Keywords: *Model Reference Adaptive Control (MRAC), BLDC Motor, Neural Network (NN), Electric vehicle.*

Table of Contents

LIST OF FIGURES

LIST OF TABLES

ACRONYMS

AMC	American Motor Car Company
BLDC	Brushless DC
CD-RW	Compact Disc, Rewriteable
DC	Direct Current
EMF	Electromotive Force
EMI	Electromagnetic Interference
EV	Electric Vehicles
EVB	Electric-Vehicle Battery
FLC	Fuzzy Logic Controller
HEV	Hybrid Electric Vehicles
ICE	Internal Combustion Engine
IGBT	Insulated-Gate Bipolar Transistor
IM	Induction Motor
Li-ion	Lithium-ion Battery
MOSFET	Metal Oxide Silicon Field Effect Transistor
MRAC	Model Reference Adaptive Control
NN	Neural Network
PI	Proportional Integral
PID	Proportional Integral Derivative
PMDC	Permanent Magnet DC
PMSM	Permanent Magnet Synchronous Motors
PWM	Pulse Width Modulation
RBS	Regenerative Braking System
SOC	State of Charge
SRM	Switched Reluctance Motor
VSI	Voltage Source Inverter
VVS	Variable Voltage Source

CHAPTER ONE

1. INTRODUCTION

1.1 Background

An electric vehicle is a vehicle whose propulsion is provided exclusively by one or more electric motors. It can draw its energy from embedded resources like a battery or be connected to an external source, for example via a catenary. The engine can be loaded, as in the case of most land vehicles, or unloaded, as in the case of cable transport. Nowadays, electric vehicles are becoming more and more popular; the sale of them has increased throughout the world for the reason that electric propulsion has better efficiency than combustion engines; they require very simple maintenance, requiring very few spare parts. With the depletion of fossil fuels and the increased environmental concerns, there is more and more interest in electric vehicles (EVs) from automobile manufacturers and governments in the entire world(Agrawal, n.d.).

In the present, electric vehicles that use battery are going to replace fuel vehicles because vehicles that use petroleum or fuel vehicles create pollution to environment, but they can generate mechanical power higher than electric vehicles. Fuel vehicles use rear differential to vary speed between left wheels and right wheels to be different and provide a balance while curving, but it causes a mechanical loss. Therefore, electric vehicles are necessary to reduce mechanical loss to make drive high performance and reduce pollution to make good environment. The selection of the appropriate electric motor is critical for electric vehicles. Various types of electric motors have previously been used in electric vehicles. However, in terms of efficiency, BLDC motor drives are the best option for electric vehicles. Permanent magnet synchronous motors are BLDC motors. They are powered by direct current voltage, but current commutation is accomplished by solid-state switches. The rotor position, which can be detected using position sensors or sensor less techniques, determines the commutation instant. (El-samahy & Shamseldin, 2018). BLDC motors are very popular in a wide variety of applications. When compared with a DC motor, it has simple structure, light weight, higher speed range, noiseless operation, maintenance free operation, large starting torque, precise and accurate control and high dynamic response. The BLDC motor uses an electric commentator rather than a mechanical commentator, so it is more reliable than the DC motor. In the present, electric vehicles that use battery are going to replace fuel vehicles because vehicles that use petroleum or fuel vehicles create pollution to but they can generate more mechanical power than electric vehicles. Fuel vehicles use a rear differential to vary speed between the left wheels and right wheels to be different and provide a balance while curving, but it causes a mechanical loss. Therefore, electric vehicles are necessary to reduce mechanical loss to make driving high performance and reduce pollution to make a good environment. The selection of the appropriate electric motor is critical for electric vehicles. Various types of electric motors have previously been used in electric vehicles. However, in terms of efficiency, BLDC motor drives are the best option for electric vehicles. BLDC motors are a type of synchronous permanent magnet motor. They are powered by direct current voltage, but current commutation is accomplished by solid-state switches. The rotor position, which can be detected using position sensors or sensor less techniques, determines the commutation instant. BLDC motors are very popular in a wide variety of applications. When compared with a DC motor, it has a simple structure, light weight, higher speed range, noiseless operation, maintenance-free operation, large starting torque, precise and accurate control, and high dynamic response. The BLDC motor uses an electric commentator rather than a mechanical commentator, so it is more reliable than the DC motor. In a BLDC motor, rotor magnets generate the rotor's magnetic flux, so BLDC motors achieve higher efficiency(Hashemnia & Asaei, 2017)(Luthra, 2017). The usual configuration of a vehicle has one motor to drive two wheels with a differential gear. However, the total mass of an electric vehicle is significantly increased by its accessories. For the above reasons, the electronic differential has been developed for use in electric vehicles to replace the rear differential or the conventional heavy gear box because it can reduce electric vehicle body mass. For electronics differential drives, include a brushless DC motor (BLDC) driven by an inverter. The Electronics Differentials characterized by some characteristics in that there is no mechanical link between the two drive wheels. The traction is separately applied to each wheel by the controller, which will apply less power to the inner wheel in curving. The goal of any electronic or electrical control system is to measure, monitor, and control a process which can accurately control itself by monitoring its output and feeding some of it back to compare the actual output with the desired output so as to reduce the error, and if disturbed, bring the output system back to the original or desired response. Proportional Integral Derivative (PID) controllers are extensively used in practical industries to control the speed of DC motors. A PID controller is an excellent choice for dc motor speed control. Because of its simplicity and ease of implementation, it is the most commonly used controller in industry . In the presence of sudden disturbances and parameter variations, conventional control methods are incapable of achieving the desired speed tracking with high accuracy. This issue can be solved by using advanced control techniques such as adaptive control, variable structure control, fuzzy control, and neural networks. The determinant structure controller is straightforward, but difficult to implement. This is due to the possibility of an abrupt change in the control signal, which could disrupt system operation. In the adaptive control, the question of control of the BLDC Motor with present-day sophistication and complexities has often been an important research area due to the difficulty in modeling, nonlinearities, and uncertainties. Model reference adaptive control is one of the main schemes used in the adaptive system. Recently MRAC has received Considerable attention and many new approaches have been applied to the practical process. The controller in the MRAC scheme is designed to ensure that the plant output converges to the reference model output based on the assumption that the plant can be linearized. As a result, this scheme works well for controlling linear plants with unknown parameters. However, it cannot guarantee control of nonlinear plants with unknown structures. Because of their higher computation rate and ability to handle nonlinear systems, artificial neural networks (ANN) have become very popular in many control applications in recent years. (Matthews & Yi, 2019).

1.2 Statement of the Problem

The reduction of greenhouse gases is important in Ethiopia to create a better environment. Since Vehicle emissions from burning gasoline and diesel fuels contain toxic pollutants including carbon monoxide, smog-causing volatile organic compounds and nitrogen oxides, Sulphur dioxides, formaldehyde and benzene. Extraction processes can generate air and water pollution, and harm local communities. Transporting fuels from the mine or well can cause air pollution and lead to serious accidents and spills. To reduce certainly the above-mentioned problems of fossil fuel-based vehicles replaced by electric vehicles which is reduce oil consumption and air pollutant emission**.** The selection of motor and controlling speed are an important things in electric vehicle which needs the efficient and appropriate control techniques. BLDC motor has better performance characteristics when it is compared with other motors. Electric vehicle speed and parameter variations caused by load excursions and varying the nature of road. In the conventional model reference adaptive controller (MRAC) scheme, the controller will be designed to realize the plant output converges to reference model output based on the plant, which is linear. This scheme is effective for controlling the linear plant with unknown parameters. However, since BLDC is nonlinear system by nature using conventional MRAC is very difficult. Hence in this thesis it proposed Neural Network and to drive a BLDC motor with better speed dynamic performance, i.e. (reduced settling time, reduced percentage overshoot, and reduced rise time of speed).

1.3 Objectives of the thesis

1.3.1 General Objective of the thesis

The main objective of this thesis is To Model Neural Network based MRAC for Electric Vehicle car in order to control speed of BLDC motor in case of Yaris Car Model.

1.3.2 Specific Objectives

The specific objectives of this thesis are:

- To analyze the tractive power and other specifications of a motor for EV propulsion
- To identify BLDC motor Controller parameters(input and output parameters)
- To develop and evaluate the performance of Neural network based Model Reference Adaptive Control System through transient analysis.
- To design Speed based Model Reference Adaptive Control
- To simulate the system by using MATLAB/ Simulink software to cheek performance.

1.4. Scope

The scope of this project is to simulate the performance of BLDC Motor using MATLAB software and train the neural network to track the reference model to the plant output. In addition to this, it is developed to compare the effectiveness of the proposed controller to improve tracking performance and modelling of BLDC Motor using the neural network based direct model reference adaptive controller in MATLAB software.

1.5 Limitations of the Study

The research work is limited to simulating the system using MATLAB/Simulink and demonstrating how the system's various components interact with one other. This is due to the difficulty in obtaining the components for the implementation of an actual system. It also necessitates the extra time and money spent on building the actual prototype implementation.

1.6 Motivation of the Study

The advancement on electric vehicle system which can replace the traditional fuel and petroleum based vehicle system is increasing in world's transportation system. This electric vehicle needs choose of suitable BLDC motor. Thus, to design Neural Network based MRAC controller algorithm is needed for the advancement of electric vehicle system.

1.7. Significance

The overall effect of EVs is to provide people with an alternative. Gasoline-powered cars will most likely never go 'out of style' due to their heritage and history. The point to having electric vehicles is simply to help people save money, save the environment, and save fossil fuels from running out prematurely.

CHAPTER TWO

2. LITERATURE REVIEW

2.1. Chapter Overview

In this chapter different electric vehicle models with their traction motors are reviewed. The performance evaluation of a brushless DC motor is compared with those of other electric motor types. Closely related works especially in speed and current regulators along with their merits and demerits are reviewed and discussed. The drive train of the BLDC motor closely related works also reviewed and discussed. This chapter also establishes the essential theory and critical assessment of the related work needed for the development of the research and it presents the main findings by different researchers of intelligence systems and how they can be used to regulate the BLDC motor especially for simple Electric Vehicle, poll oscillation with aid of Model reference adaptive control system. The related literature and similar studies mentioned in this study substantiate the arguments that support the theories and assumptions. The information gathered in this chapter provides compelling motivation to pursue the study due to the Benchmark information and baseline research that reflect meritorious works and scholarly studies conducted by experts that are relevant to the neural network based model reference adaptive controller.

2.2. Electric Vehicles

The popularity of electric vehicles (EVs) is growing for a number of reasons, including price reductions and increased environmental and climate consciousness. Many nations have pushed the development of electric vehicles to lessen reliance on oil and environmental damage. The automotive sector has grown to become one of the most significant global industries, both economically and in terms of research and development. More technology components are being added to automobiles in an effort to increase the safety of both passengers and pedestrians. Additionally, there are more cars on the roads, which makes it possible for us to travel quickly and pleasantly. But as a result, air pollution levels in urban areas have dramatically increased. Contaminants, such as particulate matter (PM), nitrogen oxides (NOX), carbon monoxide (CO), sulfur dioxide (SO2), etc. The following benefits of EVs over conventional cars(Review, 2020)(Sanguesa et al., 2021)(Zhou et al., 2015):

- Zero emissions: these vehicles don't release CO_2 or nitrogen dioxide through their tailpipes (NO_2). Although the creation of batteries has a negative impact on carbon footprint, the manufacturing procedures also tend to be more environmentally friendly.
- Simplicity: There are fewer engine components in Electric Vehicles (EVs), which results in significantly less expensive maintenance. The engines are more straightforward and small; they do not require a cooling circuit, nor are a gearshift, clutch, or components that lessen engine noise required.
- Reliability: Because these vehicles have fewer and simpler components, they are less likely to break down. Furthermore, the natural wear and tear brought on by engine explosions, vibrations, or gasoline corrosion is not experienced by EVs.
- Cost: Compared to maintenance and fuel costs of conventional combustion cars, the cost of the vehicle and the power required is significantly lower. Compared to conventional vehicles, EVs have a much lower energy cost per kilometer.
- Efficiency: Electric vehicles are more efficient than conventional cars. The efficiency of the power plant will also affect the well to wheel (WTW) efficiency as a whole. Compared to diesel cars, which vary from 25% to 37%, the total WTW efficiency of gasoline vehicles ranges from 11% to 27%. The WTW efficiency of EVs powered by a natural gas power plant, in comparison, ranges from 13% to 31%, while EVs powered by renewable energy show an overall efficiency of up to 70%.
- **Toyota Yaris Case;** The Yaris reflects Toyota's emphasis on design, with more distinct styling both inside and out. Emotional appeal while maintaining its established rational strengths, such as packaging, efficient powertrains, and durability. Yaris' rational dimensions were always extremely strong. They hoped to connect the model not only with their customers' brains, but also with their hearts. Toyota has long been known for producing cars that are reliable, with solid build quality and good levels of safety. In 2021 Driver Power survey, the Yaris finished in 21st position out of a 75-car list, which was up from 43rd place in 2020. In Ethiopia also Toyota Yaris is a good used car that comes in both sedan and hatchback body styles. The Yaris is a joy to drive thanks to its sharp steering and taut suspension. Inside, there's decent seating space and user-friendly infotainment technology

2.3. Various Types of Electric Motors Used for Electric Vehicles

In this section, different electric motors are studied and compared to see the benefits of each motor and the one that is more suitable to be used in the electric vehicle (EV) applications. DC, induction, permanent magnet synchronous, switching reluctance, and brushless DC motors are the five primary types of electric motors that are explored. Conclusion: Brushless DC and permanent magnet motors are superior to other motor types for use in electric vehicle applications, despite the fact that induction motor technology is more advanced than other motor types. Less pollution, less fuel consumption, and a higher power-to-volume ratio will result from the use of these motors. Permanent magnet and brushless DC motors are becoming more and more desirable for use in electric vehicle applications due to the falling costs of permanent magnet materials and the trend toward improved efficiency in these motor types (Hashemnia & Asaei, 2017)(Xue et al., 2009).

Table 2.1 Different model of Electric Vehicle and their motors

NO	Brand Name	Country	Capacity of passenger	Motor type
1	Toyota RAVA 4	Japan	5	BLDC
2	Nissan leaf	Japan	5	BLDC
3	Nissan/Tino	Japan	4	PMSM
4	Mitsubishi-MiEV	Japan	4	BLDC
5	Tesla	USA	5	BLDC
6	Toyota/Prius	Japan	4	PMSM
7	Honda/Insight	Japan	4	PMSM
8	Toyota/Yaris	France/Japan	4	PMSM
9	Toyota/Vitz	Japan	4	PMSM

2.3.1. DC Motors

Despite the fact that flux and torque can be easily controlled and decoupled with DC motors, their design which includes brushes and rings poses maintenance issues. As a result, the appeal of DC motors in traction applications decreased with the development of vector control for AC motors (synchronous and induction). Naturally, DC motors continue to be suitable options for low power applications. Since the commutator actually functions as a strong inverter, power electronics systems can be quite straightforward and low-cost. A hybrid electric vehicle (HEV) with the name "Dynavolt" was unveiled by the Peugeot factory in France.(Varghese et al., 2014)

2.3.2. Induction Motors

Due to their dependability, toughness, low maintenance requirements, and ability to operate in harsh settings, squirrel cage induction motors have already emerged as the leading contender. Of all the AC rivals, induction motors have the most advanced technology. Using vector control techniques, torque and field control can be separated. By using flux weakening in the constant power region, speed range can be increased. The drawbacks of induction motors include the existence of break-down torque in the constant power region, a reduction in efficiency and an increase in losses at high speeds, an inherent lower efficiency compared to permanent magnet motors due to the presence of rotor winding, and finally a low power factor. The use of dual inverters to increase the constant power region, the incorporation of doubly-fed induction motors to have excellent performance at low speeds, and the reduction of rotor winding losses during the design phase are just a few of the approaches taken by researchers to address these issues.

2.3.3. Permanent magnet synchronous (PMS) motors (or blushless AC (BLAC))

In traction applications, PMS motors pose the biggest threat to induction motors. In fact, a lot of automakers (including Toyota, Honda, and Nissan) already use these motors in their cars. Higher power density, greater efficiency, and better heat dissipation into the environment are just a few benefits of these motors. At speeds higher than the base speed, the conduction angle of the power converter can be changed, allowing for a wider speed range and greater efficiency of PMS motors. Up to three or four times the base speed can be achieved in the speed range. These motors have the drawback of being susceptible to demagnetization from heat or armature reaction.(Minuye, 2021)

2.3.4. Switched reluctance motors (SRM)

In HEV systems, switched reluctance motors are becoming more and more popular every day. These motors' benefits include fault tolerance, straightforward control, simple and sturdy design, and outstanding torque-speed characteristics. An innate ability of a switching reluctance motor allows for operation over a large constant power area. For this motor, a number of drawbacks have been mentioned, including excessive noise, high torque ripple, a unique convertor topology, and electromagnetic interference. The motor's benefits and drawbacks are both significant in EV applications.(El-samahy & Shamseldin, 2018)

2.3.5. Brushless DC motors (BLDC)

Conceptually, these motors are what result when the stator and rotor of permanent magnet DC motors are reversed. In contrast to BLAC motors, which are supplied by sinusoidal waves, they are powered by rectangular waves. The removal of the brushes, as well as their compactness, great efficiency, and high energy density, are their key advantages.(Derammelaere et al., n.d.)

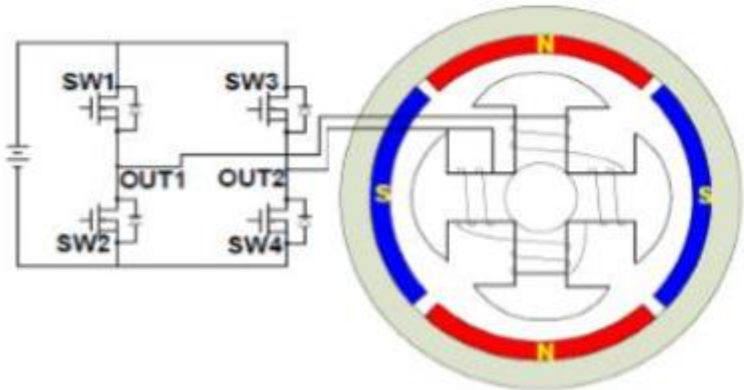

Figure 2.1 BLDC motor(Hashemnia & Asaei, 2017)

Some of the EV models by different manufacturers are listed in Table 2.1 along with the electric motor used. Since each company uses a different electric motor drive for its propulsion system accordingly. It can be seen from Table 2.1 that BLDC and induction motors are the most popular from the manufacture’s point of view.

2.4. Performance Comparison of Various Motor Types

A basic comparison of a BLDC motor's numerous machine parameters with those of DC and IM motors has shown the benefits of BLD motors over the other varieties. The comparison explains how it may be used in EVs and for the majority of other applications while still being broadly accepted in comparison to the other varieties. Additionally, the comparison reveals how BLDC motors can replace all other types due to their extensive range of advantages and ability to be used in nearly all applications where a motor is needed using only a modest drive setup.(Luthra, 2017; Varghese et al., 2014)

Table 2.1 summarizes the advantages of the BLDC motor when compared against DC and IM motors

Table 2.2 Comparison between brushed DC and brushless DC motors(Varghese et al., 2014)

Feature	BLDC motor	Brushed DC motor	Actual advantages
Commutation	Electronic commutation based on rotor position information	Mechanical brushes commutator	Electronic switches replace the mechanical devices
Efficiency	High	Moderate	The voltage drops on an electronic device is smaller than that on brushes
Maintenance	Little/None	Periodic	No brushes/commutator maintenance
Thermal performance	Better	Poor	Only the armature windings generate heat, which is transferred to the stator and connected to the BLDC's outside case. The case dissipates heat better than a rotor inside a brushed motor.
Output power/ Frame size (ratio)	High	Low	Modern permanent magnet and no rotor losses
Speed/Torque characteristics	Flat	Moderately flat	There is no brush friction to limit useful torque.
Dynamic response	Fast	Slow	Permanent magnets reduce rotor inertia.
Speed range	High	Low	No mechanical limitation imposed by brushes or commutators

Electric noise	Low	High	No arcs from brushes to generate noise, causing EMI problems.
Lifetime	High	Low	No brushes and commutators

A graphical comparison amongst various electric motors used in an EV has been made based on certain parameters like power density, cost of motors and their controller, dynamic response, efficiency operation life, and the torque versus speed characteristics(Luthra, 2017)(Joy et al., 2018). The general graphical comparison of various electric motors is shown in Figure 2:2.The BLDC motor is the most efficient motor, barring the controller and its price. Although induction and SR motors are about equally efficient, DC motors are the least effective. The DC and SR motors are more affordable than the BLDC motor, which is the most expensive.IM is the least. The IM motor trails the BLDC motor in terms of power density. And Motor SR As in the previous case, the BLDC motor and IM have a longer operational life than others. The DC motor is therefore the least susceptible to brush wear and sparking. A life of operation. The outcome demonstrates that BLDC motor has better performance metrics than diverse kinds.

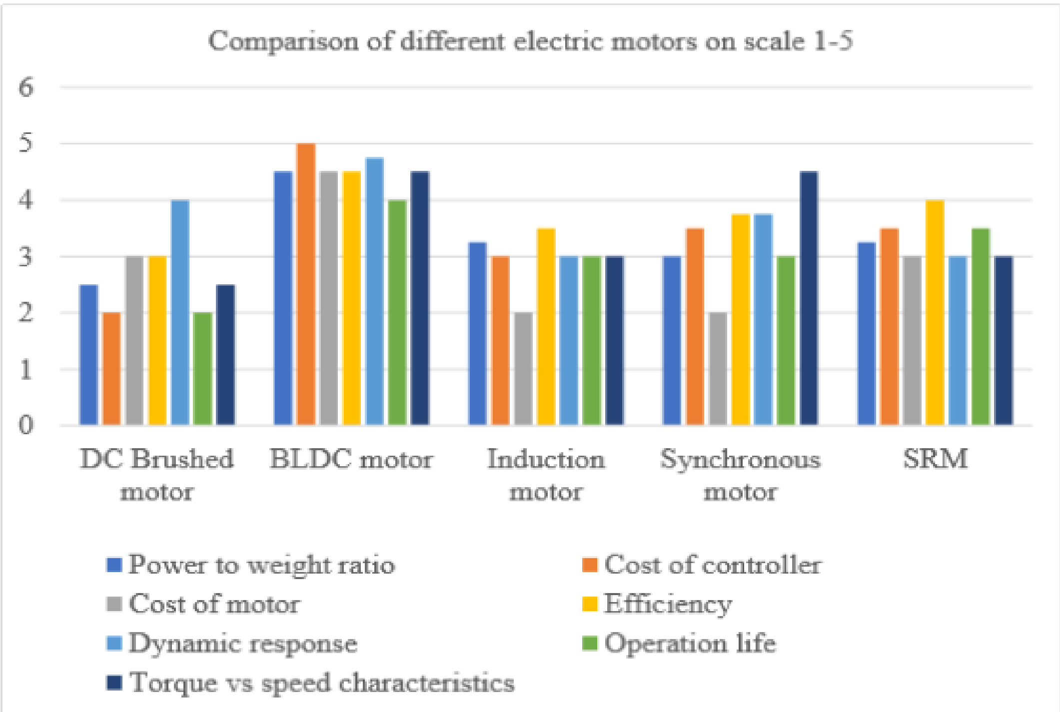

Figure 2.2 performance comparison of different electric motors

2.4 Related Works on Brushless DC Motor Drive and Electric Vehicle System

In (Anshory et al., 2019), a comparison of the control capabilities of the model reference adaptive control (MRAC) and the traditional PID controller applied to a brushless DC motor is presented. The MRAC is based on the MIT law technique, and the results are contrasted. An improved model predictive current control for PMSM drives is the subject of the study (Sun et al., 2020). A better MPCC system for PMSM drives is suggested by Circle based on Current Track. In the suggested technique, the reverse electromotive force is calculated using the stator voltage and current from the previous period to forecast the stator current for the subsequent period. The suggested MPCC determines the ideal voltage vector based on a current track circle rather than a cost function to further enhance the steady state and dynamic performance. The forecast of the current track circle is straightforward and quick in comparison to the cost function calculation.

In Combined Fuzzy and PI Control of Regenerative Braking System of Electric Vehicle driven by Brushless DC Motor (You et al., 2020), the author investigates proportional integral control and combined fuzzy management strategies. Regenerative braking systems disperse both mechanical and electrical braking forces. The paper (Using et al., 2021) BLDC Motor Controller Design Comparison for Electric Vehicles The actual speed feedback will be managed using a fuzzy logic controller and artificial neural network, which uses pulse width modulation (PWM) to control speed. This allows the actual speed to be adjusted to the intended pace.

The study (Agrawal, n.d.),suggests a fuzzy logic controller for electric vehicle speed control. The use of regenerative braking energy to regulate the speed of an electric vehicle using a fuzzy logic controller is covered in this article. A sugeno type fuzzy logic controller has been established. The output of an electric vehicle's motor controller that uses fuzzy logic acts as feedback to the motor, increasing the vehicle's speed as a result. The suggested technique involves two different types of braking forces, one of which is regenerative and the other is frictional, depending on stability and brake safety. To enable the conversion of a significant amount of kinetic energy into electrical energy, which can then be stored in a battery or other kind of energy storage. The speed control of a BLDC motor using a PID controller is shown by the author on (Motakabber et al., 2020). These kinds of motors can more effectively improve their speed control thanks to the proportional integral derivative (PID) method. The overview of the PID controller's functionality and design is the paper's main goal.

Design of speed control for brushless DC motor used in electric vehicle based on adaptive neuro-fuzzy inference system is presented by the author on (Series & Science, 2019). The configuration of the suggested approach is an adaptive neuro-fuzzy inference controller used with the dynamics model of an electric vehicle. According to the study on (Gadekar, 2020), BLDC motor drives can be made to perform better by using self-tuning PID controllers for a wide speed range. Control system advancements in recent years have made it possible to automatically tune PID controllers to achieve the best performance at varied operating speeds.

For use in brushless dc motor speed control for electric motorcycles, the author (Suryoatmojo et al., 2020) suggests an adaptive neurofuzzy inference system. Proportional-Integral-Derivative (PID) and Fuzzy-PID controllers were created, tested, and compared to ANFIS controller. ANFIS is learned using, but somewhat modified, data from Fuzzy-PID performance results. The paper (Anshory et al., 2019) offered BLDC motor system identification and artificially intelligent control-based speed optimization. Following the acquisition of the transfer function equation, simulations and analyses are carried out utilizing a variety of optimization techniques, including PID, Fuzzy, Hybrid Fuzzy PID, and, finally, the fusion of Fuzzy and PID optimized with PSO algorithm.

In general, from above literature reviewed they have drawbacks such as low accuracy, low speed, and longer running time, limited performance, Tuning the controller parameters is awkward and Inadequate gains selection for controllers which can result to the instability of the whole system. To mitigate the aforementioned difficulties the neural network based model reference adaptive controller for speed control of BLDC motor for electric vehicle was designed.

CHAPTER THREE

3. METHODOLOGY

3.1 Introduction

This chapter deals with data collection and analysis, mathematical modeling of the vehicle dynamics and BLDC motor, and design the reference model output converges to the plant output which is BLDC motor drive. A neural network-based model reference adaptive intelligent controller is employed for speed control of the motor. An online growing multilayer back propagation neural network structure is used in tandem with the traditional model reference adaptive controller architecture to implement the intelligent supervisory loop. The BLDC motor drive is then modelled as a whole. Lastly the system is simulated using the program MATLAB/2020, which supports both Simulink and script.

3.2 Materials

Software like MATLAB/2020a, Microsoft Office 2016, and Math Type 7.4 Equations are employed in this project. The computer program known as MATLAB includes Simulink and technical toolboxes. Editing of the thesis documentation is done using Microsoft Office. For composing mathematical equations and formulas in Microsoft Office word processing and PowerPoint presentation software, utilize Math Type 7.4.

3.3. Methods

For successful completion of this thesis the following formal methodologies to be followed to carry out different tasks. At the beginning, Finding the problem and defining that problem by carefully thinking. Secondly, study background of the Research is the central part of the thesis which is modeling the behavior of the nonlinear Brushless DC motor to be done based on physical parameters of the Neural Network train system. Thirdly, design and performance analysis of neural network based model reference adaptive controller for the speed control of a BLDC motor was done. During fourth phase the performance evaluation of the proposed algorithm will be done using MATLAB/SIMULINK. Lastly the conclusion, and recommendation for further work was suggested. The followed flow chart is implied in Figure 3.1 below.

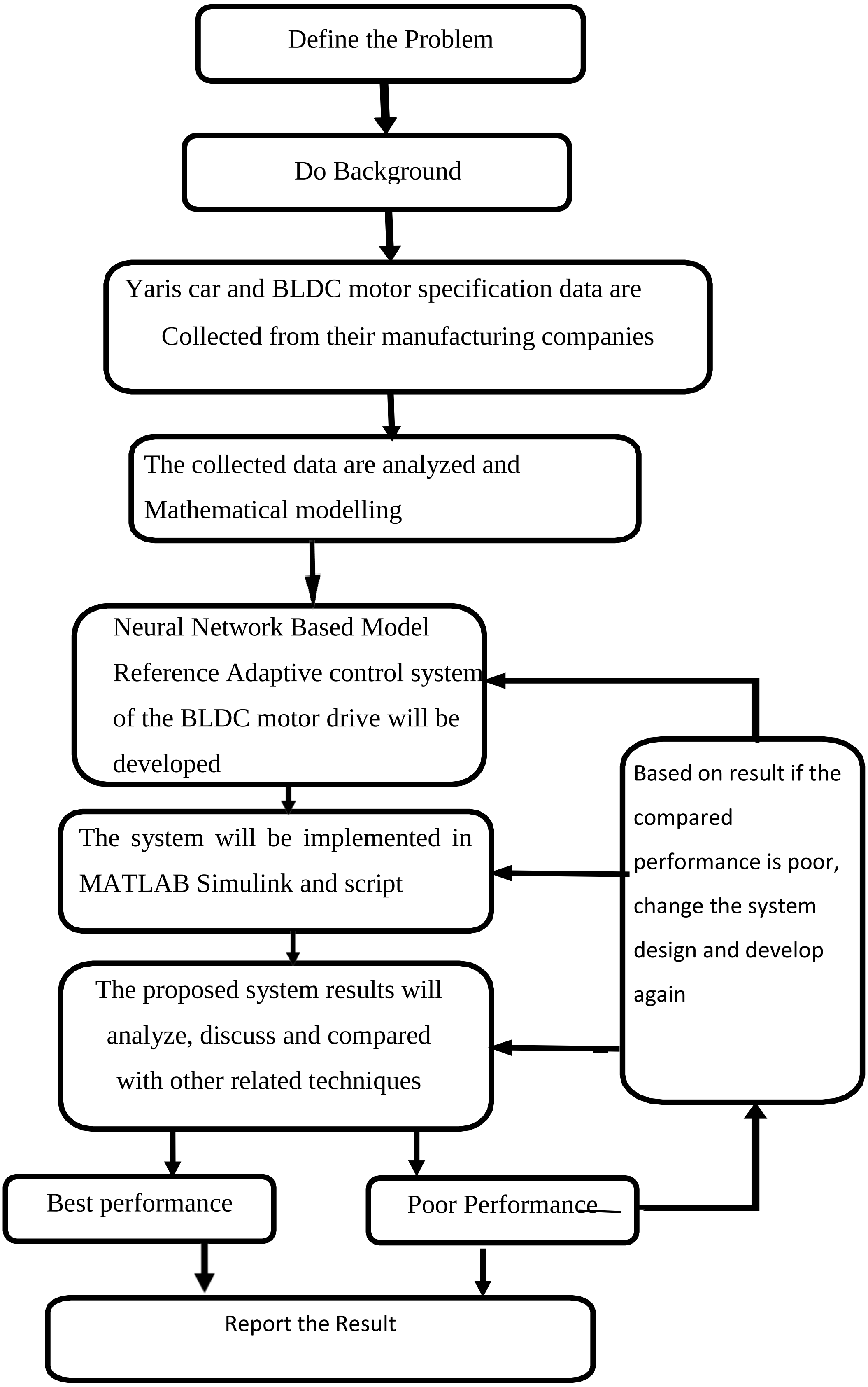

Figure 3.1 Flow chart of research Methodology

3.4 Proposed System Block Diagram

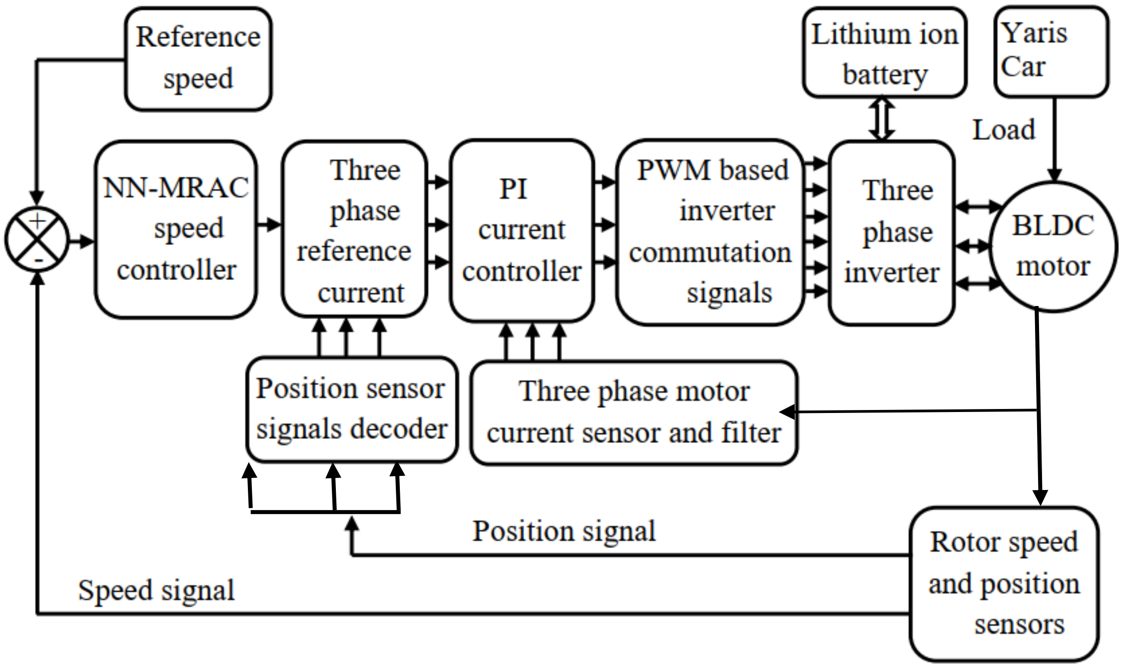

Figure 3.2 Block diagram of the proposed control system

This block diagram's operating principle is represented as follows. Utilizing a speed regulator allows for control over the discrepancy between the reference speed and rotor speed. A suggested adaptive speed controller the torque command is then issued from the speed regulator's output. The torque command is multiplied by the torque constant to get the highest reference current. Peak reference current and decoded hall are multiplied to create reference current. Sensors. Because, two phases of the stator current are considered to be the stator current feedback. Once the two current phases are understood the third phase is negative summation of the two. The difference of phase current and the corresponding reference current is controlled by using PWM current controller. PWM current controller consists of current regulator, comparator and logical circuit which is used to generate inverter driving signals.

3.5 Analysis of Yaris electric vehicles dynamics

Electric vehicles come in two different varieties. These include both fully electric and hybrid electric vehicles. Vehicles defined as pure electric vehicles if whole of the required energy for traction is contributed by on board DC source and characterized as hybrid electric vehicles if a part of traction energy contributed by ICE. In this thesis largely focuses on pure electric automobiles. In the power-train system of pure electric vehicles, the battery, drive motor, reducer, gearbox etc. Among them, Drive motor and battery are the two main components among them. To lessen the mechanical transmission device and boost transmission efficiency. The power system of pure electric car designed in this study includes motor, battery, and mechanical driving device and control system. The structure diagram of car power system as is depicted in Figure 3.3.

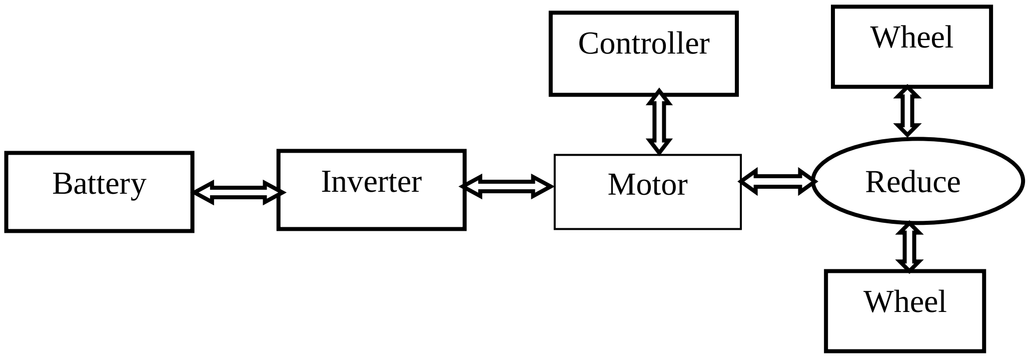

Figure 3.3 Pure Electric Vehicle Power System Structure

3.5.1 Driving force of Yaris electric vehicles

The electric car is made up of numerous parts, including a charging module, converters, controllers, batteries, and an electric motor(Ranpariya et al., 2019). In order to overcome the force caused by the load and other opposing forces acting on the vehicle, the electric motor chosen to drive it must be capable of producing enough power and torque. The motor can be rotated by the user in either a clockwise or counterclockwise direction according to the proposed design. The sensor will respond to the controller circuit according to the position of the rotor. Then the controller circuit will fix the direction of current following to the stator. When the vehicle is moving, a number of forces are at work on the platform. The balance of forces operating on the running platform, forces classed as road-load, and driving force is important for simulating the dynamics of a vehicle. The road-load force is made up of a variety of forces, including the rolling resistance of the tires, the aerodynamic drag force, and others(Joy et al., 2018). The resultant force also known as the driving force which is the sum of all these acting forces.

The acting forces produce for rotor torque design, which can be written as

$$F_T = F_R + F_G + F_A + F_a \tag{3.1}$$

Where F_T total tractive force, F_R rolling resistance force, F_G gradient force, F_A aerodynamic force and F_a force required to accelerate. Figure 3.4 below represents the changes of inclination angle in the road surface.

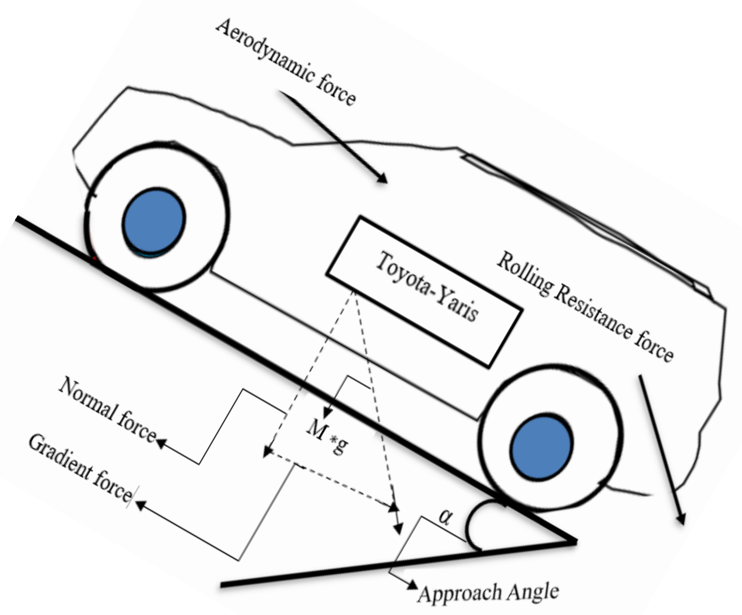

Figure 3.4 Exerted forces on moving electric vehicle

Table 3.1 Car specification from Toyota Yaris 2021 Model [L1]

Car specification	Value by Number
Gross vehicle weight	1615 Kg
Kerb weight	450 Kg
Maximum speed	175-180 Km/hr.
Acceleration 0-100 Km/hr	10.2 sec
Seating capacity	5 person
Approach angle	26°
Battery type	Lithium-ion

Number of Wheel	4

3.5.1.1 Rolling Resistance

Rolling Resistance is the force necessary to propel a vehicle over a particular surface. The worst surface type that the vehicle could possibly encounter should be taken into account. It is essentially the resistance experienced by the car as a result of the tires' contact with the road, and it is computed using equation 3.2

$$F_R = C_{rr} * M * g * \cos(\alpha) \tag{3.2}$$

$$F_R = 0.01 * 1615kg * 9.81m/s^2 * \cos(26^0) = 142.252N$$

Where M is the Gross mass of the vehicle (kg), **α** is the gradient angle (rad), g is the acceleration due to gravity (m/s^2**)** and C_{rr} is the rolling resistance coefficient. Table 3.2 shows the different material rolling resistance Coefficient. The power required to overcome the rolling resistance of the 142.252 N.

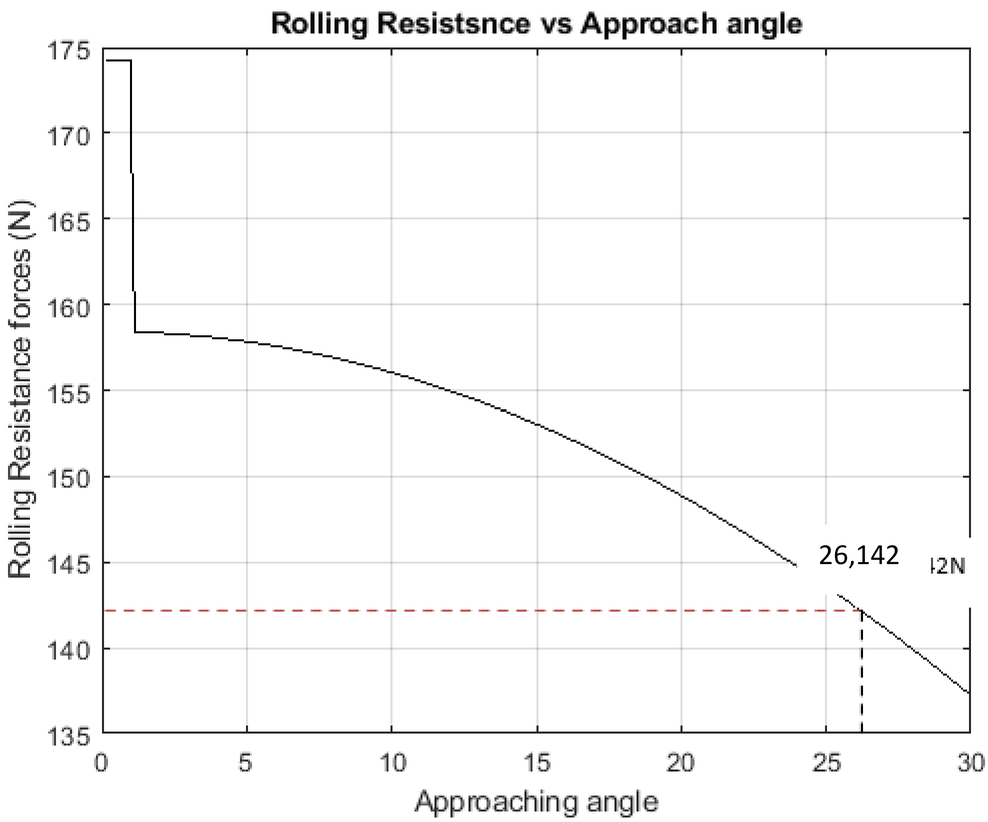

Figure 3.5 Rolling Resistance vs Approach Angle

$$P_R = F_R * \text{Veocity}(\frac{m}{sec}) \quad (3.3)$$

$$= 142.252N * 180 * \frac{1000m}{3600s} = 7.12Kw$$

Table 3.2 Coefficient of frictions for different types of surfaces (Akhtar, 2018)(Grunditz, 2014)

Contact surface	Coefficient of friction
Concrete surface (good/fair/	0.010/0.015/0.02
Asphalt (good/fair/poor)	0.012/0.017/0.022
Macadam (good/fair/poor)	0.015/0.022/0.037
Snow/dirt	0.025/0.037
Mud (firm/medium/smooth)	0.037/0.09/0.15
Grass (firm/soft)	0.055/0.037
Sand (firm/soft/dune)	0.060/0.15/0.3

3.5.1.2 Gradient Resistance

The force required to move a vehicle up a slope or "grade" is known as grade resistance. The highest angle or grade that the vehicle is anticipated to climb during normal operation must be used in this calculation. The angle between the ground and slope of the path is represented as α as shown in figure (3.4).

$$F_G = M * g * \sin(\alpha) \quad (3.4)$$

$$= 1615Kg * 9.81m / s^2 * \sin(26^0) = 6945.179N$$

Where M is the mass of the vehicle in (kg), g is the acceleration due to gravity (m / s^2) , α is the road or the hill-climbing angle, road slope (rad.). The power required to overcome the hill-climbing force at a speed of 180km/hr. is:

$$P_G = F_G * speed(\frac{m}{sec}) \tag{3.5}$$

$$= 6945.179N * 60 * \frac{1000m}{3600s} = 115.257Kw$$

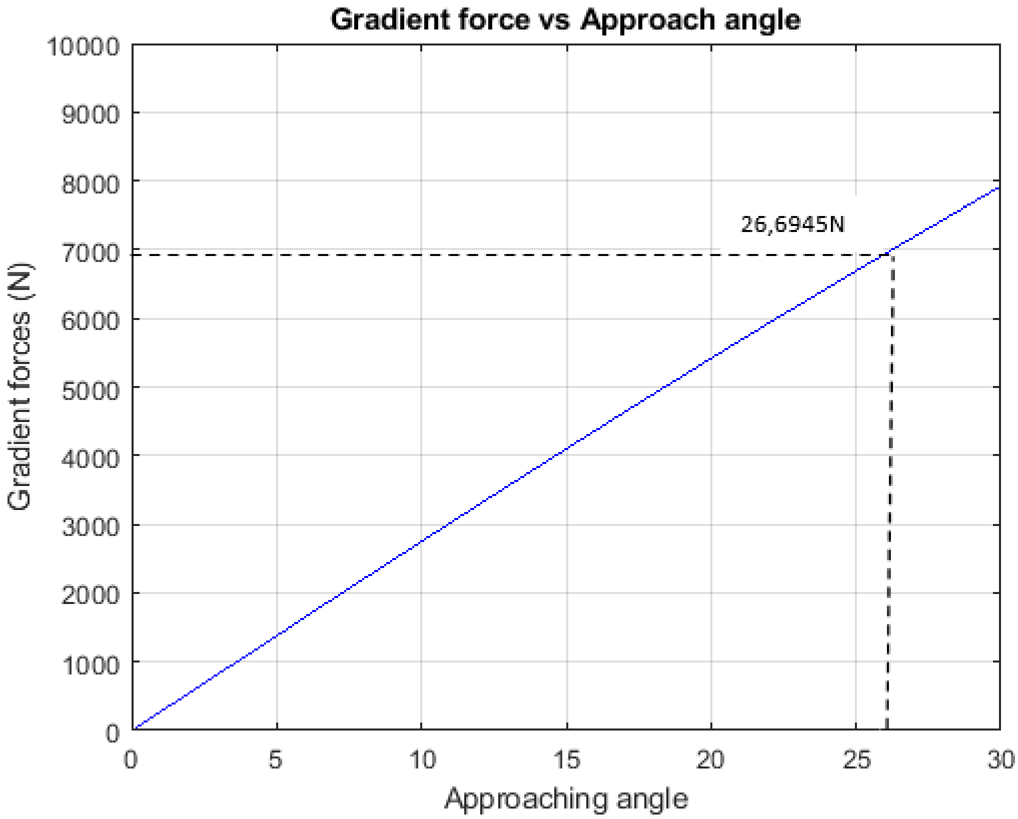

Figure 3.6 Gradient force vs Approach Angle

3.5.1.3. Aerodynamic Drag Force

The force opposing the motion of the vehicle platform due to air drag is known as the aerodynamic drag force. When a vehicle is moving, there will be an area where the air pressure is high in front of the vehicle platform and low in the area behind the platform. These two zones will oppose the motion of the platform. Shape drag is the resultant force on the vehicle (Akhtar, 2018)(Grunditz, 2014). Skin friction, which is produced when two air molecules move at different speeds, is the second element of aerodynamic drag. Since the air, close to the vehicle platform, moves almost with the same speed as the vehicle platform, in contrast to the air speed far away from the vehicle, there Friction occurs (System, 2016). The linear velocity of the vehicle platform, V, which is a function of the aerodynamic drag force, can be written as

$$F_A = 0.5\rho * A * C_d * (V + V_a)^2 \tag{3.6}$$

Where A is the frontal area of the vehicle, C_d is the aerodynamic drag coefficient, V and V_a are the speed of vehicle and air, respectively. The power needed to overcome it can therefore be disregarded because the air speed is lower than the vehicle speed. When developing the dynamics of an electric vehicle, additional factors such aerodynamic lift must be taken into account. Force, wheel force, and others. Assume V_a =0

$$F_A \text{ at } 60km/hr = 0.5*1.2*2*0.5*(16.67)^2 = 166.733N$$
$$F_A \text{ at } 180km/hr = 0.5*1.2*2*0.5*(50)^2 = 900N$$

Power calculated as follows;

$$P_A \text{ at maxiumam Speed} = F_A * V \tag{3.7}$$
$$= 900N * 50m/s = 4500W = 4.5KW$$
$$P_A \text{ at Gradient Speed} = 166.733N * 16.67m/sec = 2.779KW$$

Usually, they are minimal compared to the two forces mentioned above and can be considered as a maximum of 4.5kW. As a result, the maximum tractive power necessary to move a four-wheel electric vehicle under all conditions of motion that is, the required maximum power for a BLDC motor will be as follows:

$$P_{out\ total}(max) = 4.5Kw + 115.752Kw + 7.112Kw = 123.869Kw$$

These are the three fundamental power that affect a moving object while it travels at a constant speed; however, when an object accelerates or decelerates, inertia-related forces also have an impact on the object. Gradient forces rise as the road's approaching angle rises, and if the vehicle's speed is believed to be constant, the aerodynamic force is constant. Beside to this, the losses due to the transmission of power to the vehicle wheel must be considered (Akhtar, 2018). The mechanical output power required to drive the vehicle is given by Equation (3.8).

$$P_{total\ driven\ power} = \frac{P_{out\ total}(max)}{\eta_{gear\ transimission\ efficient}} \tag{3.8}$$
$$= \frac{123.869}{0.95} \approx 130Kw$$

When the vehicle is fully loaded and traveling at a speed of 60 km/h, the maximum tractive power is provided when it clamps a hill with a maximum approaching angle of 26 degrees. In order to increase torque while using the batteries and the motors limited power output, the vehicle's speed must be decreased while clamping a hill. If we need to use larger battery size and motor of larger power rating the penalty is cost and weight increment. Figure (3.6) illustrates how much power the motor must produce to move the vehicle at a constant speed of 60 km/h while approaching from different directions.

3.5.1.4. The Effect of vehicle Speed on the Power Requirement

Figure 3.7 analyzes and plots the relationship between the vehicle's speed and driving force. This demonstrates the linear relationship between vehicle power consumption and speed in km/hr. The power consumption of a vehicle rises as its speed does [23][24]. The vehicle has a top speed of 180 km/h and a 130 kW power requirement. The determined maximum power requirement is satisfied by this relationship.

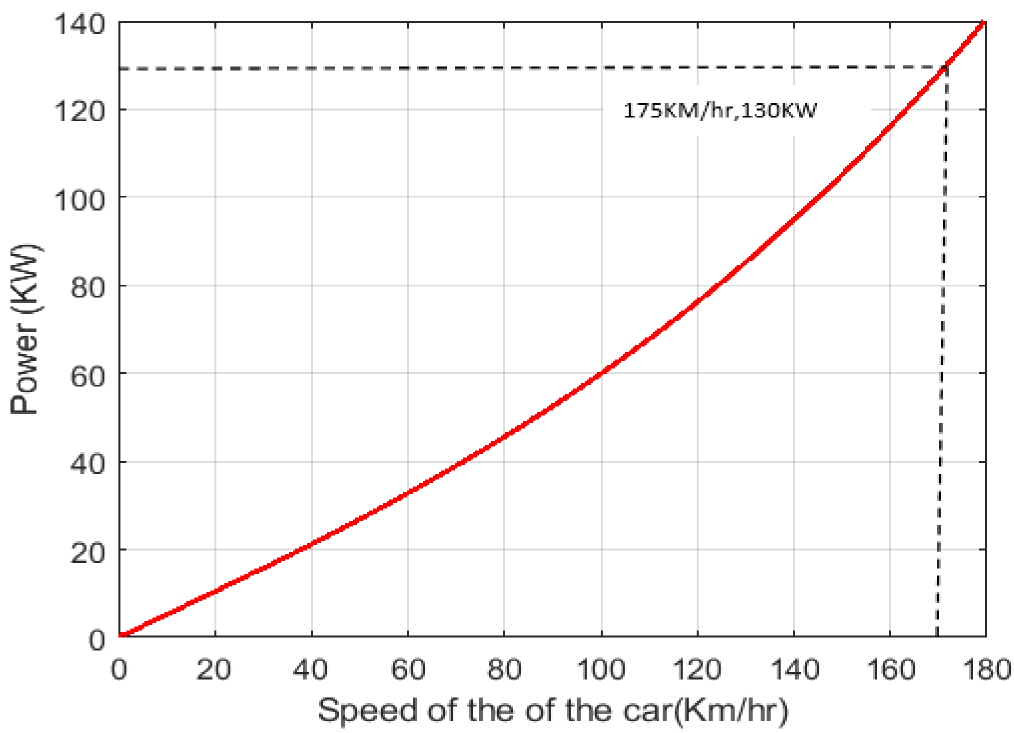

Figure 3.7 speed of the car vs power

3.5.1.5 Motor Rated Power and Peak Power Matching

The torque versus speed characteristic curve's specifications should be followed when choosing the rated speed, torque, and power of the BLDC motor (System, 2016). When the vehicle starts, the motor speed is low and works in constant torque state, as long as the speed is higher than the rated speed, it works in constant power state (Singh, 2014). The rated torque and output of the 4800rpm base speed electric car BLDC motor have a value of 148.8Nm and 75KW respectively as illustrated in Figure 3.8.

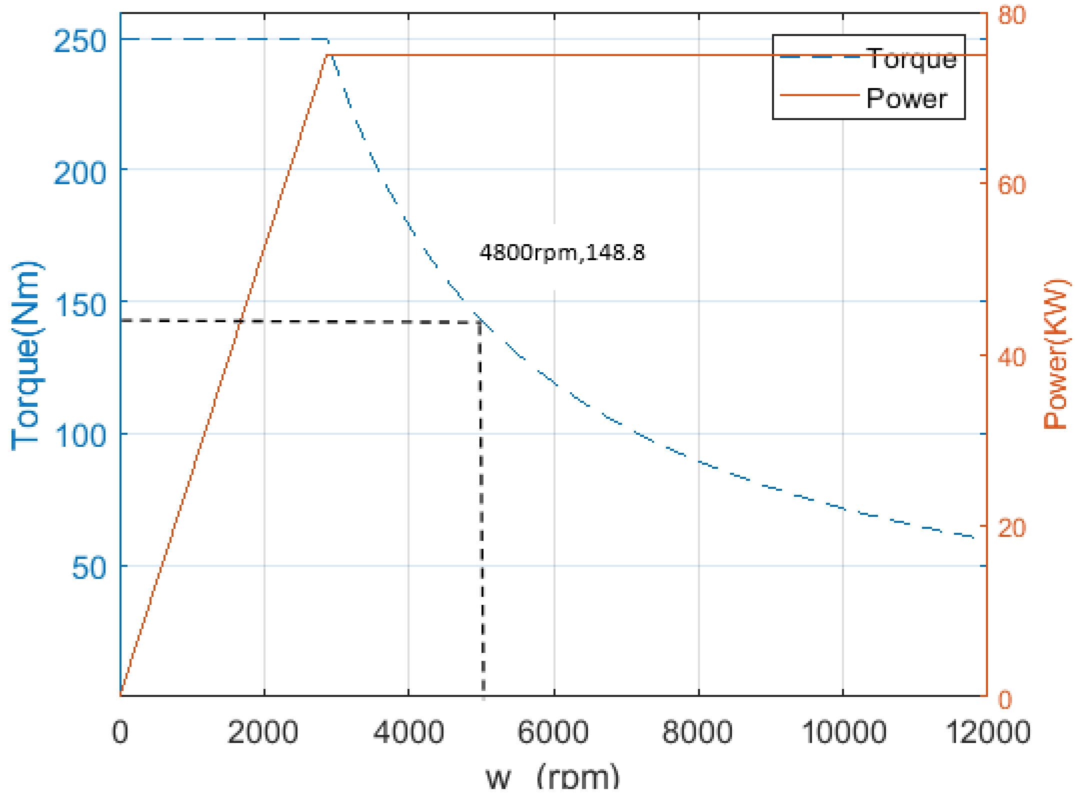

Figure 3.8 Torque versus speed characteristics of the BLDC motor

3.5.2 Electric Vehicle Toyota Yaris specification

Table 3.3 Electric Vehicle Toyota Yaris Car driving motor specification

Parameters	Values
Maximum power	130 kW
Gross weight	1615Kg
Rated power	75 kW
Maximum torque	250N-m
Rated torque	148.8 N-m
Rated speed	100Km/hr.
Departure angle	26°
Seating capacity	5 persons

3.5.3 Reducer and Gear Specification

Because a vehicle's need for torque changes with speed, reducers are widely utilized in cars for power transmission. A reducer's main functions are to alter the gear ratio between the motor crankshaft and the vehicle's drive wheels and to generate the torque necessary to move the vehicle under various road, environment, and load conditions. Reverse and neutral gear changes allow the vehicle to move forward and stop and start, respectively. Table 3.4 provides a description of the Toyota Yaris's gearbox. The company that manufactures hybrid electric automobiles gave the essential information.

Table 3.4 Gear box specifications(Wase, 2020)

Parameters	Values
Maximum Speed	6000rpm
Maximum Torque	250Nm
Differential gear ratio	2.834:1

3.5.4. Traction Motor specification

Depending on the maximum power of the electric vehicle, some of the BLDC motor specifications are taken from the manufacturing company and others are taken from literature. The torque and back EMF constants are computed using the following derivations from the motor's two phase equations. The motor's rated power is determined by multiplying the motor current by the back EMF when there are two phases involved.

$$\text{power}_{\text{rated}} = 2E_m * I_m \tag{3.9}$$

$$E_m = \frac{\text{power}_{\text{rated}}}{2 * I_m} = \frac{75\text{Kw}}{2 * 212\text{A}} = 176.886\text{V}$$

Emf constant (ke) calculated as

$$k_e = \frac{E_m}{\omega_{\text{rated}}} \tag{3.10}$$

$$= \frac{176.886V}{4800(\frac{2\pi}{60})} = 0.352(\frac{V}{rad/sec})$$

If two phase operating system of BLDCM is considered $k_b = 2 * 0.352 = 0.704$

$$Torque_{(rated)} = k_t * I_m \quad (3.11)$$

$$= \frac{2E_{m*}I_m}{\omega_{rated}} = \frac{2 * 176.886V * 212A}{4800(\frac{2\pi}{60})} = 148NM$$

$$k_t = \frac{Torque_{(rated)}}{I_m} = \frac{148NM}{212A} = 0.701$$

Table 3.6 shows the parameter specifications of three phase BLDC motor used for the study

Table 3.5 Parameter specifications of BLDC motor used in this thesis (Mullick, 2017)

Parameters	Value
Number of poles	4
Power factor	0.95
Efficiency at rated	95.7 [%]
Control input rated voltage	352 [V]
Rated motor current	212 [A]
Rated motor power	75 [kW]
Armature phase Resistance	1.2 [**Ω**]
Armature phase inductance	0.56[H]
Rated speed	4800 [rpm]
Viscous friction model	0.001 [N·s/m]
Torque constant	0.701 [N·m/A]
Back emf coefficient	0.352[V·s/rad]
Inertia moment of the rotor	0.0089 [kg]
L(Self-inductance)	2[MH]
M (Mutual inductance)	0.5[MH]
λ_p (Flux amplitude turns)	0.105[Web]
J (moment of Inertia)	0.000925kg. m^2
B (Viscous Coefficient)	0.001NMS

3.5.5 Battery Specifications

Batteries serve as the pure electric vehicles' power source. Since lithium batteries have a long lifespan and a high energy density, they are chosen as the power source for electric cars. The proposed system equations considered for the battery are as follow

$$P = P_{max} 0.5 * 0.95 * P_{(zero\ grade)} \tag{3.12}$$

$$P_m = \frac{P}{\eta_m} \tag{3.13}$$

$$W_{road} = P_m * t = \frac{P_m S}{V} \tag{3.14}$$

$$SOC(\%) = \frac{(W_{rated} - W_{road})x100\%}{W_{rated}} \tag{3.15}$$

where P is the power required for the vehicle at a constant speed, S is endurance mileage, Wroad is the energy needed for mileage S, Pm is the input power of the motor drive and ηm is the efficiency of motor and motor drive assembly(Minyamer Gelawe Wase, 2020)

Table 3.6 Parameter specifications of Lithium-ion battery

Parameters	Value
Cell type	Lithium-ion
Total battery power pack	42.2[kWh]
Capacity	120[Ah]
Nominal voltage	4.3[V]
Rated voltage	352[V]
Energy density	155 [Wh/kg]
Operating temperature	-10 to 50 [^{0}C]
Energy	666 [Wh]

3.6. Modeling of BLDCM Drive for Electric Vehicle Propulsion

An accurate and precise model of the electric motor drive design is needed for the electric vehicle power system component(Tashakori et al., 2011). A detailed model of the BLDC motor is needed in order to construct the control system for the electric vehicle's propulsion. This thesis work takes into account the three-phase star-connected BLDC motor with hall rotor position sensor control system. An accurate model of the BLDC motor that provides the precise values of rotor speed, armature current, torque, and back EMF is needed to study the various control schemes of the motor drive. In this section, the modeling of BLDC motor and the whole motor driving systems are examined theoretically and mathematically.

3.6.1 Three-Phase VSI PWM inverter

The three-phase VSI uses at 120^0 mode operation to regulate the power circuit for a BLDC motor. A six-step bridge with six switches is used to operate three-phase inverter, and each phase has two switches that are operated. Each step in the process is referred to as a time shift in the proper order from one MOSFET to the next. An inverter with six steps would have 360^0 cycle, with each step would have 60^0 intervals. .Vs is the three-phase source voltage and the MOSFET switches are S_1, S_2, S_3, S_4, S_5 and S_6. The outcomes V_a, V_b and V_c are shown in Figure 3.9.Three BLDC motors feed this output terminal and n is the three-phase BLDC neutral terminal. The inverter is power circuit diagram is identical to that shown in Figure 3.9. Each transistor the 120^0 mode VSI conduct for 120^0 of the cycle. To complete one cycle of the output AC voltage the 120^0 mode inverter takes six steps each of which is 60^0 long. S_1 conducts for 120^0 in this inverter, but neither S_1 nor S_4 conduct for the next 60^0 .Now S_4 is turned on at 180^0 and conducts for 120^0 i.e from 180^0 to 300^0 between the S_4 stops conducting at 300^0 and a 60^0 delay passes until S_1 turns on again at 360^0 .The S_3 is turned on at 120^0 and conducts for 120^0 before being switched off in the bottom row. The S_4 is turned on at 300^0 and conducted for 120^0 and S_3 is turned back on after the 60^0 interval has passed. The firing sequences for the six MOSFET switches are identical to those used in the 180^0 mode inverter. In this situation, just two switches one from the upper group and one from the lower group are active in each step.

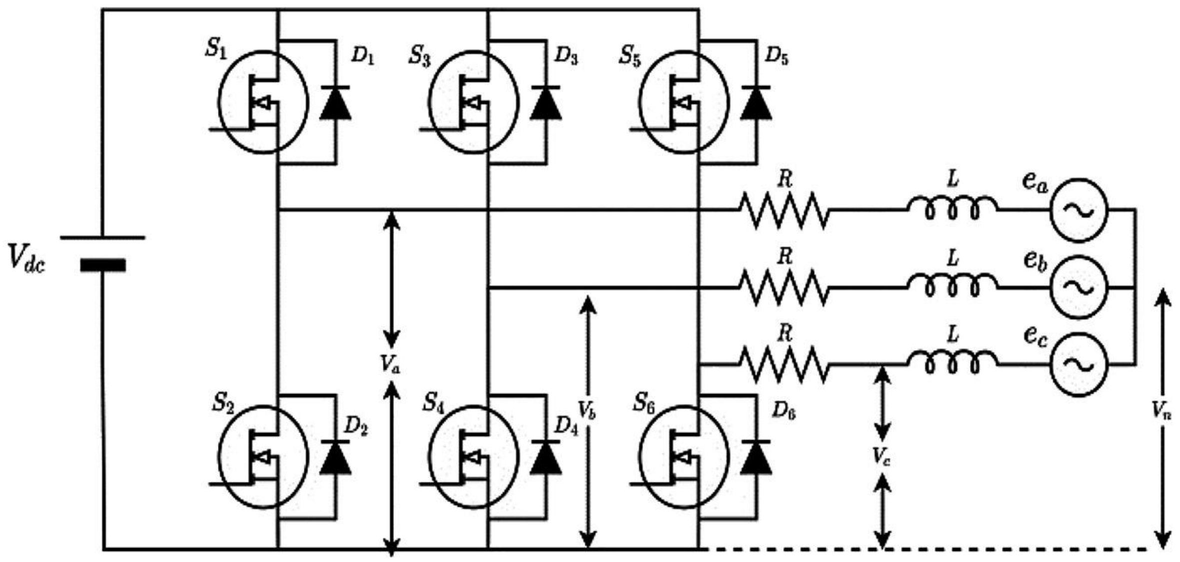

Figure 3.9 BLDC motor with 3-phase Inverter as electronic commutator

3.6.2 Rotor Position Hall Sensors Modeling

The stator windings need to be energized sequentially in order to turn the BLDC motor. Knowing the rotor location is necessary to determine which winding should be used. Integrated Hall sensors in the stator on the motor's non-driving end experience the Rotor's orientation. As the rotor poles approach With Hall Effect sensors, a high or low signal is produced. In order to properly commute, the current every time a magnet pole changes, it must alter its polarity and traverses the sensor. In the brushed DC motor, the commutator and brushes perform the polarity reversal. In the BLDC motor, the polarity reversal is performed by power MOSFETS, which must be switched in synchronism with the rotor position. The switching sequence used to obtain phase currents is described in Table 3.7. To rotate the BLDC motor, the stator windings must be excited sequentially. Each commutation sequence energizes one winding to positive power, the second to negative power, and the third to non-energized. To determine the energizing sequence, the rotor position must be known. (Tashakori et al., 2011)(Lake et al., 1984)

Table 3.7 Hall Effect signals and inverter switches status of the BLDC motor(Tashakori et al., 2011)(Jain, 2017)

Electrical Degree	Hall A	Hall B	Hall C	Inverter Switch					
				S_1	S_2	S_3	S_4	S_5	S_6
0-60	0	1	0	on	off	off	off	off	on
60-120	1	1	0	on	off	off	on	off	off
120-180	1	0	0	off	off	off	on	on	off
180-240	1	0	1	off	on	off	off	on	off
240-300	0	0	1	off	on	on	off	off	off
300-360	0	1	1	off	off	on	off	off	on

3.6.3. Mathematical Modeling of Brushless DC Motor

A three-phase inverter is needed in the front end of a BLDC motor, which is classified as an electronic motor and is depicted in Figure 3.10. The inverter functions as an electronic commutator in self-control mode, receiving the switching logical pulse from the position sensors (Tashakori et al., 2011). The motor is referred to as an electronic commutated motor as well. The BLDC motor has a permanent magnet on the rotor and three stator windings (Lake et al., 1984). Because magnets and stainless steel have high resistivity's, rotor-induced currents can be disregarded. The following assumptions are made to simplify the overall BLDC motor mathematical equation.

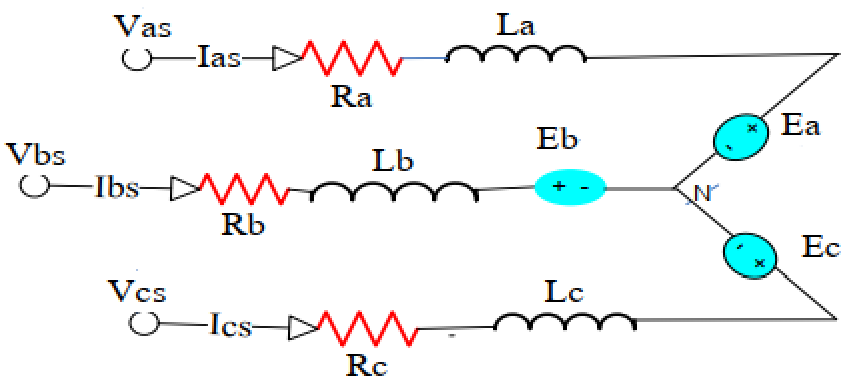

Figure 3.10 Stator connected three phase BLDC motor winding

Following assumptions are made to simplify the mathematical equations and the overall BLDC motor model.

- Magnetic circuit saturation is ignored;
- The corresponding stator resistance, self-inductance and mutual inductances

of each phase are equal;

- Hysteresis and eddy current losses are eliminated;
- Inverter semiconductor switches are ideal

From Figure 3.10 V_S drop through R_S , L_S ,M and E where V_S ,is supply voltage on stator winding, R_S ,stator resistance, L_S ,self-inductance of stator, M, is mutual inductance for each phase and E total back emf. Let

$$V_{as} = R_s i_a + L\frac{di_a}{d_t} + M\frac{di_b}{d_t} + M\frac{di_c}{d_t} + e_a \tag{3.16}$$

$$V_{bs} = R_s i_b + L\frac{di_a}{d_t} + M\frac{di_b}{d_t} + M\frac{di_c}{d_t} + e_b \tag{3.17}$$

$$V_{cs} = R_s i_c + L\frac{di_a}{d_t} + M\frac{di_b}{d_t} + M\frac{di_c}{d_t} + ec \tag{3.18}$$

Where

$$L_S = La = Lb = Lc \tag{3.19}$$

$$R_S = R_a = Rb = Rc \tag{3.20}$$

The above formula by matrix form

$$\begin{bmatrix} V_{as} \\ V_{bs} \\ V_{cs} \end{bmatrix} = \begin{bmatrix} R_S & 0 & 0 \\ 0 & R_S & 0 \\ 0 & 0 & R_S \end{bmatrix}\begin{bmatrix} i_a \\ i_b \\ i_c \end{bmatrix} + \begin{bmatrix} L_S & M & M \\ M & L_S & M \\ M & M & L_S \end{bmatrix}\begin{bmatrix} \phi_a \\ \phi_b \\ \phi_c \end{bmatrix} + \begin{bmatrix} e_a \\ e_b \\ e_c \end{bmatrix} \tag{3.21}$$

Where $\phi = \frac{di}{d_t}$ beside to this from fundamental of Dc motor $e_a \propto \omega_r$, ω_r is motor speed

The induced voltage of each phase winding is directly proportional of speed of the motors.

$$e_a = k_a \omega_r \tag{3.22}$$

, where k_a , angular position of the rotor constant for the other phase also the same fashion.

$$e_b = k_b \omega_r \tag{3.23}$$

$$e_c = k_c \omega_r \tag{3.24}$$

From the figure 3.10 the connection is star and current of star connection is the summation is equal to zero.

$$i_a + i_b + i_c = 0,\ i_b + i_c = -i_a \tag{3.25}$$

$$V_{as} = R_s ia + L\frac{dia}{dt} + M\frac{d(i_b + i_c)}{dt} + e_a \tag{3.26}$$

$$V_{as} = R_s ia + L\frac{dia}{dt} + M\frac{d(-ia)}{dt} + e_a \tag{3.27}$$

$$V_{as} = R_s ia + (L - M)\frac{dia}{dt} + e_a \tag{3.28}$$

By the same fashion;

$$V_{as} = R_s i_a + (L - M)\frac{di_a}{dt} + e_a \tag{3.29}$$

$$V_{bs} = R_s i_b + (L - M)\frac{di_b}{dt} + e_b \tag{3.30}$$

$$V_{cs} = R_s i_c + (L - M)\frac{di_c}{dt} + e_c \tag{3.31}$$

$$\begin{bmatrix} V_{as} \\ V_{bs} \\ V_{cs} \end{bmatrix} = \begin{bmatrix} R_s & 0 & 0 \\ 0 & R_s & 0 \\ 0 & 0 & 0 \end{bmatrix} \begin{bmatrix} i_a \\ i_b \\ ib \end{bmatrix} + \begin{bmatrix} L-M & 0 & 0 \\ 0 & L-M & 0 \\ 0 & 0 & L-M \end{bmatrix} \begin{bmatrix} \phi a \\ \phi b \\ \phi c \end{bmatrix} + \begin{bmatrix} e_a \\ e_b \\ e_b \end{bmatrix} \tag{3.32}$$

Equation (3.33) written as following

$$\begin{aligned} \frac{di_a}{dt} &= -\frac{Ri_a}{L-M} + \frac{V_{as}}{L-M} - \frac{e_a}{L-M} \\ \frac{dib}{dt} &= -\frac{Ri_b}{L-M} + \frac{V_{as}}{L-M} - \frac{e_b}{L-M} \\ \frac{di_c}{dt} &= -\frac{Ri_c}{L-M} + \frac{V_{as}}{L-M} - \frac{e_c}{L-M} \end{aligned} \tag{3.33}$$

From the above equations, the system state equations are written in the following

$$\dot{X}(t) = Ax + B(V - e) \tag{3.34}$$

Where the states are chosen as

$$x = [i_a \quad ib \quad i_c]^T \tag{3.35}$$

Where the state space matri

$$A = \begin{bmatrix} -\frac{R}{L-M} & 0 & 0 \\ 0 & -\frac{R}{L-M} & 0 \\ 0 & 0 & -\frac{R}{L-M} \end{bmatrix} \tag{3.36}$$

$$B = \left[\frac{1}{L-M}\right] \tag{3.37}$$

$$V = \begin{bmatrix} V_{as} \\ V_{bs} \\ V_{cs} \end{bmatrix} \tag{3.38}$$

$$e = \begin{bmatrix} e_a \\ e_b \\ e_c \end{bmatrix} \tag{3.39}$$

3.6.4 Modeling of Ideal Back-EMF

The back EMF signals have a phase shift of 120 electrical degrees with respect to each other due to symmetrical distribution of the phase winding in the stator. Hence the back-EMF voltages are a function of the electrical rotor angle θ, motor speed ω, and flux linkage λ. Each phase in the balanced three phase system is in phase with each other with a 120^0 phase shift. The rotor angle functions $f_a(\theta), fb(\theta)$ and $f_c(\theta)$ have the same shape as, and with a maximum magnitude of ±1. Equations (3.39), (3.40), and (3.41) show the mathematical functions of the rotor angle in a three-phase system.

$$f_a(\theta)=\begin{cases} \frac{6}{\pi}\theta \ , & 0<\theta\leq\frac{\pi}{6} \\ 1 \ , & \frac{\pi}{6}<\theta\leq\frac{5\pi}{6} \\ -\frac{6}{\pi}\theta+6 \ , & \frac{5\pi}{6}<\theta\leq\frac{7\pi}{6} \\ -1 \ , & \frac{7\pi}{6}<\theta\leq\frac{11\pi}{6} \\ -\frac{6}{\pi}\theta-1 \ , & \frac{11\pi}{6}<\theta\leq\frac{12\pi}{6} \end{cases} \tag{3.40}$$

$$f_b(\theta) = f_a(\theta+\frac{2\pi}{3}) \tag{3.41}$$

$$f_c(\theta) = f_a(\theta-\frac{2\pi}{3}) \tag{3.42}$$

The trapezoidal rotor position function is limited between +1 and -1 and these functions are modeled as the following diagram**.**

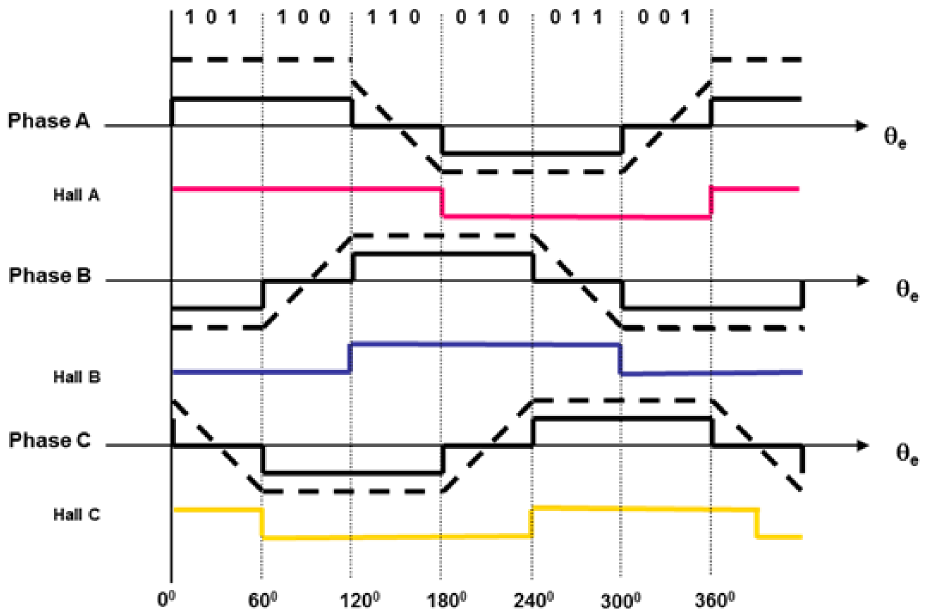

Figure 3.11 Phase voltage, current and hall-sensor waveforms with respect to rotor electrical

3.6.5 Open loop s-domain analysis of three-phase BLDC motor

Absolutely no difference between the mathematical model of a BLDC motor and that of a traditional DC motor. The main difference mathematical modeling of BLDC and dc i.e., BLDC involved three phase and dc motor is single phase. The resistive and inductive components of the BLDC motor configuration are notably affected by the phases. Consider one of the single phase equivalent circuit of the three-phase machine.

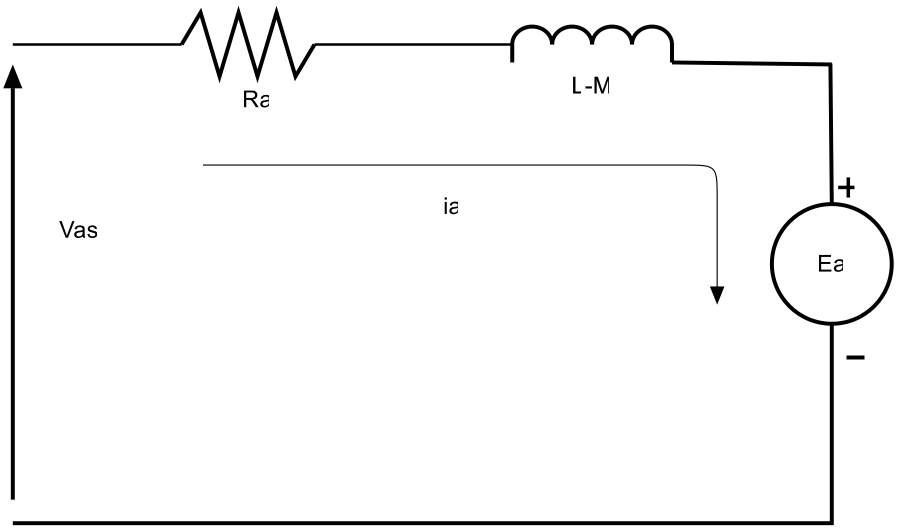

Figure 3.12 simplified single-phase equivalent circuit of the three-phase BLDC motor

The basic component of each of the three phase windings are armature resistance R, winding inductance L, mutual inductance M and the back-electromotive force(back-EMF). Using Kirchhoff's voltage low (KVL) in the above equivalent circuit the following equation obtained.

$$\frac{di_a}{dt} = -\frac{Ri_a}{L-M} + \frac{V_{as}}{L-M} - \frac{e_a}{L-M} \tag{3.43}$$

Where;

V_{as} = The stator phase winding voltage
i_a = stator phase winding current
e_a = back – EMF produced in the phase a winding

In the same fashion, considering the mechanical properties of the motor, from Newton's second law of motion, the mechanical properties relative to the torque of the system arrangement would be the product of the inertia load, J and the rate of angular velocity ω_m is equal to the sum of all torques;

$$\frac{d\omega}{dt} = -\frac{B\omega}{J} - \frac{T_L}{J} + \frac{T_e}{J} \tag{3.44}$$

Where;

T_e = The electrical torque produced by the motor
T_L = Load torque
J = The moment of inertia of the motor
B = air gap friction constant
ω_m = angular speed of the motor

The back-EMF produced in each stator winding phase is directly proportional with the rotor speed and it can be written as follows;

$$e_a = k_a \omega_m \tag{3.44}$$

Where, K_e is the back-EMF constant which is the function of the motor PM flux linkage (λ_m) and also, the electrical torque produced is also a direct relation with the stator phase current applied and given by the following relation;

$$T_e = k_t i_a \tag{3.45}$$

Where, k_t is the torque constant which is dependent on the mass of the shaft and the radius. Therefore, re-writing equations (3.42) and (3.43) then equations (3.44) and (3.45)

$$\frac{di_a}{dt} = -\frac{Ri_a}{L-M} + \frac{V_{as}}{L-M} - \frac{k_e\omega_m}{L-M} \tag{3.46}$$

$$\frac{d\omega}{dt} = -\frac{B\omega}{J} - \frac{T_L}{J} + \frac{i_a k_t}{J} \tag{3.47}$$

Using Laplace transfer to evaluate equations (3.45) and (3.46), the following are obtained approximately (all initial conditions are all assumed to be zero) from equation (3.45)

$$L\left\{\frac{di_a}{dt} = -\frac{Ri_a}{L-M} + \frac{V_{as}}{L-M} - \frac{k_e\omega_m}{L-M}\right\} \tag{3.48}$$

This implies that;

$$si_a = -\frac{Ri_a}{L-M} + \frac{V_{as}}{L-M} - \frac{k_e\omega_m}{L-M} \tag{3.49}$$

By the same fashion; the Laplace transform of equation (3.47)

$$s\omega_m = -\frac{B\omega}{J} - \frac{T_L}{J} + \frac{i_a k_t}{J} \tag{3.50}$$

$$L\left\{\frac{d\omega}{dt} = -\frac{B\omega}{J} - \frac{T_L}{J} + \frac{i_a k_t}{J}\right\} \tag{3.51}$$

At no load for $T_L = 0$ the equation 3.51 becomes

$$s\omega_m = -\frac{B\omega}{J} + \frac{i_a k_t}{J} \tag{3.52}$$

From equation 3.41 the stator phase current can be obtained;

$$i_a = -\frac{s\omega_m + \frac{B}{J}\omega_m}{\frac{k_t}{J}} \tag{3.53}$$

By directly substitute equation 3.53in equation 3.51

$$\frac{s\omega_m + \frac{B}{J}\omega_m}{\frac{k_t}{J}}\left(s + \frac{R_a}{L-M}\right) = -\frac{k_e}{L-M}\omega_m + \frac{1}{L-M}V_a \tag{3.54}$$

By simplifying the above equation it becomes

$$V_a = \left(\frac{s^2 J(L-M) + sB(L-M) + sRJ + BR_a + k_e k_t}{k_t}\right)\omega_m \tag{3.55}$$

The transfer function G(s) can be obtained as the ration of angular speed to the source voltage;

$$G(s) = \frac{\omega_m}{V_a} = \frac{k_t}{s^2 J(L-M) + sB(L-M) + sRJ + BR_a + k_e k_t} \tag{3.56}$$

By multiplying the whole equation by $J(L-M)$ the above equation be come

$$G(s) = \frac{\omega_m}{V_a} = \frac{\frac{k_t}{J(L-M)}}{s^2 + s\left(\frac{B}{J} + \frac{R_a}{L-M}\right) + \frac{BR_a + k_e k_t}{J(L-M)}} \tag{3.57}$$

By Considering, the following assumptions;

1) The friction constant is very small ($B \approx 0$) tends to zero, that implies that

2) $R_a J >> B(L-M)$ And

3) $k_e k_t \gg R_a B$

And the negligible values zero, the transfer function is finally written as;

So, by re-arrangement and mathematical manipulation on "J(L-M)", by multiplying top and bottom of the equation (3.57)

$$\frac{R_a}{k_e k_t} \mathrm{x} \frac{1}{R_a} \tag{3.58}$$

From the above transfer function becomes

$$G(s) = \frac{\omega_m}{V_a} = \frac{\frac{1}{k_t}}{\frac{JR_a}{k_e k_t} X \left(\frac{L-M}{R_a}\right) s^2 + \frac{JR_a}{k_e k_t} s + 1} \tag{3.59}$$

From equation (3.59) the following constants are gotten, The mechanical time constant τ_m which is given by;

$$\tau_m = \frac{JR_a}{k_e k_t} \tag{3.60}$$

The electrical time constant τ_e which is given by;

$$\tau_e = \frac{L-M}{R_a} \tag{3.61}$$

Substituting, equations (3.59) and (3.60) in equation (3.61), it yields;

$$G(s) = \frac{\omega_m}{V_a} = \frac{\frac{1}{k_t}}{s^2 \tau_e \tau_m + s\tau_m + 1} \tag{3.62}$$

By the same fashion three phase winding of BLDC motor have similar equation, total torque and speed is contribution of each phase. Both electrical and mechanical time constant are affected important parts of modeling parameters. Based on this assumption the following two point is concluded

- All the stator windings of the Three phases of BLDC motor is constant and equal which is represented by (R)
- All the difference inductance (L-M) in each phase of the three phase windings are all equal and represented by L.

From this concept the mechanical and electrical time constant three-phase BLDC motor is listed as below;

$$\tau_m = \frac{3JR_a}{k_e k_t} \text{ and } \tau_e = \frac{L}{3R_a} \tag{3.63}$$

Table 3.8 Table Parameter of BLDC Motor

Motor Parameter	Values
Per phase resistance (R)	1.2ohm
Per phase inductance (L)	0.56mH
Per mutual inductance (M)	0.00025Nm/rad/sec
Factious constant (B)	0.0005 kgm2
Moment of inertia (J)	0.00025 V.rad/sec
Number of poles(P)	4
Back-EMF constant (Ke)	0.352V.rad/sec
Torque constant(Kt)	0.701Nm/A
DC-bus voltage(Vdc)	12V

From the above table other remaining parameters are calculated as follows;

$$\tau_m = \frac{3JR_a}{k_e k_t} = 0.0171\text{s}$$

$$k_e = \frac{3RJ}{0.0171\text{s}k_t} = 0.0763\frac{\text{V}-\text{sec}}{\text{rad}}$$

$$\tau_e = \frac{L}{3R_a} = 0.0005556\text{s}$$

Then we get G(s) to be:

$$G(s) = \frac{\omega_m}{V_a} = \frac{\frac{1}{k_t}}{s^2\tau_e\tau_m + s\tau_m + 1} \tag{3.64}$$

$$= \frac{13.11}{0.00000266s^2 + 0.0171s + 1} = \frac{49228571.43}{s^2 + 6428.57s + 375939.85}$$

3.7 Controller Design

3.7.1 Adaptive Control

An adaptive control system can be broadly described as a control system that have the ability to customize the design of parameter controls such as online controls based on the input received. Adaptive controllers are also controllers with adjustable parameters and a mechanism for adjusting parameters. System adaptive control has two loops, one loop is normal feedback with process and the other loop is parameter adjustment. Adaptive control system is very beneficial to design control systems with improved performance and functionality.

3.7.2 Model Reference Adaptive Controller (MRAC)

Model reference adaptive control is one schemes of Adaptive control where the system output follows the reference model output. MRAC can considered as an adaptive servo system where the desired performance is expressed in the form of a reference model, which gives the desired response to the signal order. The following is the block diagram of the MRAC controller

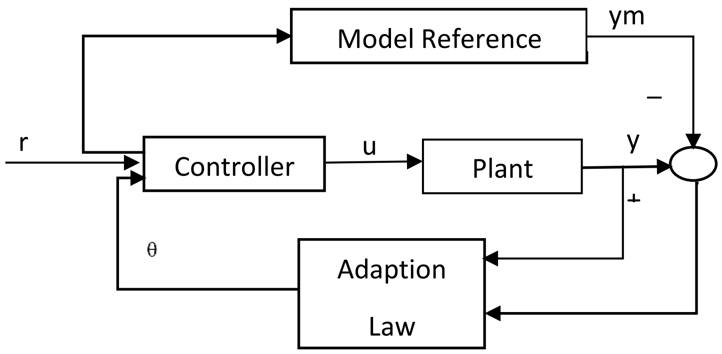

Figure 3.13 Model Reference Adaptive control of BLDC motor

Adjustment of a system parameters in MRAC can be obtained in two ways

- ❖ Gradient Method (MIT Rule)
- ❖ Lyapunov Stability Theory

3.7.2.1 Design of MRAC Controller with MIT Rule

The MIT Rule will be used to establish an adaptive parameter update mechanism on the controller. Furthermore, the equation for updating is referred to as a function Sensitivity derivative.

$$e = y - y_m \tag{3.65}$$

Cost function;

$$J(\theta) = \frac{1}{2}e^2 \tag{3.66}$$

Where θ a vector of controller parameter change the parameter is changes the parameter in the direction of negative gradient of the error square.

$$\frac{d\theta}{dt} = -\gamma\frac{\delta J}{\delta\theta} = -\gamma e\frac{\delta e}{\delta\theta} \tag{3.67}$$

$\frac{de}{d\theta}$ is called the sensitivity derivative .it indicates how error is influenced by the adjustable parameter θ.Then it is assumed that the controller has adaptive feedback (θ_1) and adaptive feedback (θ_2) . Next is to derive adaptive feedback (θ_1) and adaptive feedback (θ_2) to get. However, the input can be rewritten using both feedbacks, this feedback can be used to get equality.

Control law

Control output is obtained in terms of controller gain;

$$U = \theta_1 r - \theta_2 y \qquad (3.68)$$

Plant output in terms of controller output;

$$y = G(s)U = G(s)[\theta_1 r - \theta_2 y] \qquad (3.69)$$

$$= \frac{49228571.43}{s^2 + 6428.57s + 375939.85}(\theta_1 r - \theta_2 y)$$

$$= \frac{49228571.43\theta_1}{s^2 + 6428.57s + 375939.85 + 49228571.43\theta_2} r$$

From the controller is obtained;

$$U = (1 - \frac{49228571.43}{s^2 + 6428.57s + 375939.85 + 49228571.43\theta_2})\theta_1 r$$

Adaption law

$$e = y - y_m = \frac{49228571.43}{s^2 + 6428.57s + 375939.85 + 49228571.43\theta_2}\theta_1 r - G_m(s)r$$

$$\frac{\delta e}{\delta \theta 1} = \frac{49228571.43\theta_1 r}{s^2 + 6428.57s + 375939.85 + 49228571.43\theta_2}$$

$$\frac{\delta e}{\delta\theta_2} = -\frac{(49228571.43)^2\theta_1 r}{(s^2+6428.57s+375939.85+49228571.43\theta_2)^2}$$

$$= -\frac{(49228571.43)^2 y}{(s^2+6428.57s+375939.85+49228571.43\theta_2)^2}$$

The sensitivity derivative obtained contains the parameters of the plant. If the model is close to the actual plant, the model characteristics can be adjusted to the plant characteristics, thus giving a sensitivity derivative as follows:

$$s^2+6428.57s+375939.85+49228571.43\theta_2 \approx s^2+a_{1m}+s+a_{0m}$$

$$\frac{\delta e}{\delta\theta 1} = \frac{a_{1m}s+a_{0m}}{s^2+a_{1m}s+a_{0m}} r \tag{3.70}$$

$$\frac{\delta e}{\delta\theta 2} = \frac{a_{1m}s+a_{0m}}{s^2+a_{1m}s+a_{0m}} y \tag{3.71}$$

Next is to implement MIT Rule, the update parameter rules for each are derived. So for filtering the error values and become:

$$\frac{d\theta_1}{dt} = -\gamma\frac{\delta e}{\delta\theta 1}e = -\gamma\left(\frac{a_{1m}s+a_{0m}}{s^2+a_{1m}s+a_{0m}}\right)re \tag{3.72}$$

$$\frac{d\theta_2}{dt} = -\gamma\frac{\delta e}{\delta\theta_2}e = -\gamma\left(\frac{a_{1m}s+a_{0m}}{s^2+a_{1m}s+a_{0m}}\right)ye \tag{3.73}$$

The reference model used follows the equation:

$$G_m(s) = \frac{\omega_n^2}{s^2+2\zeta\omega_n+\omega_n} \tag{3.74}$$

The design of the reference model is with ζ = 1, and t_s = 0.03, obtained ω_n = 133.33 which is based on the 2% criterion for the setting time value, then the transfer function of the reference model becomes:

$$G_m(s) = \frac{\omega_n^2}{s^2+2\zeta\omega_n+\omega_n} = \frac{17776.88}{s^2+266.66s+17776.88}$$

$$\frac{a_{1m}s + a_{m0}}{s^2 + a_{1m}s + a_{m0}} = \frac{17776.88}{s^2 + 266.66s + 17776.88}$$

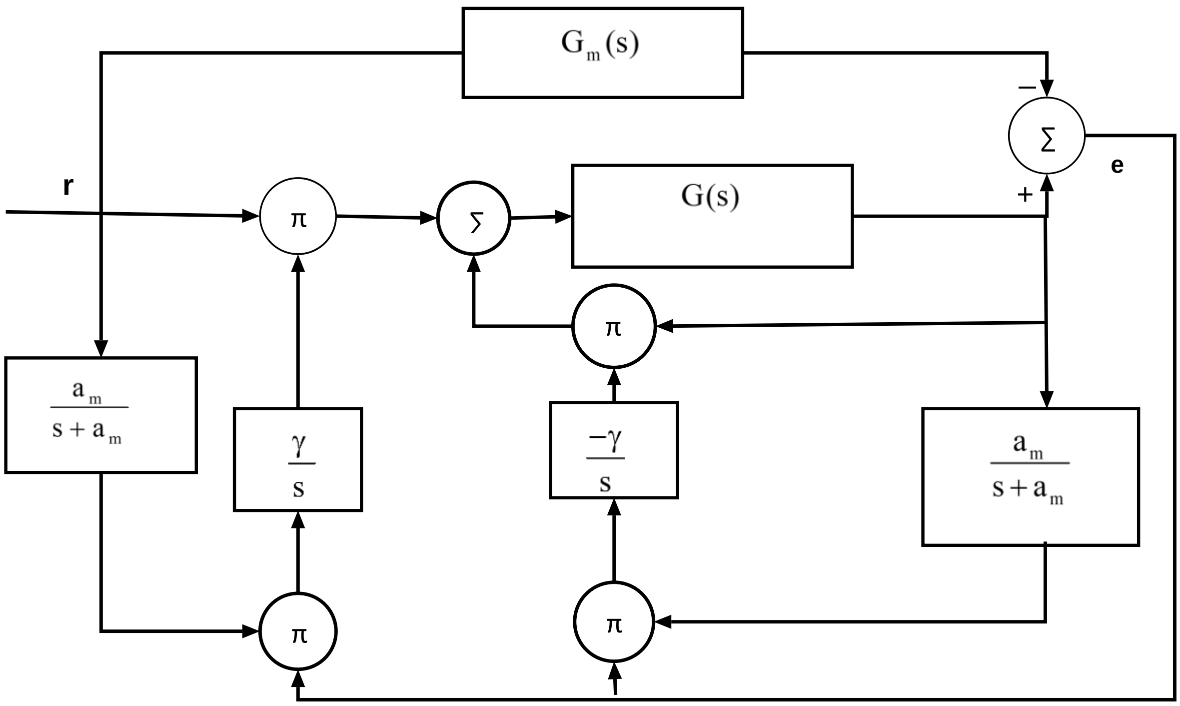

Figure 3.14 Design of MRAC-MIT controller

3.7.2.2 Design of MRAC Controller with Lyapunov Stability Theory

The lyapunov stability method is an important class of adaptive control. This method attempts to find the lyapunov function and an adaption mechanism in such away the error between plant and model goes to zero.

By considering second order BLDC motor model

$$\frac{d^2y}{dt^2} = -a\frac{dy}{dt} + bU \tag{3.75}$$

And second order Reference Model

$$\frac{d^2y_m}{dt^2} = -a_m\frac{dy}{dt} + b_m r \tag{3.76}$$

Control law

Let control input;

$$U = \theta_1 r - \theta_2\frac{dy}{dt} \tag{3.77}$$

Tracking error;

$$e = y - y_m \tag{3.78}$$

By substituting equation 3.75and 3.76 into equation 3.78

$$\frac{d^2e}{dt^2} = \frac{d^2y}{dt^2} - \frac{d^2y_m}{dt^2} = -a\frac{dy}{dt} + bU - (-a_m\frac{dy}{dt} + b_m r) \tag{3.79}$$

Replacing in equation 3.77 into equation 3.79

$$\frac{d^2e}{dt^2} = -a\frac{dy}{dt} + b(\theta_1 r - \theta_2\frac{dy}{dt}) - (-a_m\frac{dy}{dt} + b_m r) \tag{3.80}$$

By adding and deducting with equation 3.80

$$\frac{d^2e}{dt^2} = -a\frac{dy}{dt} + a_m\frac{dy}{dt} + b\theta_2\frac{dy}{dt} - a_m\frac{dy}{dt} + a_m\frac{dy_m}{dt} + b\theta_1 r - b_m r \tag{3.81}$$

Taking the same terms in one place

$$\frac{d^2e}{dt^2} = -a_m(\frac{dy}{dt} - \frac{dy_m}{dt}) + (-a + a_m + b\theta_2)\frac{dy}{dt} + b\theta_1 r - b_m r) \tag{3.82}$$

Finally equation 3.82 becomes;

$$\frac{d^2e}{dt^2} = -a_m\frac{de}{dt} - (a - a_m - b\theta_2)\frac{dy}{dt} + (b\theta_1 - b_m)r \tag{3.83}$$

By integrating equation 3.83;

$$\frac{de}{dt} = -a_m e - (b\theta_2 - a_m + a)y + (b\theta_1 - b_m)r \tag{3.84}$$

From error dynamic it is observed that the tracking error will go to zero. If

$$b\theta_2 = a_m - a \tag{3.85}$$

$$b\theta_1 = b_m \tag{3.86}$$

Let the lyapunov function for the error dynamic

$$v(e,\theta_1,\theta_2) = \frac{1}{2}\left\{e^2 + \frac{1}{b\gamma}(b\theta_2 + a - a_m)^2 + \frac{1}{b\gamma}(b\theta_1 - b_m)^2\right\} \tag{3.87}$$

Where $b\gamma > 0$

$$v(e,\theta_1,\theta_2) = \frac{1}{2}e^2 + \frac{(b\theta_2 + a - a_m)^2}{2b\gamma} + \frac{(b\theta_1 - b_m)^2}{2b\gamma} \tag{3.88}$$

This function is zero when e is zero and the controller parameter are equal to the correct values .for valid lyapunov function time derivative of lyapunov function must be Negative.

This derivative is given by e

$$\frac{dv(e,\theta_1,\theta_2)}{dt} = e\frac{de}{dt} + \frac{1}{\gamma}(b\theta_2 + a - a_m)\frac{d\theta_2}{dt} + \frac{1}{\gamma}(b\theta_1 - b_m)\frac{d\theta_1}{dt} \qquad (3.89)$$

Substituting the value of $\frac{de}{dt}$ from equation 3.87 in to equation 3.89

$$\frac{dv(e,\theta_1,\theta_2)}{dt} = -a_m e^2 - (b\theta_2 - a_m + a)y + (b\theta_1 - b_m)r + \frac{1}{\gamma}(b\theta_2 + a - a_m)\frac{d\theta_2}{dt} + \frac{1}{\gamma}(b\theta_1 - b_m)\frac{d\theta_1}{dt} \qquad (3.90)$$

$$= -a_m e^2 + \frac{1}{\gamma}(b\theta_2 - a_m + a)(\frac{d\theta_2}{dt} - \gamma ye) + \frac{1}{\gamma}(b\theta_1 - b_m)(\frac{d\theta_1}{dt} + \gamma re) \qquad (3.91)$$

If the parameter are updates as follows

$$\frac{d\theta_1}{dt} = -\gamma re \qquad (3.92)$$

$$\frac{d\theta_2}{dt} = -\gamma ye \qquad (3.93)$$

$$\theta_1 = \frac{-\gamma re}{s} \qquad (3.94)$$

$$\theta_2 = \frac{-\gamma ye}{s} \qquad (3.95)$$

θ_1 and θ_2 are the control parameter with adjustable gain γ and the block diagram of lyapunov rule is shown in the figure below.

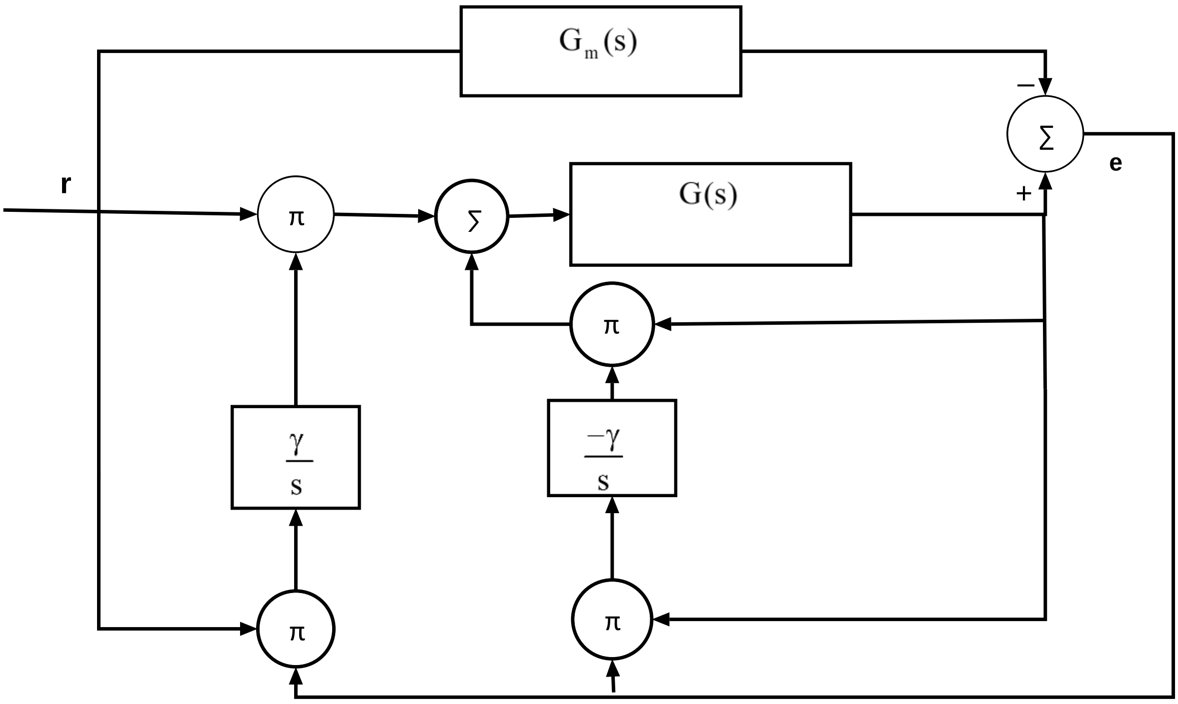

Figure 3.15 Design of MRAC Controller with Lyapunov Stability

3.7.2.3 PID (Proportional Integral Derivative)

A PID controller (Proportional, Integral, and Derivative) is a controller that can enhance the level of precision of a plant system that has feedback characteristics. The PID controller calculates and minimizes the error value, or difference between the process output and the input/set point given to the system. The PID controller is made up of three components: proportional, integral, and derivative, which can be employed together or separately depending on the intended response to a system or plant. Each component is explained below.

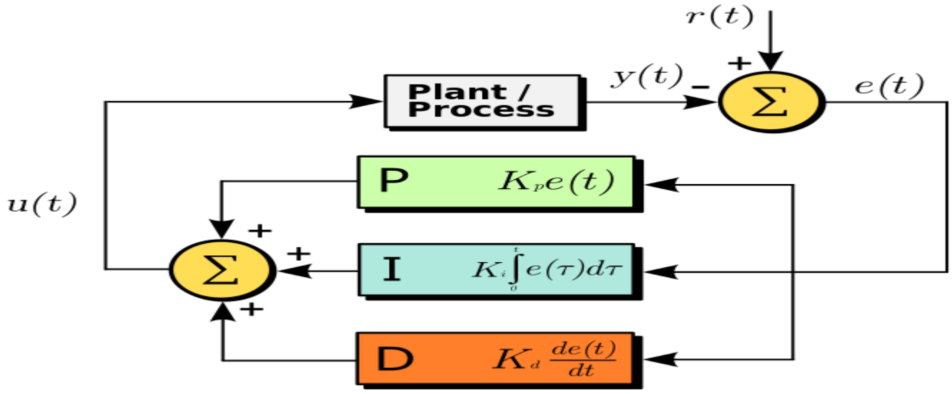

Figure 3.16 Schematic of PID

The proportional/gain controller acts as an amplifier, changing the output of the system proportionally without having any dynamic effect on the controller's performance. The proportional controller's response can be expressed as equality.

$$P_{out} = K_c E(t) \quad (3.96)$$

Where: P_{out} = output of proportional controller

K_c = constant gain

E (t) = error expressed in continuous time

On-off control often causes oscillations is that the system overreacts because a small change in error will create manipulated variables change over the full range. This effect is avoided in proportional controls where controller characteristics are proportional to the control error for small errors.

This control is characterized by a nonlinear function. Control characteristics proportional must give the limits and of the control variables. Linear range can be determined either by giving a range over which the characteristic is linear. This range is usually centered on the set point.

Integral Controller; An integral/reset controller is a controller that functions to repair the system's steady state response in order to minimize system errors. The integral controller's response can be expressed mathematically.

$$I_{out} = K_i \int_0^t E(\tau)d\tau \tag{3.97}$$

Where: I_{out} = integral controller output

K_i = integral constant

$E(\tau)$ = error expressed continuously

τ = integral variable

The integral action's primary function is to ensure that the process outputs match a stable set point. When using proportional control, the control error is usually constant. With integral action, a small positive error will always result in an increase in the control signal, while a small negative error will always result in a decrease in the control signal, regardless of how small the error is.

Derivative Controller; A derivative/rate controller is a controller whose primary function is to improve the system's transient response. The response of a derivative controller can be expressed as follows:

$$D_{out} = K_d \frac{d}{dt} E(t) \tag{3.98}$$

Where; D_{out} = derivative controller output

K_d = derivative constant

E (t) = error expressed in continuous time

The derivative action's goal is to improve closed-loop stability. Because of the process dynamics, it will take a long time for changes in the control variables to be visible in the process output. As a result, the control system will be slow to correct errors.

Proportional Integral Derivative (PID); PID is a controller which consists of a combination of three basic control actions namely Proportional, Integral and Derivative.

The general form of PID control is as follows:

$$U(t) = K_p e(t) + K_i \int_0^t e(t) + K_d \frac{de}{dt} \tag{3.99}$$

$$e(t) = r(t) - y(t) \tag{3.100}$$

Where u (t) represents the control signal, y (t) represents the output signal, r(t) represents the reference signal, and e(t) represents the error signal. The coefficients K_p, K_I, and K_d in the equation represent proportional, integral, and derivative constants, respectively. Equation 3.99 is transformed into Laplace form to yield:

$$\frac{U(s)}{E(s)} = K_p + \frac{K_I}{s} + K_d s \tag{3.101}$$

If the applied reference signal is to follow the output signal, the controller gain values must be adjusted. K_p, K_I, and K_d values must be found tuning appropriately. PID coefficients can be found using the closed loop. The PID controller can be built using the Ziegler-Nichols approach, the relay feedback method, or another method by modifying the root locus curve to achieve acceptable performance. In this study, the constraints PID parameters were used (ÇAKAR et al., 2020).

3.7.2.4 Controller Design of MRAC-PID

Because motor inductance is very low, the order of the speed dependent transfer function of the motor can be considered second order in order to simplify controller design (ÇAKAR et al., 2020) . a_0, a_1, a_2 And b_0 are constants in the equation from equation 3.64

$$G(s) = \frac{y(s)}{u(s)} = \frac{b_0}{a_2 s^2 + a_1 s + a_0} \tag{3.102}$$

$$= \frac{13.11}{0.00000266 s^2 + 0.0171 s + 1}$$

Transfer function of reference model as stated;

$$G_m(s) = \frac{\omega_n^2}{s^2 + 2\zeta\omega_n + \omega_n} \tag{3.103}$$

Control law

Control output is obtained in terms of controller gain;

$$U(t) = K_p e(t) + K_i \int_0^t e(t)dt + K_d \frac{dy(t)}{d(t)} \tag{3.104}$$

Where y is the plant output; and (t) = (t) - (t), with (t) as the input of the reference model.

The representation of Laplace transform of equation 3.104 is listed as

$$U(s) = K_P E(s) + \frac{1}{s} K_i E(s) - sK_d Y(s) \tag{3.105}$$

The output (s) of the motor can be found as follows:

$$G(s)U(s) \tag{3.106}$$

Substitute equation 3.105 in to 3.106

$$G(s)[K_P E(s) + \frac{1}{s} K_i E(s) - sK_d Y(s)] \tag{3.107}$$

The closed loop system is;

$$G(s)E(s)[K_P + \frac{1}{s} K_i) - sK_d G(s)Y(s)] \tag{3.108}$$

Error can be stated as followed

$$E(s) = R(s) - Y(s) \tag{3.109}$$

Then substitute in terms of E(s) in to equation 3.109

$$G(s)(R(s) - Y(s)[K_P + \frac{1}{s} K_i) - sK_d G(s)Y(s)] \tag{3.110}$$

By arranging equation 3.110

$$Y(s) = \frac{[sK_p G(s) + K_i G(s)]R_{in}(s)}{s^2 K_d G(s) + (1 + K_p G(s))s + K_i G(s)} \tag{3.111}$$

PID coefficients are unknown. It is necessary to determine them in such a way that the PID controller exhibits adaptive behavior in response to variations in the parameters of the process to be controlled. The PID controller is then designed in the time domain. Because of this, equation (3.112) can be written as in the time domain. The model parameters vary at every moment of time and the adaptive controller must change its parameters also at every moment of time. A differential operator is used to convert equation (3.103) to the time domain equation (3.112) Represents the cost function from equation (3.66).

The representation of Equation 3.112 in the time domain is:

$$y(t)=\frac{[pK_p g(t)+K_i g(t)]r(t)}{p^2K_d g(t)+(1+K_p g(t))p+K_i g(t)} \tag{3.113}$$

Where p; is a differential operator

The tracking error of the closed-loop system and the reference model is

(3.114)

$$E(t)=y(t)-y_m(t) \tag{3.115}$$

Substitute equation 3.103 in to 3.114 and 3.115

$$E(t)=\frac{[pK_p g(t)+K_i g(t)]r(t)}{p^2K_d g(t)+(1+K_p g(t))p+K_i g(t)}-\frac{\omega_n{}^2}{p^2+2\xi\omega_n p+\omega_n{}^2} \tag{3.116}$$

E (t) is the error between the transition behavior of the closed-loop system and the reference model. The criterion for compensating in equation (3.102) is given by equation(3.117).

The expressions of the sensitivity functions of the closed-loop system error towards the controller parameters are derived by differentiating equation(3.118). These expressions are defined as follows:

$$\frac{dE(t)}{dK_P}=\frac{g(t)e(t)p}{K_d g(t)p^2+(1+K_p g(t))p+K_i g(t)} \tag{3.119}$$

$$\frac{dE(t)}{dK_i}=\frac{g(t)e(t)p}{K_d g(t)p^2+(1+K_p g(t))p+K_i g(t)} \tag{3.120}$$

$$\frac{dE(t)}{dK_d}=\frac{g(t)e(t)p^2}{K_d g(t)p^2+(1+K_p g(t))p+K_i g(t)} \tag{3.121}$$

To make sure that there is a perfect tracking error, let assume that, the time behavior of the process is equal to the time behavior of the reference model, as follows:

$$\frac{g(t)}{K_d g(t)p^2+(1+K_p g(t))p+K_i g(t)}=\frac{\omega_n{}^2}{p^2+2\xi\omega_n p+\omega_n{}^2} \tag{3.122}$$

The gradient method described in equation (3.104) is applied to find the expressions of the control parameters:

$$\frac{dK_p}{dt}=(-\gamma_p)E(t)[\frac{\omega_n{}^2}{p^2+2\xi\omega_n p+\omega_n{}^2}]e(t) \tag{3.123}$$

$$\frac{dK_i}{dt} = (-\gamma_i)E(t)[\frac{\omega_n^2}{p^2 + 2\xi\omega_n p + \omega_n^2}]e(t) \tag{3.124}$$

$$\frac{dK_d}{dt} = (\gamma_d)E(t)[\frac{\omega_n^2}{p^2 + 2\xi\omega_n p + \omega_n^2}]y(t) \tag{3.125}$$

Where; γ_p, γ_i and γ_d are adaption gain

Generally PID controller is stated as follows

$$\begin{aligned} u(t) = (-\gamma_p)E(t)[\frac{\omega_n^2}{p^2 + 2\xi\omega_n p + \omega_n^2}]e(t) + (-\gamma_i)E(t)[\frac{\omega_n^2}{p^2 + 2\xi\omega_n p + \omega_n^2}]e(t) \\ +(\gamma_d)E(t)[\frac{\omega_n^2}{p^2 + 2\xi\omega_n p + \omega_n^2}]y(t) \end{aligned} \tag{3.126}$$

3.7.2.4 Model Reference controller with Neural Network (MRAC-NN)

Brushless DC (BLDC) motor control systems are made up of a multi-variable, non-linear, strong-coupling system that is used to provide robust and adaptive capabilities. The popularity of emerging intelligent BLDC motor controllers has skyrocketed. Neural Network-based control method in which the available data is the result of measuring the system's dynamic behavior. This capability is well suited for use in adaptive control systems where the controller must adapt due to changes in system behavior. The inverse model of BLDC motor speed was built using NN. This model was then used as a controller. The MRAC concept was used to develop control schemes with good dynamic responses. (Sanguesa et al., 2021)(Priti, 2016)

Several measurements of the MRAC speed controller gains were used to train the networks in order to train and validate Neural Network. The current work employs a four-layer feed forward back propagation NN. As shown in Figure 3.16, the input, two hidden, and output layers each have three (3, 6), four, and one neuron, respectively. The number of neurons in the hidden layer is an essential component of network architecture. The hidden layer has no direct interaction with the outside world (Premkumar & Manikandan, 2015). This layer has a significant impact on the final output, and the number of neurons in this layer must be sufficient.

The NN architecture input is chosen from adaptation gain and the summation of adaptation gains, using the forward selection method to find the best network architecture. The Sigmoid function is used as an activation function to design and establish network behavior. A sigmoid transfer function can be used to introduce nonlinearity into a model and/or to ensure that certain signals stay within a certain range. The final neural network structure used in this work is depicted in Figure 3.17.

The input of neural network are expressed as follows

From equation (3.94)

$$\theta_1(t) = -\gamma r \int_0^t e(t)dt \tag{3.127}$$

$$\theta_2(t) = \gamma y \int_0^t e(t)dt \tag{3.128}$$

The third input is the summation of two adaption gain of the MRAC in the case of lypounov stability rule.

- The procedure to create and train a network using the toolbox is as follow:
- Inputs (two adaption gain and the summation of adaption gain) and target vectors are generated and loaded to the workspace in MATLAB.
- A four layer feed forward back propagation network created in the MATLAB/script
- Trainlim and Tansig were chosen as training and transfer function, respectively.
- Input and target vectors were introduced to the created network.
- Training parameters such as the epochs and error goal were adjusted.
- The specified network was trained gradually. This process is finished when the defined error was reached. During the training, weights and biases of the network were iteratively adjusted to minimize the network performance function.
- Finally, after training the network, the Simulink block is generated.

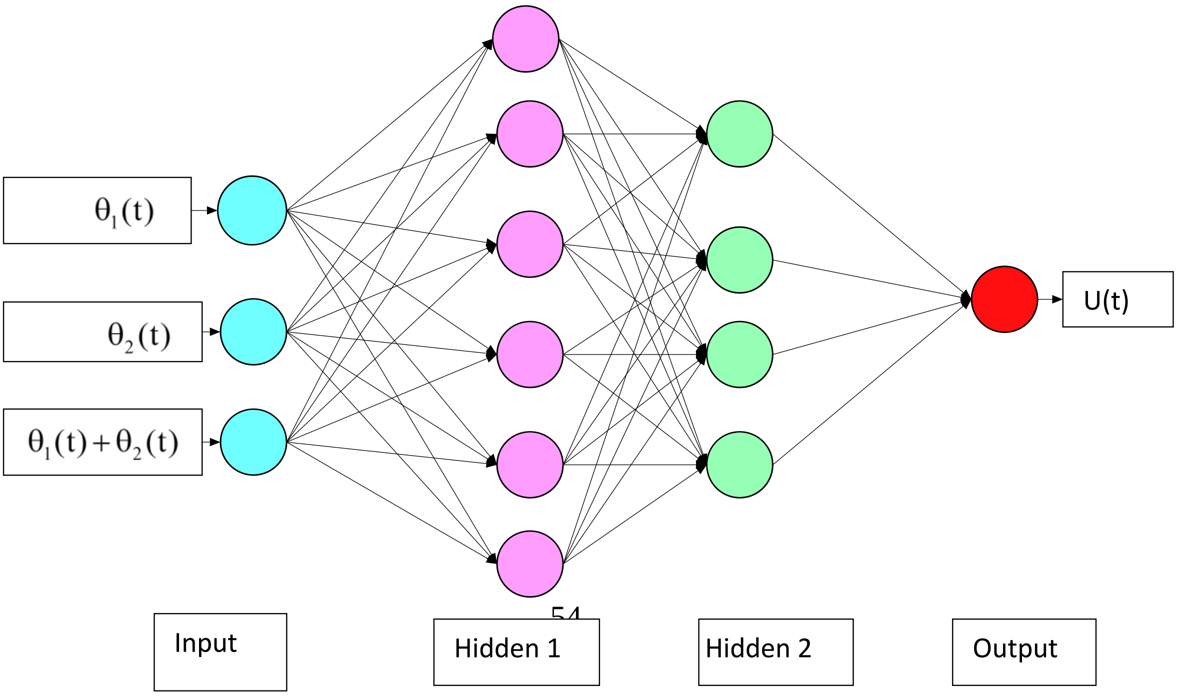

Figure 3.17 Neural network structure used in this thesis

Where the idea of U(t) (control signal) is taken from Equations (3.77) of MRAC-lypounov stability

$$U(t) = \theta_1(t)r(t) - \theta_2(t)\frac{dy}{dt} \qquad (3.129)$$

Figure 3.18 depicts the flowchart of the neural network training of the proposed neural network structure in the speed control system of the BLDC motor.

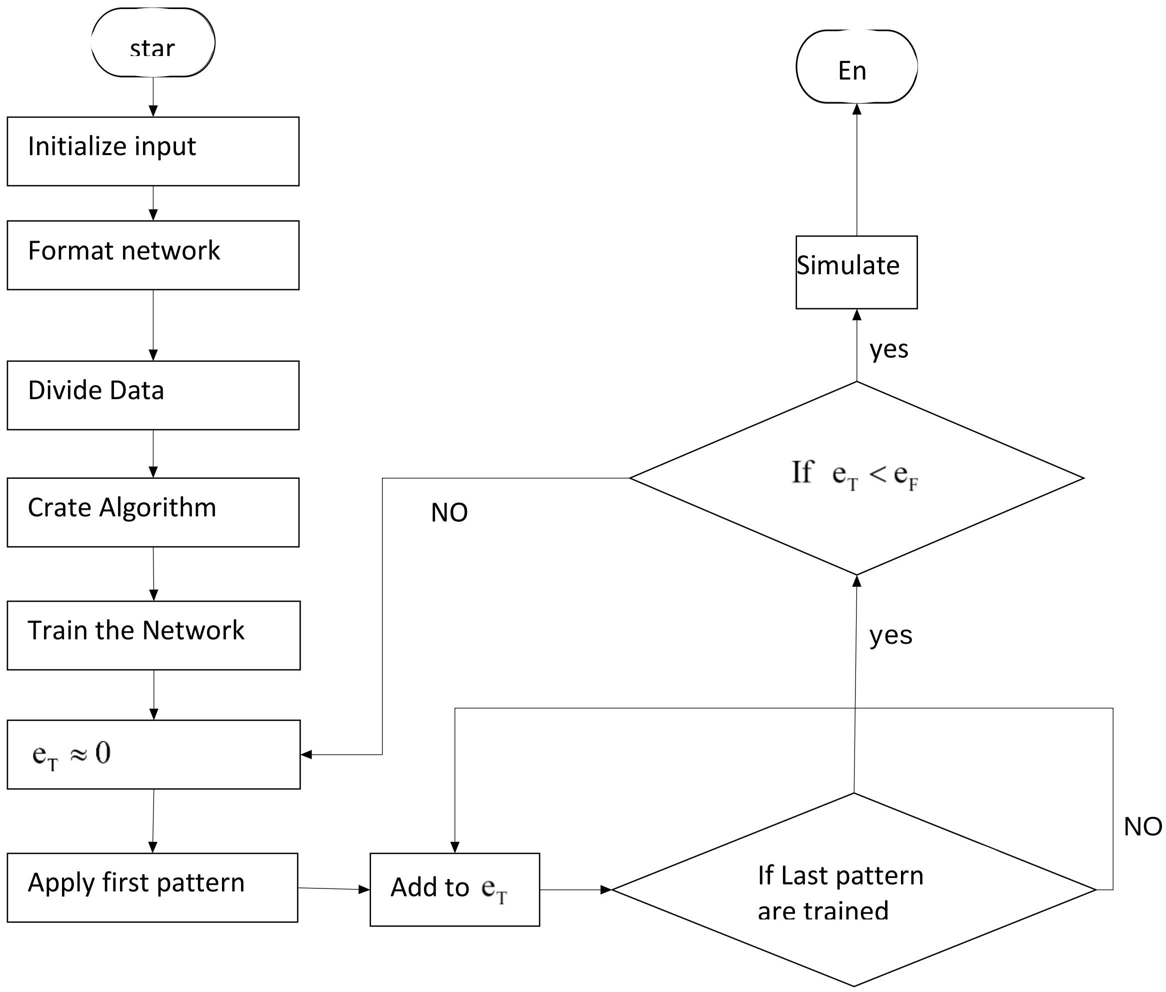

Figure 3.18 Artificial Neural Network Flowchart

The input and output data are generated from Model Reference Adaptive control (MRAC) –in the case of lypounov stability based result Simulink implementation as shown in Figure 3.19.

After the simulation time is completed, the data are transferred from Simulink to the workspace in the form of vectors.

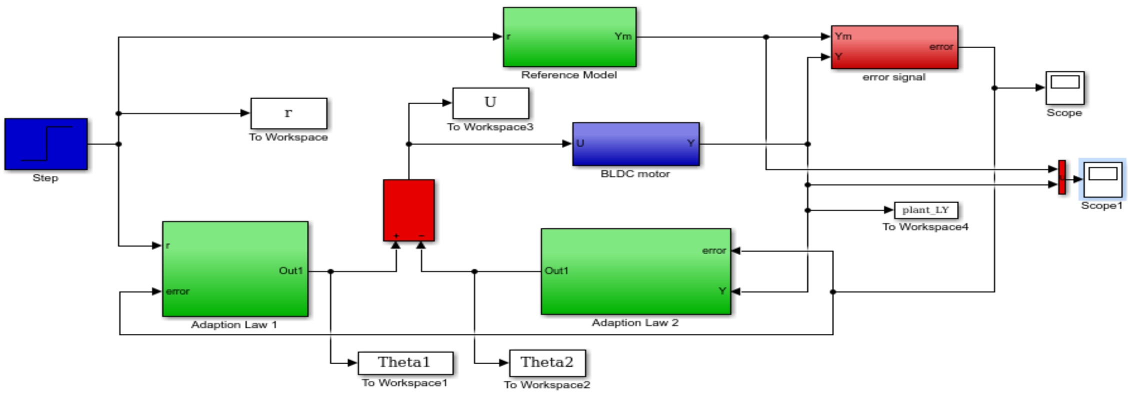

Figure 3.19 Generating the input and output data from MRAC-Lypounov control system

Below the MATLAB/code is the sample code for the neural network used in this thesis. The Levenberg-Marquardt backpropagation is used to train the network and Tansig is the default transfer (activation) function of the network. The network has three input parameters and one output parameter as described above. Each input and one output have 10000 data. After several trainings of the network based on trial and error, the number of hidden layers and their neurons are selected based on the performance evaluation toolbox results.

```
I=[r,Theta1,Theta2]';
T=[U]';
net=newff(minmax(I),[1,6,1],{'tansig','tansig','purelin'},'trainlm');
net=init(net);
net.trainParam.show=1;
net.trainParam.lr=0.06;
net.trainParam.mc=0.075;
net.trainParam.epochs=100000;
net.trainParam.goal=1e-12;
net=train(net,I,T);
%To generate the NN on Simulink block gensim(net,-1)
```

After executing the above code, several performance measurements of the trained network are available. The Figure 3.20 depicts the validation of the mean squared error and its value. At the training epoch of 413 the mean squared error is $5.2703x10^{11}$.

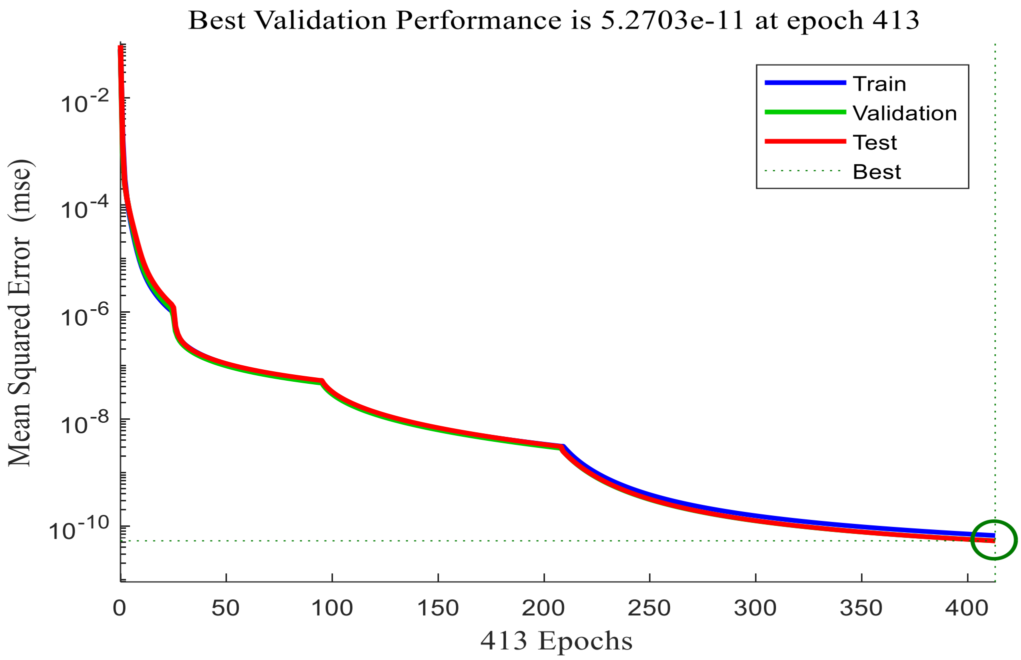

Figure 3.20 Validation of the mean squared error

The training state plots shows the gradient descent is a combination of two words the 'gradient', which means a slope and the 'descent', which means to incline. Therefore, with gradient descent, the slope of gradients is descended to find the lowest point with the smallest error. It is an iterative process until the correction of the error in the NN learning model. The following figure 3.21 shows the training state.

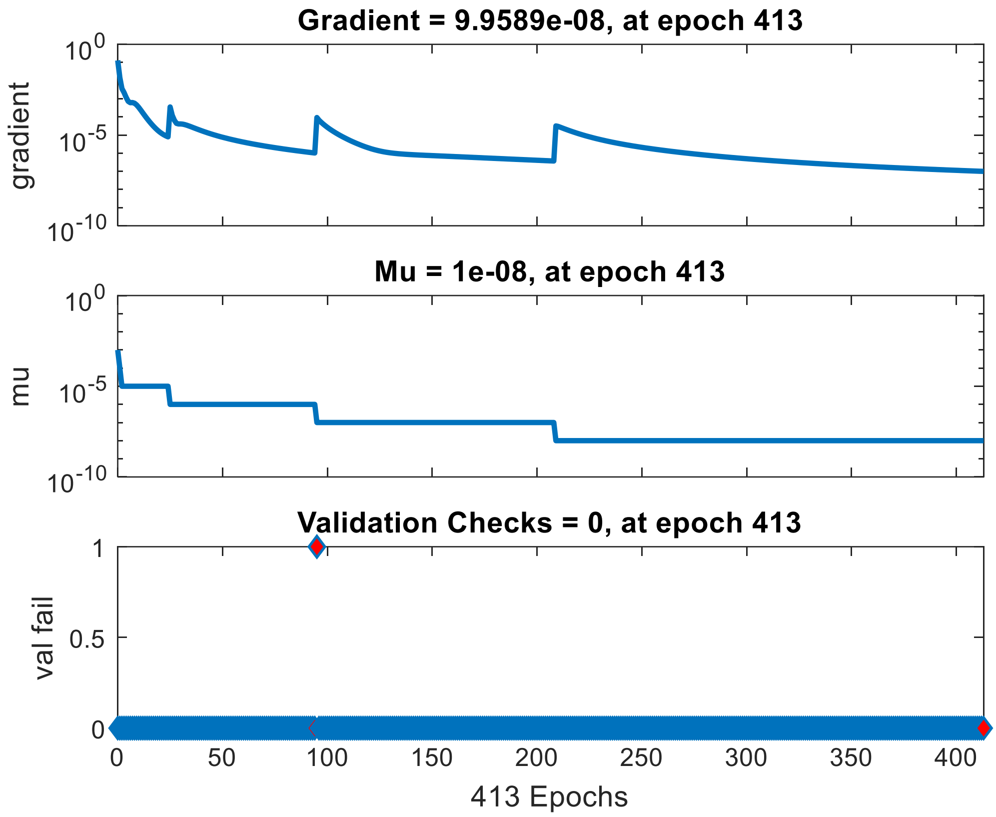

Figure 3.21 Training state of gradient and validation check of neural network structure

The other most important in neural network train tools is error histogram graphs. This future shows the error must going to zero.by subtracting the output from targets. Figure 3.22 shows the error histogram.

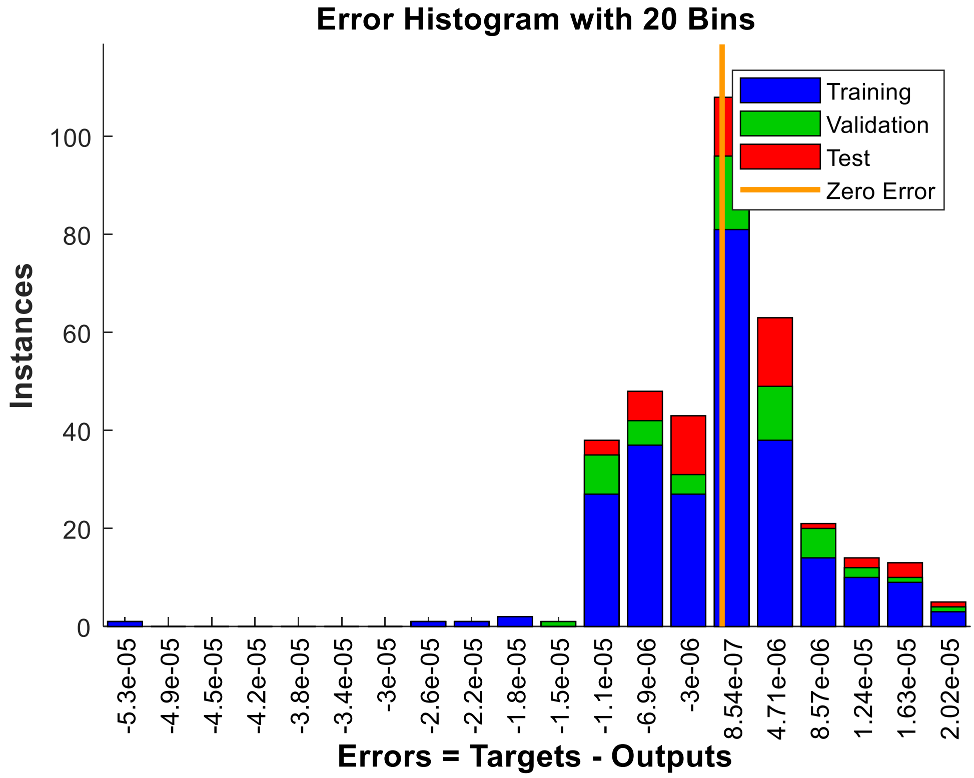

Figure 3.22 Error Histogram of neural network structure

The regression plots also display the network outputs with respect to targets for training, validation, and test sets as shown below in Figure 3.23. For a perfect fit, the data should fall along a 45-degree line, where the network outputs are equal to the targets. In this work, the neural network has been retrained many times to have the perfect fit for its output and target. This is done by changing the hidden layers and their neurons. This change updates every time the weights and biases of the network, and it produce an improved network after retraining. For this work, the fit is perfect for all data sets, with R values in each case is 1.

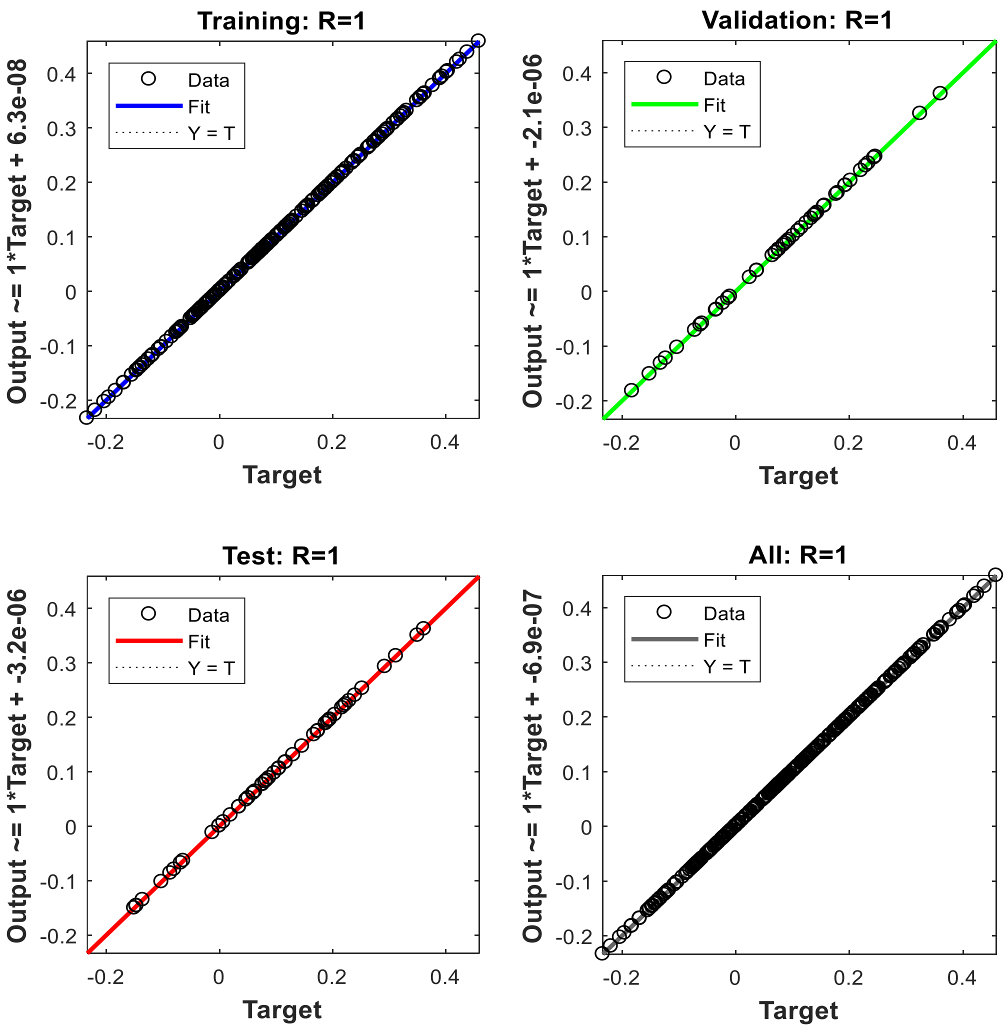

Figure 3.23 Regression plots of the training, validation, and test sets

After training of the network, the following Simulink block in Figure 3.24 is generated. It includes the input and output of trained data, the structure of the network, the weights, and the biases of each layer and neurons.

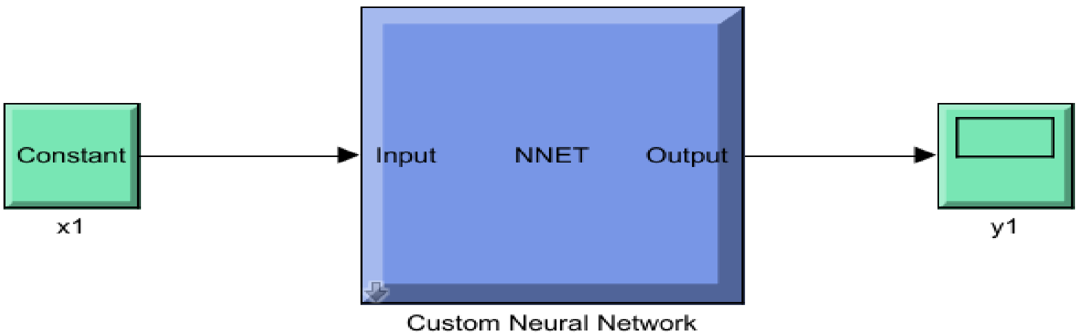

Figure 3.24 The Simulink block of the trained neural network structure

CHAPTER FOUR

4. RESULTS AND DISCUSSION

The simulation results explained in this chapter is performed for the same values the system parameters under study. First simulation result for BLDC without any controller i.e. open loop response is presented. Then the simulation result of BLDC motor with controller such that Model Reference Adaptive Controller (MRAC) using Gradient Method (MIT Rule), Model Reference Adaptive Controller (MRAC) using Lyapunov Stability Theory, Model Reference Adaptive Controller (MRAC) with Proportional Integral Derivative (PID) and Model Reference Adaptive Controller (MRAC) with Neural Network are respectively presented. At the end of this chapter the performance of the above mentioned controller are compared with each other and the best controller is selected for BLDC motor.

4.1 Open-loop Response for BLDC Motor

The open loop response for the system BLDC motor is shown on figure 4.1 demonstrates the open loop response of BLDC motor drive system model. The reference input for open loop is 3000rpm.

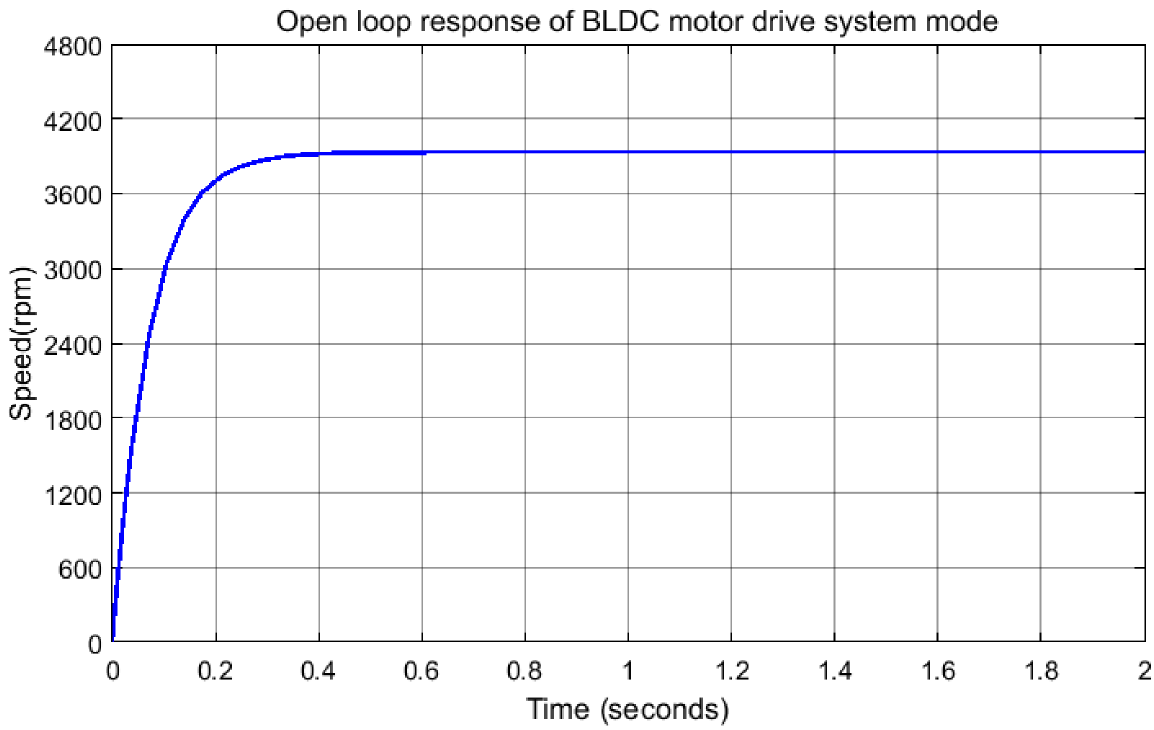

Figure 4.1 Open loop response of BLDC motor drive system mode

From figure 4.1 the error between the reference and the output cannot be reflected in determining its control input. Figure 4.2 is shows the reference speed input for open loop BLDC motor. The error between open loop output and input is very large.to minimize this error we must use controller.

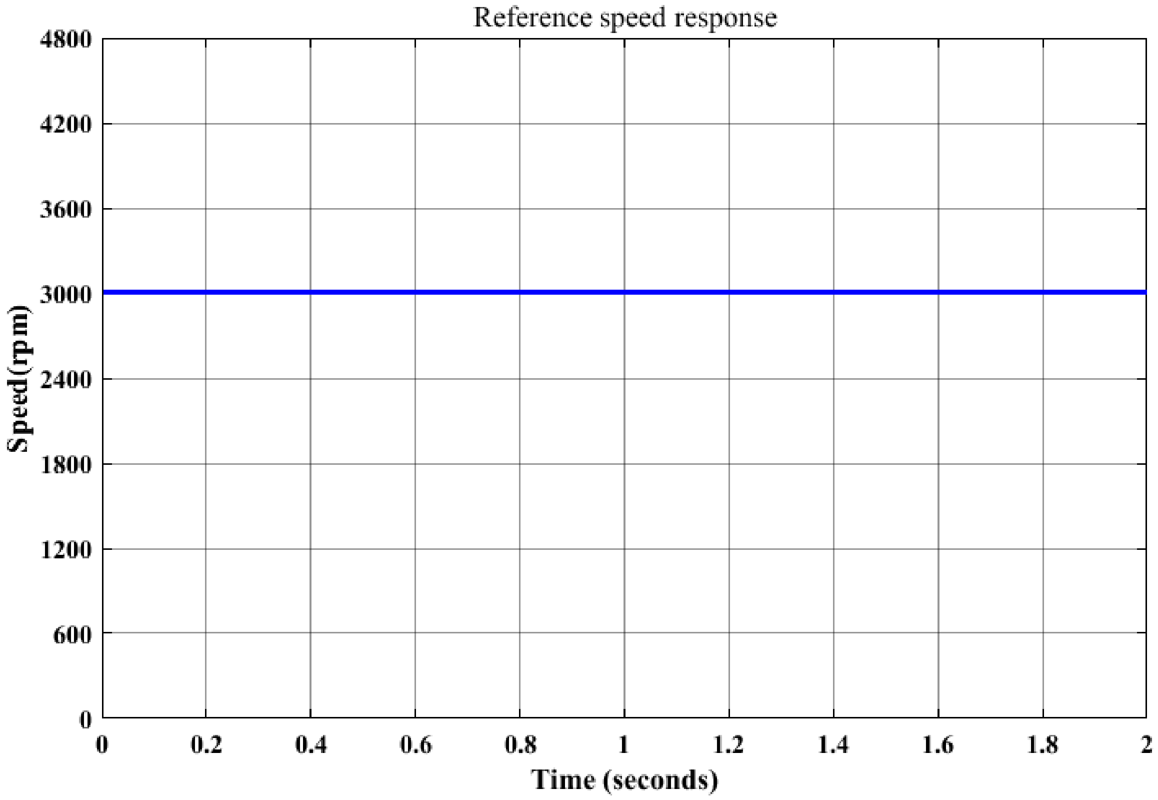

Figure 4.2 the corresponding Reference speed

4.2 Simulation Result of Model Reference

Model Reference is used to give an idyllic response of the adaptive control system to the reference input.In the control Design part of this thesis the suitable reference model for the closed loop system dynamics was selected and then a control law for the plant for achieve the primary control objective such as tracking the reference input. Reference model must be linear and stable. The performance of model reference response is shown in Figure 4.3. From open loop speed simulated result shows in Figure 4.3 the rising time is short and acceptable which is 0.0257sec, settling time is 0.0438 and the overshoot of the response is very closed to zero which is 0.0363%.from this transient response the the selected performance of model reference is best.

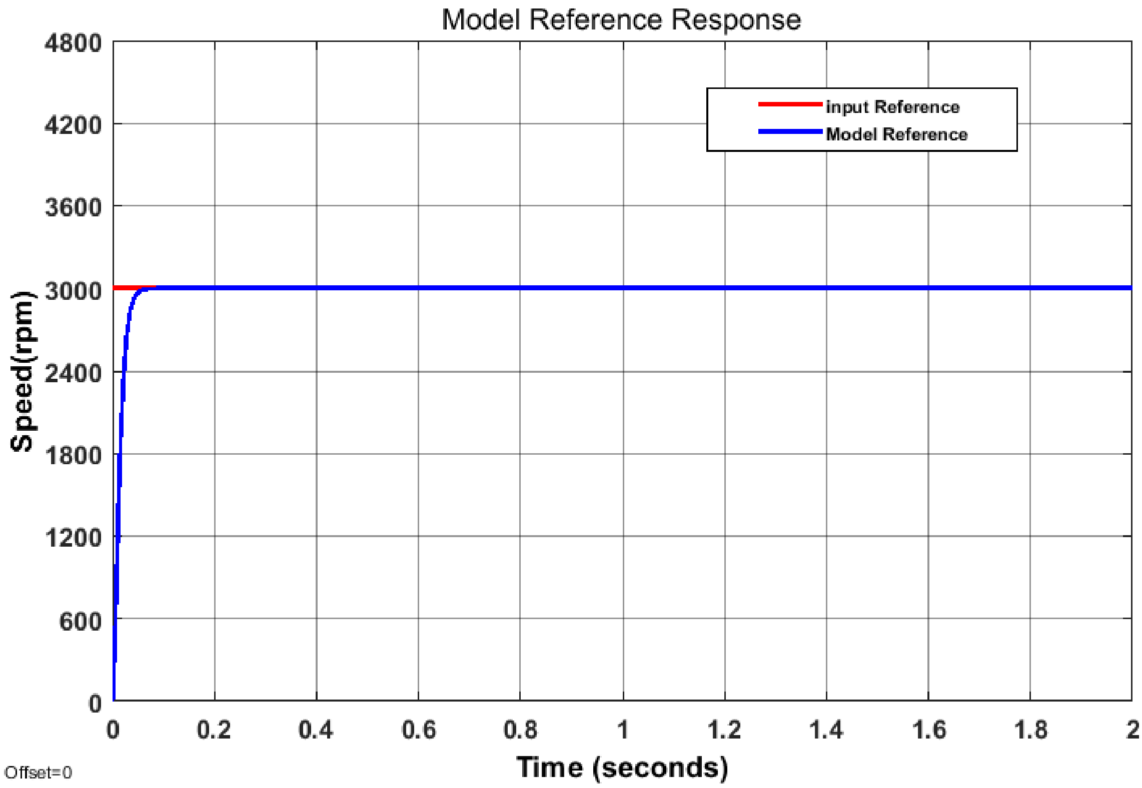

Figure 4.3 the corresponding phase current of BLDC motor mode

4.3 Simulation Results using MRAC by MIT Rule

This method is the original method developed for adaptive control design before other methods. In the simulation of the MRAC-MIT controller, the output of the closed-loop system to follow the output of the reference model. Therefore, the main aim is to minimize the error. By designing a controller that has two adjustable parameters such that a certain cost function is minimized. The MRAC gradient approach adaptive controller gain design is then simulated again using MATLAB Simulink. Both the output of the system responses are shown in Figure 4.5. From closed loop speed simulated result shows in Figure 4.3 the rising time is short and acceptable which is 0.0203 sec,settling time is 0.2415 sec and the overshoot of the response is not good which is 59.4499%. So from MRAC with MIT rule the controller result from above is satisfactory and the settling time is not bad. The only drawbacks of the controller are the overshoot intransient point or time for problem must be solved in next controller three method of using MRAC controller with different technique.

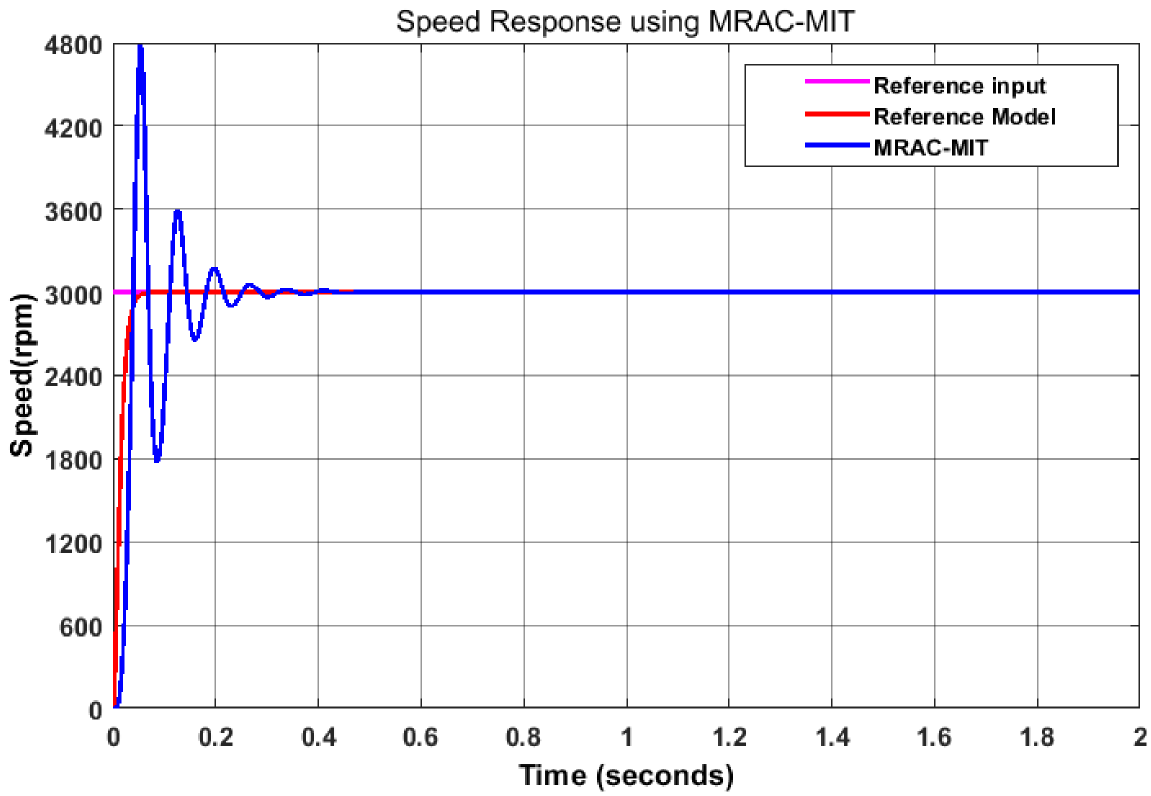

Figure 4.4 BLDC Motor Speed Response using MRAC-MIT

On the other hand Model reference controller the output response for plant is not perfectly follows the reference model. It can be said that the system is a perfect model following system, such that the error should be go to zero. The adaptive controller gain is again simulated but this time with gamma γ values of 20 and -20.

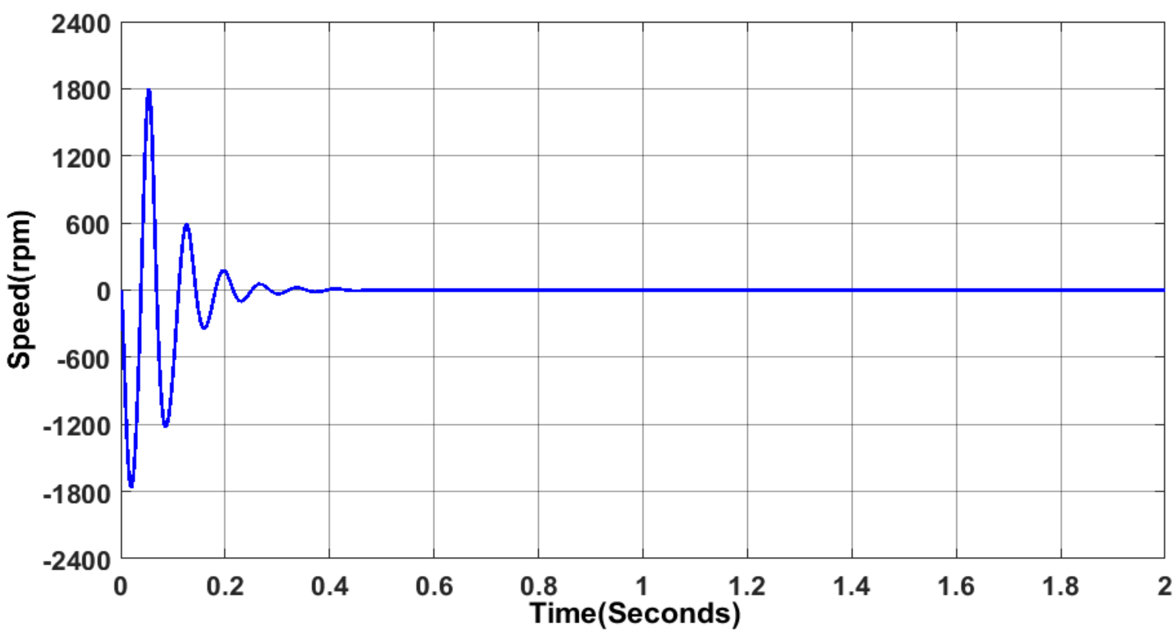

Figure 4.5 Error signal using MRAC-MIT

4.4 Simulation Results using MRAC Controller with Lyapunov Stability Theory

In this method also the aim is to minimizing the tracking error plant output and model reference. The model are simulated in Matlab Simulink which are shown in Figure 4.6. The Performance difference between MRAC-MIT and MRAC-Lyapunov is visible in this simulation. The adaption gain in this case are chosen in controller design and used in the simulation under consideration. The two adaption gain is lasted in terms of gamma γ and the values is 80 and -80. The input speed to the system is consider as 3000rpm.

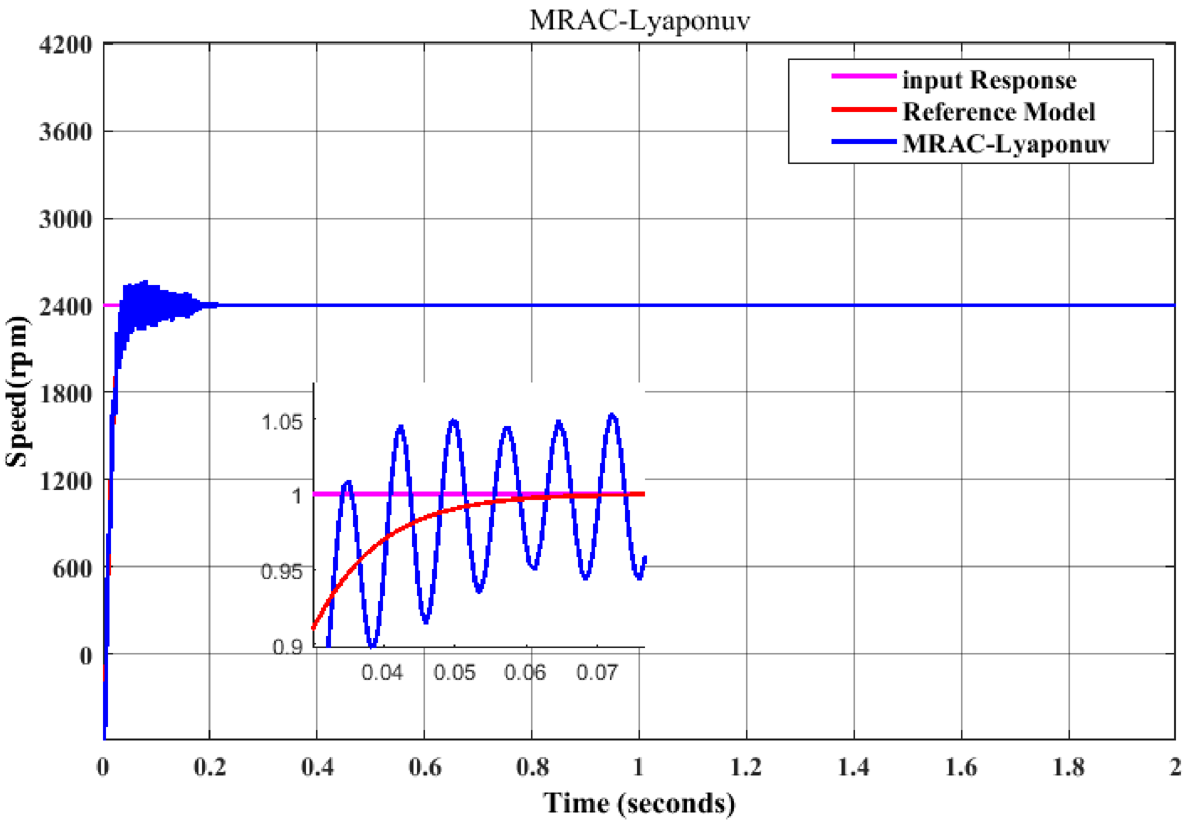

Figure 4.6 BLDC Motor Speed Response using MRAC-Lypounov Rule

The output response for plant is better follows the reference model when its compared with MRAC-MIT rule. From closed loop speed simulated result shows in Figure 4.6 the rising time is short and acceptable which is 0.0209 sec, settling time is 0.1663sec and the overshoot of the response is also good when we compare with MRAC-MIT, which is 5.6357%. So from MRAC with Lypounov rule the controller result from above is satisfactory and the settling time is not bad. The only drawbacks of the controller are the overshoot intransient point or time for problem must be solved in next controller two method of using MRAC controller with different technique.

The error between reference model and plant output is shown as Figure 4.7.after few time the error is going to zero. But it is not rapid

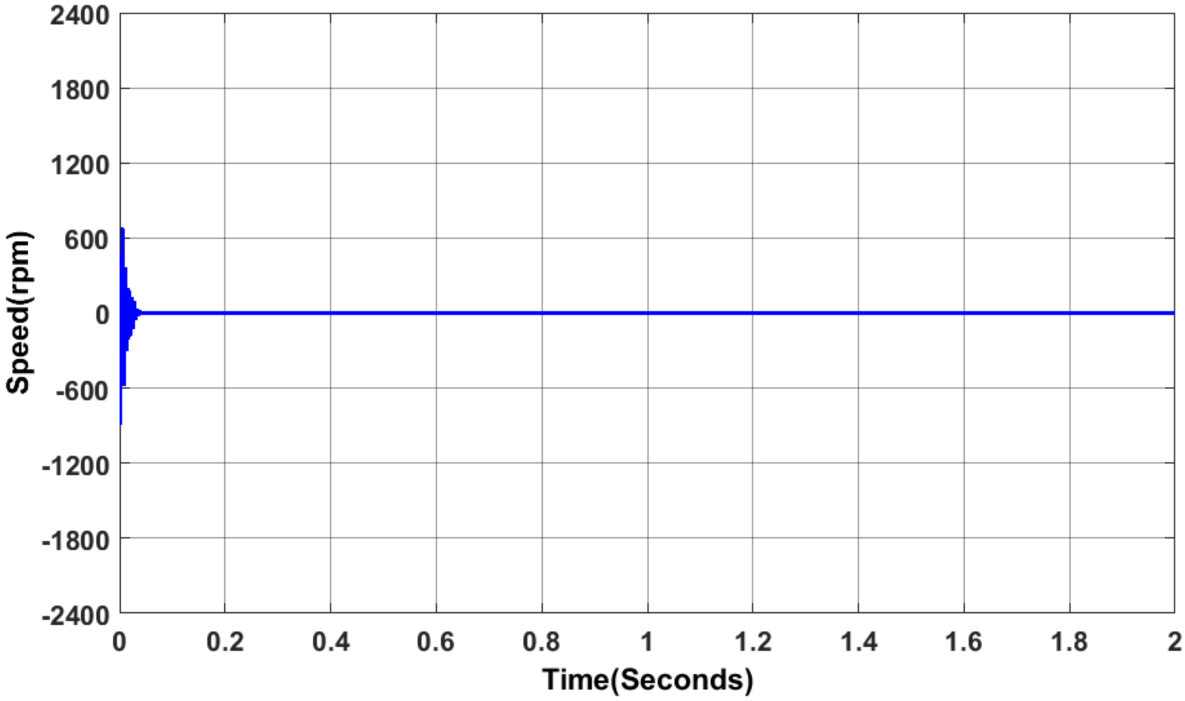

Figure 4.7 Error signal using MRAC-Lypounov rule

4.5 Simulation Results using MRAC-PID Controller

In this method also the aim is to minimizing the tracking error plant output and model reference. The model are simulated in Matlab Simulink which are shown in Figure 4.8. The Performance difference between MRAC-Lyapunov and MRAC-Lyapunov with PID is visible in this simulation. The adaption gain in this case are chosen in controller design and used in the simulation under consideration. The two adaption gain is lasted in terms of gamma γ and the values is 80 and -80. For compensator PID controller those gain is selected using Ziegler Nicholas. The value of Kp, Ki and Kd are 79,20 and 0.05 respectively. The input speed to the system is consider as 3000rpm. From closed loop speed simulated result shows in Figure 4.8 the rising time is short and acceptable which is 0.000109sec,settling time is 0.1959sec and the overshoot of the response is also good when we compare with MRAC-MIT, but in other way no big difference when we compare with MRAC- Lyaponuv which is 5.4354%.

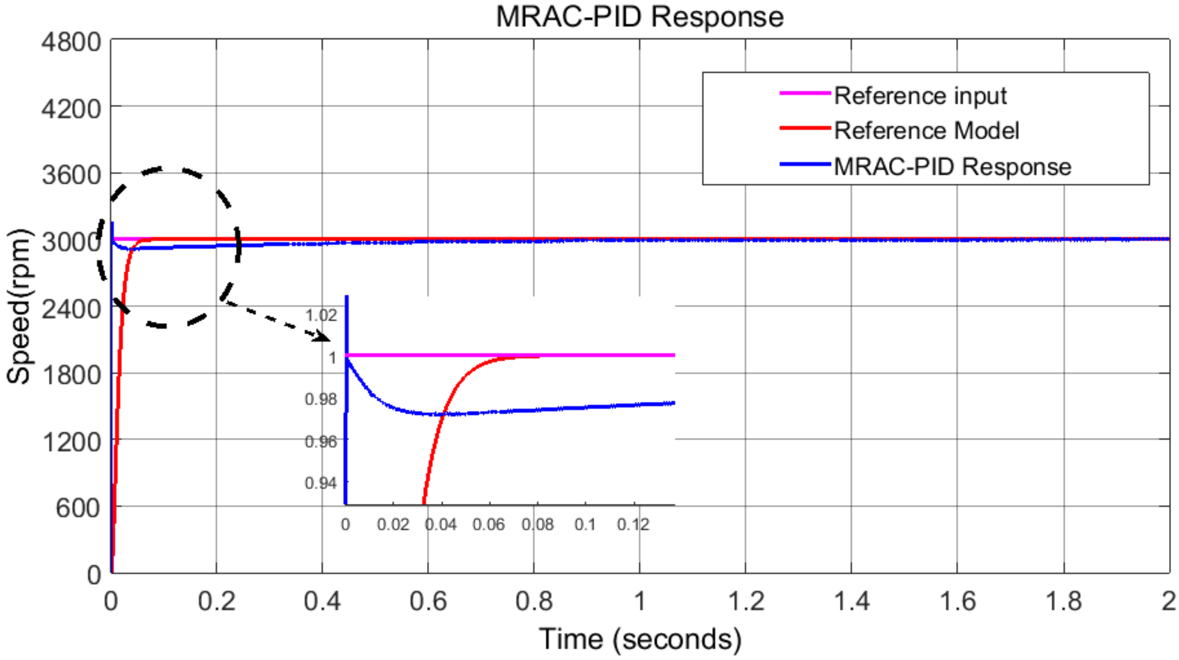

Figure 4.8 BLDC Motor Speed Response using MRAC-PID

The error between plant output and model reference is simulated as Figure 4.9

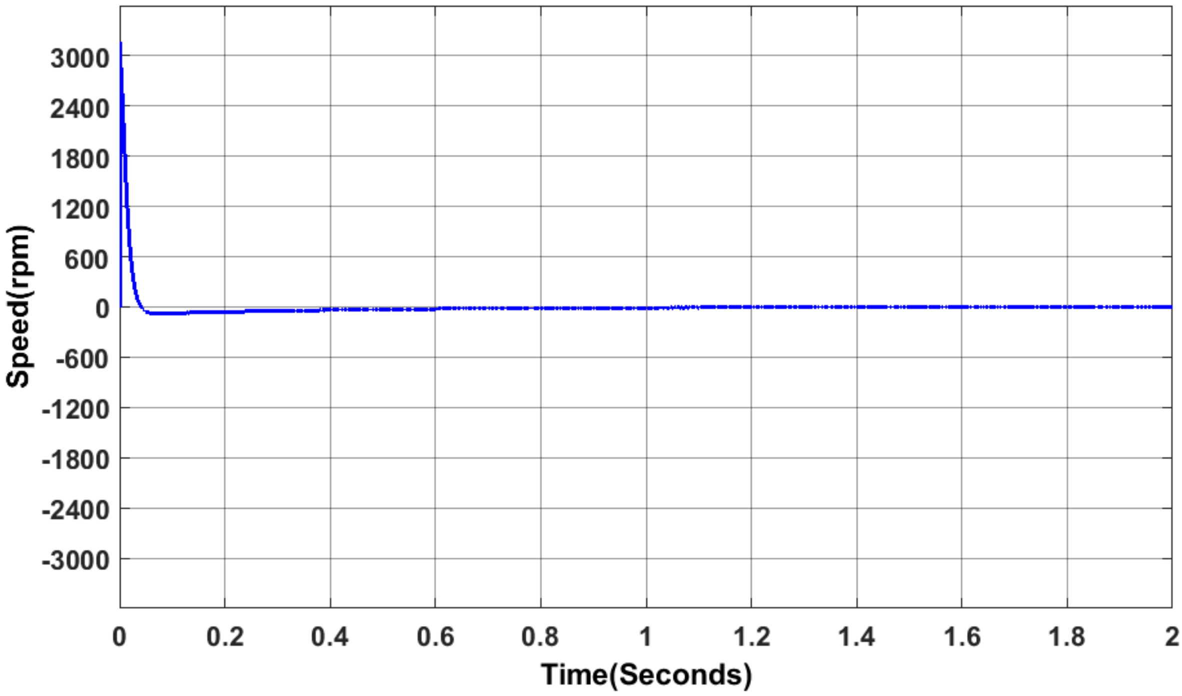

Figure 4.9 Error signal using MRAC-PID

4.6 Simulation Results using MRAC Controller based on NN

The goal of this method is to minimize the tracking error in plant output and model reference. Figure 4.10 depicts the simulation of the model in Matlab Simulink. In this simulation, the performance MRAC-NN is shown with best performance. In this case, the adaption gain is chosen during controller design and used in the simulation under consideration. The two adaption gain is lasted in terms of gamma γ and the values is 80 and -80. The input speed to the system is consider as 3000rpm. The NN architecture input is chosen from adaptation gain and the summation of adaptation gains, using the forward selection method to find the best network architecture. The Sigmoid function is used as an activation function to design and establish network behavior. A sigmoid transfer function can be used to introduce nonlinearity into a model and/or to ensure that certain signals stay within a certain range.

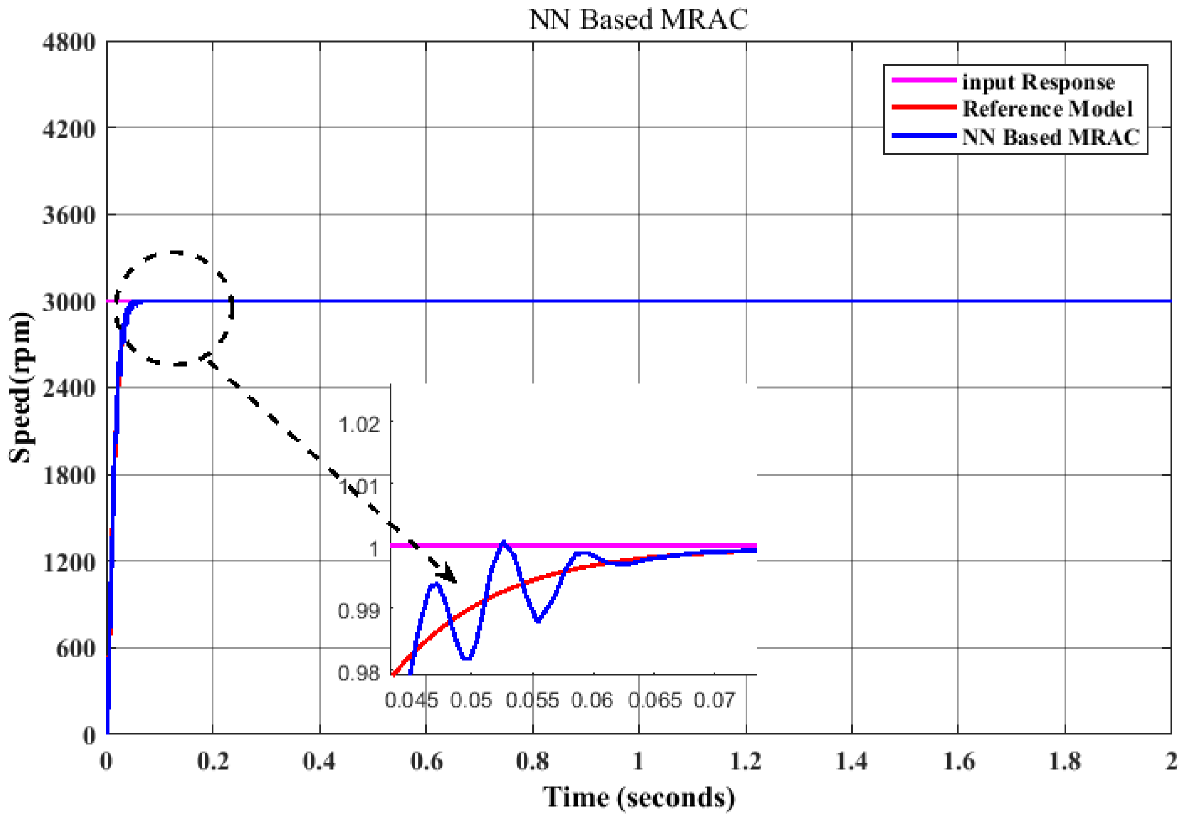

Figure 4.10 BLDC Motor Speed Response using MRAC-NN

The rising time is 0.0236 sec, the settling time is 0.0450sec, and the overshoot of the response is the best when compared to other, which is 0.0736 percent, according to the closed loop speed simulated result shown in Figure 4.10. So the controller result from MRAC-NN is satisfactory, and the settling time very shorten. Figure 4.11 depicts the error between the reference model and the plant output after a few times. However, it is so quick.

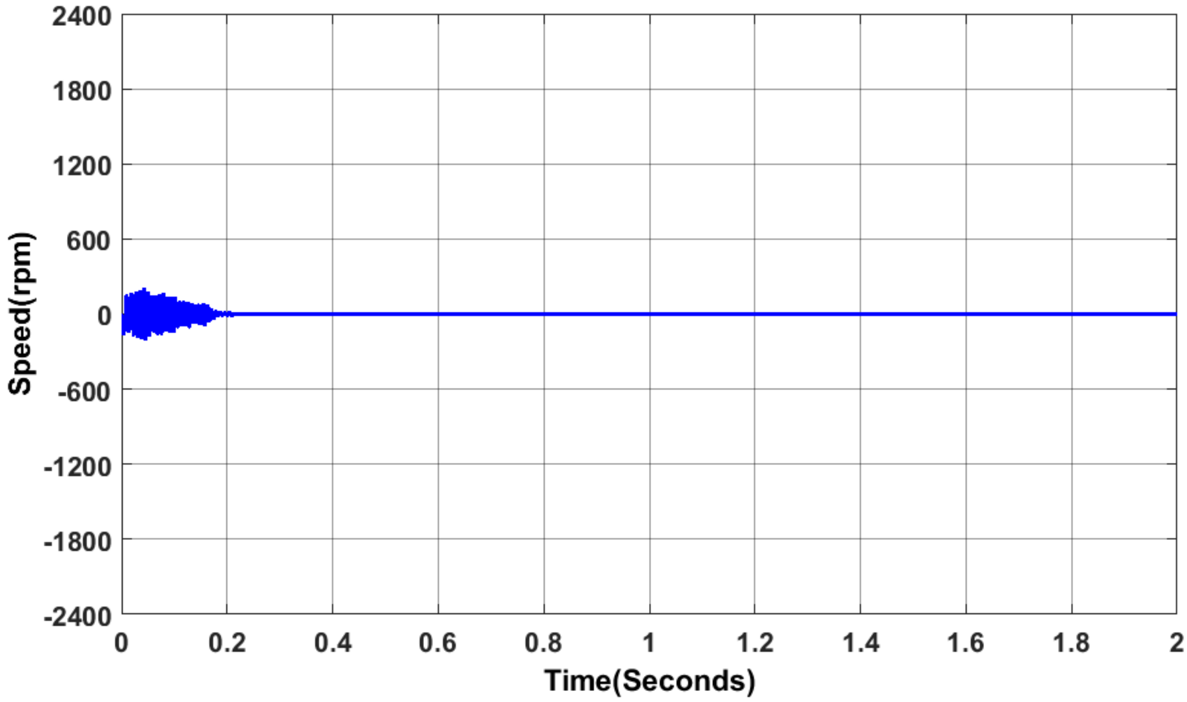

Figure 4.11 Error signal using MRAC-NN

4.7 Discussion of the results

From the result of this thesis simulation the best one is Neural Network based Model Reference Adaptive controller. Because of the performance of this controller is best when it compare with Conventional Model Reference Adaptive controller (MIT rule and Lyaponuv stability theory) and PID based Model Reference Adaptive Controller. The result comparison is simulated as Figure 4.12.

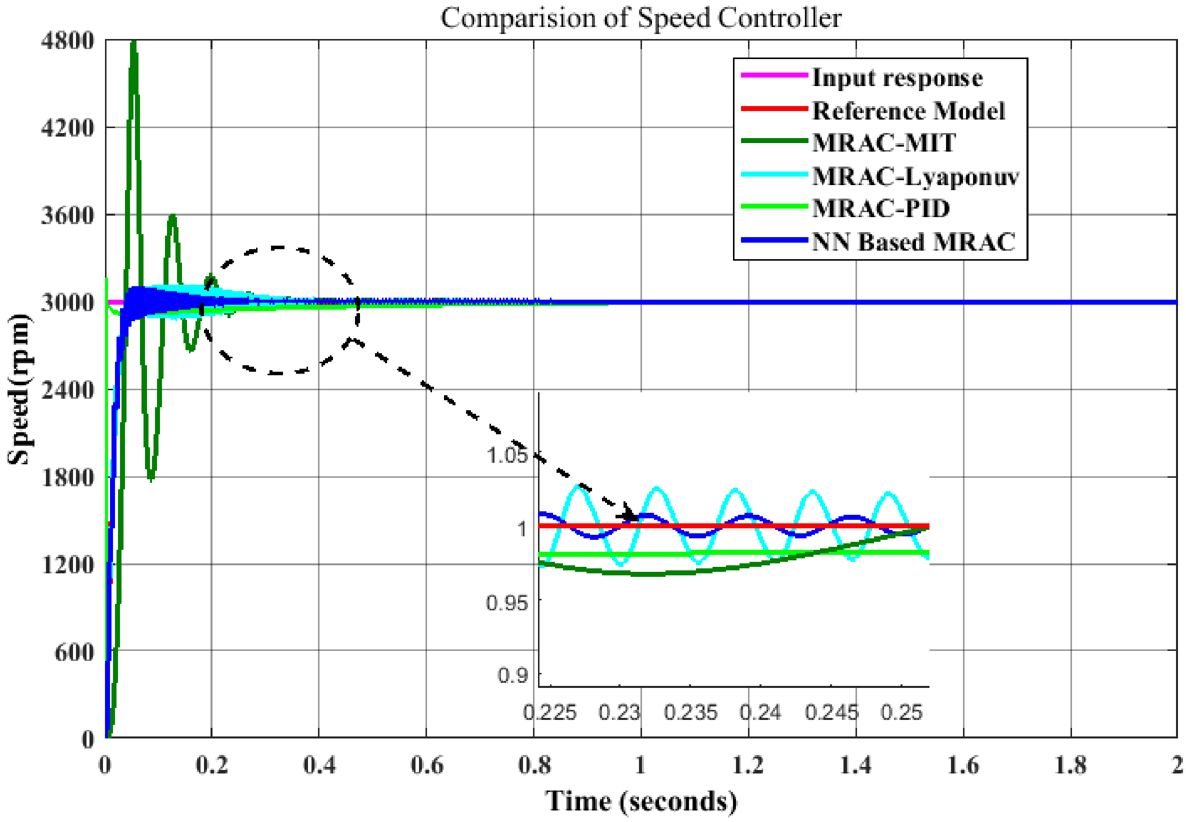

Figure 4.12 BLDC Motor Speed Response comparison

From simulation the performance of all controller is compared as Table 4.1

Table 4.1 Speed controller comparison of performance parameter results

Speed Controller	Performance Parameter Result				
	Rising Time(sec)	Settling Time(sec)	Peak time	overshoot	Steady State error
Model Reference	0.0257	0.0438	0.09171	0.0363	0
NN-MRAC	0.0236	0.0450	0.0575	0.0736	0
PID-MRAC	0.00010842	0.1388	0.539	5.7299	0
MRAC-Lyaponuv	0.0209	0.1663	0.793	5.6357	0
MRAC- MIT	0.0203	0.2415	0.0535	59.4499	0

The comparison result shown in figure 4.12 is listed in table 4.1 in terms of control performance. From control theory the system is said to have better speed dynamic performance if it has the lower rise time, lower percent overshoot, lower settling time as well as lower peak time. But in Model reference adaptive control case after selecting model reference if dynamic performance is the same with model reference performance

That system have to be better speed dynamic performed. From Table 4.1 the NN Based MRAC is better dynamic performance when it compare with PID Based MRAC and conventional MRAC. Because of the speed performance of NN based MRAC is small difference with the performance of Model Reference control. Not only this one but also if the error between the system and model reference is quickly going to zero that controller better. In Figure 4.13 in the case of NN based MRAC the difference between the system and model reference is quickly going to zero.

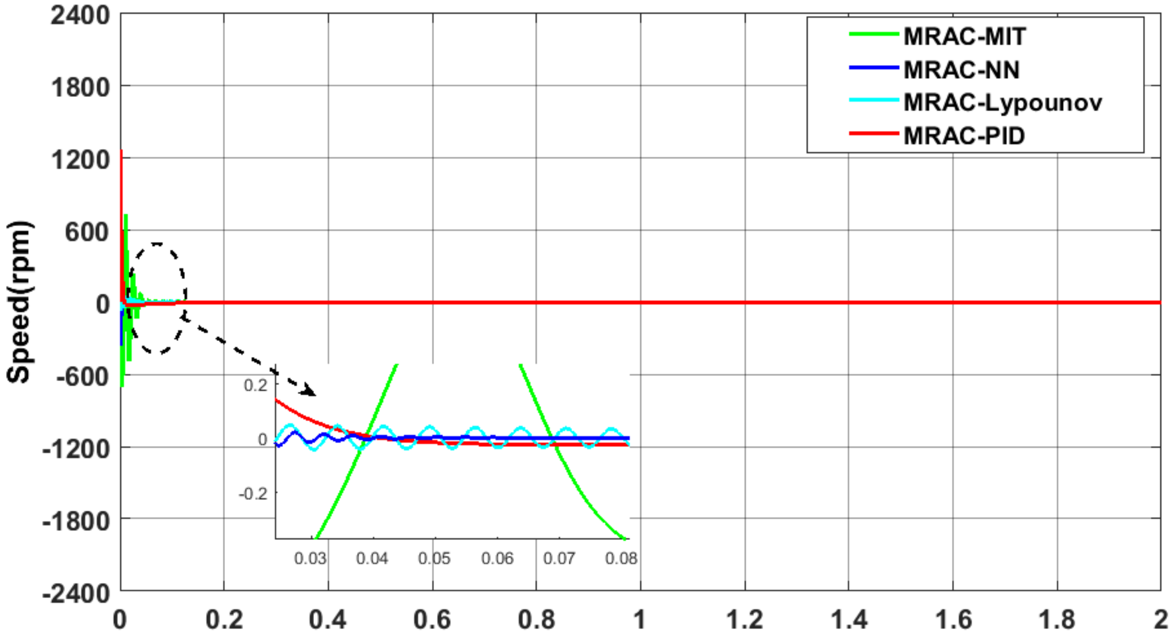

Figure 4.13 Error signal comparison

In this thesis adaption gain at each controller are the same. Now if the Adaptation gain (α) is varied in a range from 0.1 to 1000 then it changes the values of control parameters θ1 and θ2.Figure 4.14 show the variation of control parameters with time for different values of adaptation gain. The dynamic error is reducing with the increment in adaptation gain and at value α=20. It implies that by MRAC the plant output is following the desired output which was the main aim behind the control action

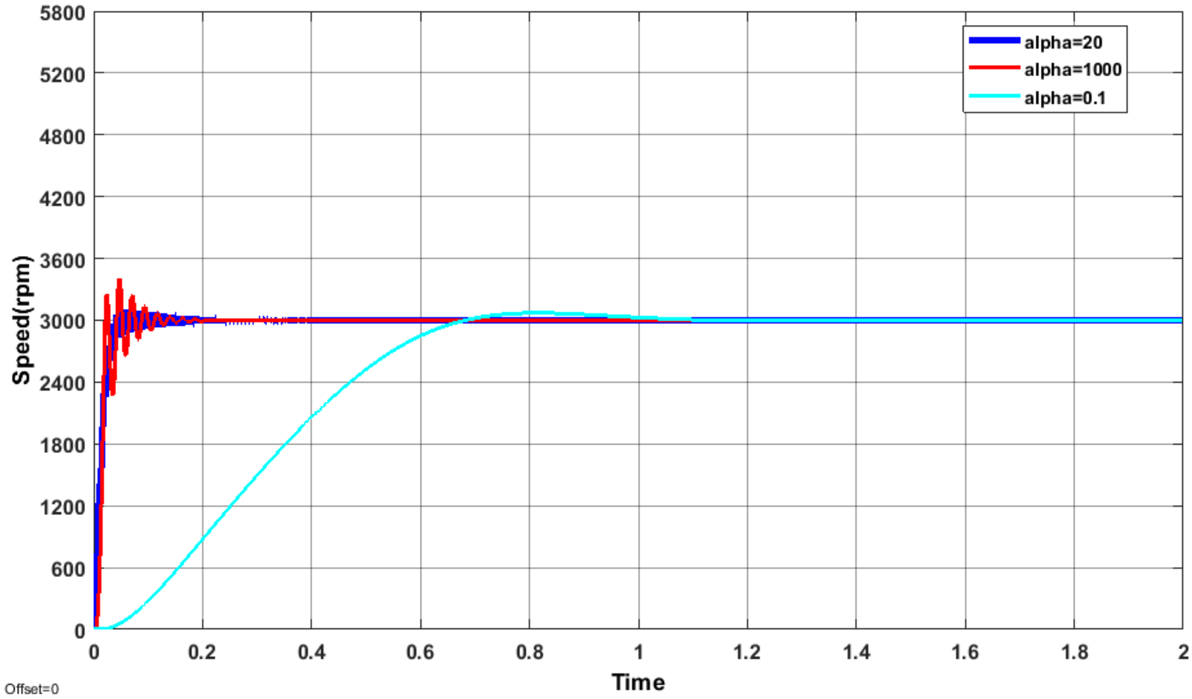

Figure 4.14 Effect of α on time response characteristic

CHAPTER FIVE

5. CONCLUSION AND RECOMMENDATION

5.1 Conclusion

This thesis investigated the modeling and design of neural network-based model reference adaptive control of nonlinear systems using MATLAB software to overcome the tracking performance of conventional model reference adaptive control to an equilibrium point for different disturbances. For updating the controller parameters online, an adaptive law based on the Gradient method and the Lyapunov stability criteria has been developed.

The simulation results show that neural network-based model reference adaptive control outperforms conventional model reference adaptive control (with MIT and Lyapunov stability criteria) and model reference adaptive with PID for regulating output. The result of the conventional model reference adaptive controller and MRAC-PID is not satisfactory to the highest degree of accuracy condition even it introduces a steady state error in the system. The neural network controller is proposed to update the controller parameters for BLDC Motor speed controller, which has advantages over traditional MRAC. The controller's transient and steady-state performances are improved by updating neural network parameters (weight and biases). Simulation studies using MATLAB/SIMULINK are used to evaluate the performance of the proposed NN-based MRAC, MRAC-PID, and Conventional MRAC. The simulation results show that the proposed neural network-based MRAC has 0.0036sec rise time, 0.0050sec settling time and overshoot 0.073 percent .Whereas, the conventional model reference adaptive control has not perform like this. Under different disturbances, the proposed system is applicable for Electric Vehicle speed controller manipulator to perform its task for maximum speed and time using neural network based model reference adaptive control than Conventional MRAC. Despite unknown parameter variation, unknown nonlinear system, and nonlinear uncertainty, the proposed NN-based MRAC is capable of maintaining vehicle speed for different disturbances and different input for BLDC Motor within tolerable limits.

5.2 Recommendation

The simulation results show that the neural network-based model reference adaptive controller for a BLDC motor speed controller good performs over the conventional model reference adaptive controller. As a result, it is recommended that the NN-based MRAC be implemented on the actual operation of a speed controller of electric vehicle to validate these simulation results. Furthermore, further research should focus on extending this scheme to a higher order nonlinear system like autopilot, quadcopters, and induction machine modeling for better performance control due to artificial intelligence with that of adaptive control.

REFERENCE

Agrawal, S. (n.d.). Speed Control of Electric Vehicle Using Fuzzy Logic Controller.

Akhtar, J. (2018). Propulsion system design of electric vehicle. December 2015. https://doi.org/10.1109/PESA.2015.7398900

Anshory, I., Robandi, I., & Ohki, M. (2019). SYSTEM IDENTIFICATION OF BLDC MOTOR AND OPTIMIZATION SPEED CONTROL USING. 10(07), 1–13.

ÇAKAR, Y., ORMAN, Y., & KİZİR, S. (2020). Design of a Model Reference Adaptive Pid Controller for Dc Motor Position Control: Compared With Pid and Fuzzy Controllers. Mugla Journal of Science and Technology, 25–35. https://doi.org/10.22531/muglajsci.668552

Derammelaere, S., Haemers, M., Viaene, J. De, Verbelen, F., & Stockman, K. (n.d.). A quantitative comparison between BLDC , PMSM , Brushed DC and Stepping Motor Technologies.

El-samahy, A. A., & Shamseldin, M. A. (2018). Brushless DC motor tracking control using self-tuning fuzzy PID control and model reference adaptive control. Ain Shams Engineering Journal, 9(3), 341–352. https://doi.org/10.1016/j.asej.2016.02.004

Gadekar, K. (2020). Performance Improvement in BLDC Motor Drive Using Self-Tuning PID Controller. 1162–1166.

Grunditz, E. A. (2014). BEV Powertrain Component Sizing With Respect to Performance , Energy Consumption and Driving Patterns.

Hashemnia, M. N., & Asaei, B. (2017). Comparative study of using different electric motors in the electric vehicles. October 2008. https://doi.org/10.1109/ICELMACH.2008.4800157

Jain, A. M. (2017). MODELLING AND SIMULATION OF THREE PHASE BLDC MOTOR FOR ELECTRIC BRAKING USING MATLAB / SIMULINK PRINCIPLE AND OPERATING. 7, 48–53.

Joy, A., Jose, A., Joseph, J., Fortel, J., P, R. V., & Alias, A. E. (2018). BLDC Motor Drive for Electric Vehicles. 1679–1683. https://doi.org/10.15662/IJAREEIE.2018.0704020

Lake, S., Mondal, S., Mitra, A., & Chattopadhyay, M. (1984). Mathematical modeling and Simulation of Brushless DC motor with Ideal Back EMF for a Precision speed control.

Luthra, G. (2017). Comparison of Characteristics of Various Motor Drives Currently Used in Electric Vehicle Propulsion System. International Journal of Mechanical And Production Engineering, 5, 2320–2092. http://iraj.in

Matthews, M. T., & Yi, S. (2019). Model Reference Adaptive Control and Neural Network Based Control of Altitude of Unmanned Aerial Vehicles. 1.

Minuye, S. A. (2021). Particle Swarm Optimization (PSO) Based PID Speed Control of BLDC Motor Drive with Regenerative Breaking for Electric Vehicle Application.

Minyamer Gelawe Wase. (2020). Artificial Intelligence Based Non-linear PID Speed and Current Control of Brushless DC Motor for Electric Vehicle Drive. (The Case of Bajaj Qute) (Vol. 4, Issue 1) [Adama Science and Technology University]. Motakabber, S. M.

A., Alam, A. H. M. Z., & Nordin, A. N. (2020). Control BLDC Motor Speed using PID Controller. March. https://doi.org/10.14569/IJACSA.2020.0110359

Mullick, J. A. (2017). Fuzzy Controller for Speed Control of BLDC motor using MATLAB Jahir Abbas Mullick Va = R * ia + L * Vb = R * ib + L * Vc = R * ic + L * + ea. 1270–1274.

Premkumar, K., & Manikandan, B. V. (2015). Speed control of Brushless DC motor using bat algorithm optimized Adaptive Neuro-Fuzzy Inference System. Applied Soft Computing Journal, 32, 403–419. https://doi.org/10.1016/j.asoc.2015.04.014

Priti, T. (2016). Brushless DC Motor Design for Electric Traction System. 02(04), 18–22.

Ranpariya, A., Shah, B., Salecha, R., Shah, V., & Sharma, P. (2019). Optimization of Required Power for an Electric Vehicle. 4605–4608.

Review, A. (2020). Technology Development of Electric Vehicles : A Review. 1–29.

Sanguesa, J. A., Torres-sanz, V., Garrido, P., Martinez, F. J., & Marquez-barja, J. M. (2021). smart cities A Review on Electric Vehicles : Technologies and Challenges. 372–404.

Series, I. O. P. C., & Science, M. (2019). Design of speed control for brushless DC motor used for electric vehicle based on adaptive neuro-fuzzy inference system Design of speed control for brushless DC motor used for electric vehicle based on adaptive neuro-fuzzy inference system. https://doi.org/10.1088/1757-899X/612/4/042066

Singh, A. K. (2014). Analysis of Induction Motor for Electric Vehicle Application Based on Drive Cycle Analysis.

Sun, X., Member, S., Wu, M., & Lei, G. (2020). An Improved Model Predictive Current Control for PMSM Drives Based on Current Track Circle. 0046(c). https://doi.org/10.1109/TIE.2020.2984433

Suryoatmojo, H., Pratomo, D. R., & Ridwan, M. (2020). ROBUST SPEED CONTROL OF BRUSHLESS DC MOTOR BASED ON ADAPTIVE NEURO FUZZY INFERENCE SYSTEM. 16(2), 415–428. https://doi.org/10.24507/ijicic.16.02.415

System, P. (2016). Parameter Matching and Optimization of a Series Hybrid Electric Vehicle PARAMETER MATCHING AND OPTIMIZATION OF A SERIES HYBRID ELECTRIC. November. https://doi.org/10.1115/IMECE2016-66312

Tashakori, A., Iaeng, M., Ektesabi, M., Iaeng, M., & Hosseinzadeh, N. (2011). Modeling of BLDC Motor with Ideal Back- EMF for Automotive Applications. II, 4–8.

Using, V., Logic, F., & Neural, A. (2021). Comparison of BLDC Motor Controller Design for Electric Vehicles Using Fuzzy Logic Controller and Artificial Neural Network. 6, 1–9. https://doi.org/10.15199/48.2021.06.01

Varghese, A. J., Roy, R., & Thirunavukkarasu, S. (2014). Optimized Speed Control for BLDC Motor. Article in International Journal of Innovative Research in Science Engineering and Technology, 3297(1), 1019–1030. https://www.researchgate.net/publication/348930291

Wase, M. G. (2020). Artificial Intelligence Based Non-linear PID Speed and Current Control of Brushless DC Motor for Electric Vehicle Drive. (The Case of Bajaj Qute).

Xue, X. D., Cheng, K. W. E., & Cheung, N. C. (2009). Selection of Electric Motor Drives for

Electric Vehicles. January.

You, A., Be, M. A. Y., & In, I. (2020). Combined fuzzy and PI control of regenerative braking system of electric vehicle driven by brushless DC motor Combined Fuzzy and PI Control of Regenerative Braking System of Electric Vehicle driven by Brushless DC Motor. 040005(April).

Zhou, M., Zhao, L., Zhang, Y., Gao, Z., & Pei, R. (2015). Pure Electric Vehicle Power-train Parameters Matching based on Vehicle Performance. International Journal of Control and Automation, 8(9), 53–62. https://doi.org/10.14257/ijca.2015.8.9.06

APPENDIXES

Appendix A: Appendixes related to analysis of data

MATLAB code for the analysis driving power vs speed of the Electric vehicle(Yaris)

```
clear all; close all;
m=1615;% Mass of the car
fric=0.01;%Friction coefficient
g=9.81;%gravitational acceleration
a=1;% Acceleration (m/sec)
r=0.25324; % Radius of the wheel in meter
K_friction=0.01; %Coefficient of friction by considering the asphalt road
F_tot=0; Tot_effcen.M=0.95; Cw=0.3; v=16.66; %speed of the rotor in m/se=100km/h
Adnsty=1.2; Af=2; vo=0; %Kd/m3 , %area in m2 , and %air velocity in m/s respectively
Vkph=0; Vkph1=0; d_Vkph=1e-2; %Initial conditions and unit step increment
Vkph_final=180; x=1; n=1; %final value in km/hr. and initial conditions
while(Vkph<Vkph_final),
Vmps=Vkph*(1000/3600);
Fadyna=0.5*Adnsty*Cw*Af*(Vmps+vo)^2;
if Vkph<=100*d_Vkph;
statfric=0.1;
else
statfric=0;
end
F_tot=m*g*(K_friction+statfric)+Fadyna+m*a; % Total force(Nm)
Power=F_tot*Vmps/0.95; % Required input power (Watt)
Vkph=Vkph+d_Vkph;
if x>16,
Powern(n)=Power/1000; %Power in KW
Vkphn(n)=Vkph; n=n+1; x=1;
end
x=x+1;
end
plot(Vkphn,Powern,'r','LineWidth',2);
set(gca,'FontSize',12)
axis([0 180 0 140]);
grid
xlabel('Speed of the of the car(Km/hr)')
ylabel('Power (KW)')
```

MATLAB code for analysis of the effect of the gradient angle in the power of the vehicle

```
clear all; close all;
m=1615;% Mass of the car
fric=0.01;%Friction coefficient
g=9.81;%gravitational acceleration
a=1;% Acceleration (m/sec)
r=0.25324; % Radius of the wheel in meter
c_ofriction=0.01; %Coefficient of friction by considering the asphalt road
```

```
d=0.25324; Cw=0.5; Tot_effcen.M=0.95; v=16.67; %speed of the rotor in m/se=60km/h
Adnsty=1.2; Af=2; vo=0; %Kd/m3, %area in m2, and %air velocity in m/s respectively
angleR=0; angleR1=0; d_angleR=1e-6; %Initial condition and %unit step increment
angleR_final=26; x=1; n=1; %final value in degree and initial conditions
while(angleR<angleR_final),
Fadyna=0.5*Adnsty*Cw*Af*(v+vo)^2;
theta=angleR*2*pi/360; %Degree to radian conversion
F_tot=m*g*(sin(theta)+c_ofriction*cos(theta))+Fadyna+m*a; % Total force(Nm)
Power=F_tot*v; angleR=angleR+d_angleR; %W
if x>16,
Powern(n)=Power/1000+1.5; thetan(n)=angleR; n=n+1; x=1;%Power in KW
end
x=x+1;
end
plot(thetan,Powern,'b','LineWidth',2);
axis([0 26 0 140]);
grid
xlabel('The approaching angle in degree')
ylabel('Power (kW)')
```

MATLAB code for torque versus speed characteristics curve

```
V1=180; %Km/hr
Wrated=16; %KWhr
Pm=12; %KW
S=0; d_S=1e-4; S_final=190; %unit step increment and % Km final value
x=1; n=1;
while(S<=S_final),
W=Pm*S/V1;
SOC=(Wrated-W)*190/Wrated;
S=S+d_S;
if x>16,
SOCn(n)=SOC; Sn(n)=S; n=n+1; x=1;
end
x=x+1;
end
figure(1);
plot(Sn,SOCn,'r','LineWidth',2);
axis([0 100 0 190]); set(gca,'xticklabel')
xlabel('Distance in Km')
ylabel('SOC (%)')
title('State of charge vs distance in KM')
grid
```

Appendix B: Appendixes related to system modeling

The proposed NN based NPID speed controller MATLAB code

```
I=[r,Theta1,Theta2]';
T=[U]';
net=newff(minmax(I),[1,6,1],{'tansig','tansig','purelin'},'trainlm');
```

```
net=init(net);
net.trainParam.show=1;
net.trainParam.lr=0.06;
net.trainParam.mc=0.075;
net.trainParam.epochs=100000;
net.trainParam.goal=1e-12;
net=train(net,I,T);
```

Appendix C: BLDC motor MATLAB/Simulink model

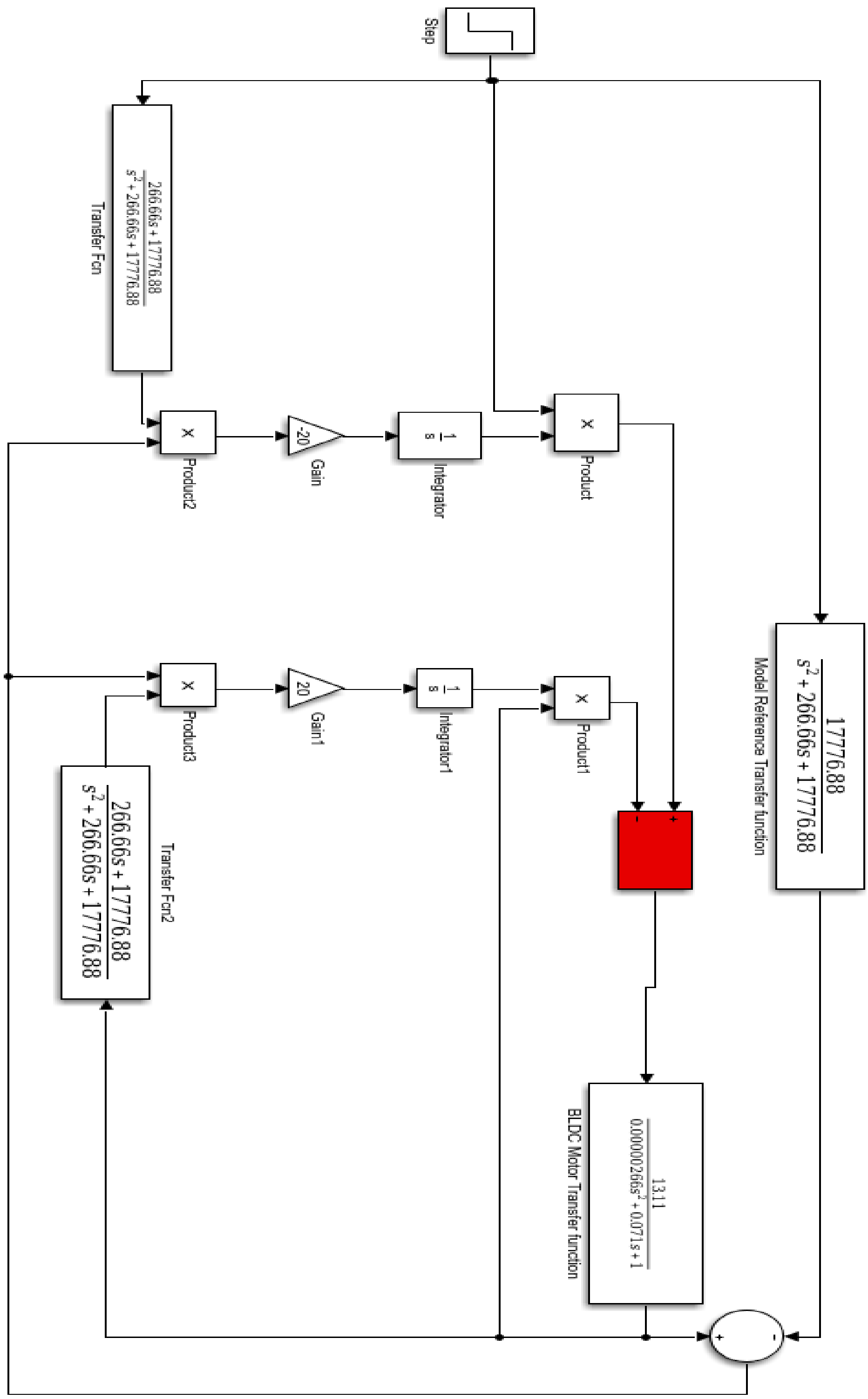

MRAC-MIT speed controller Simulink block for BLDC motor

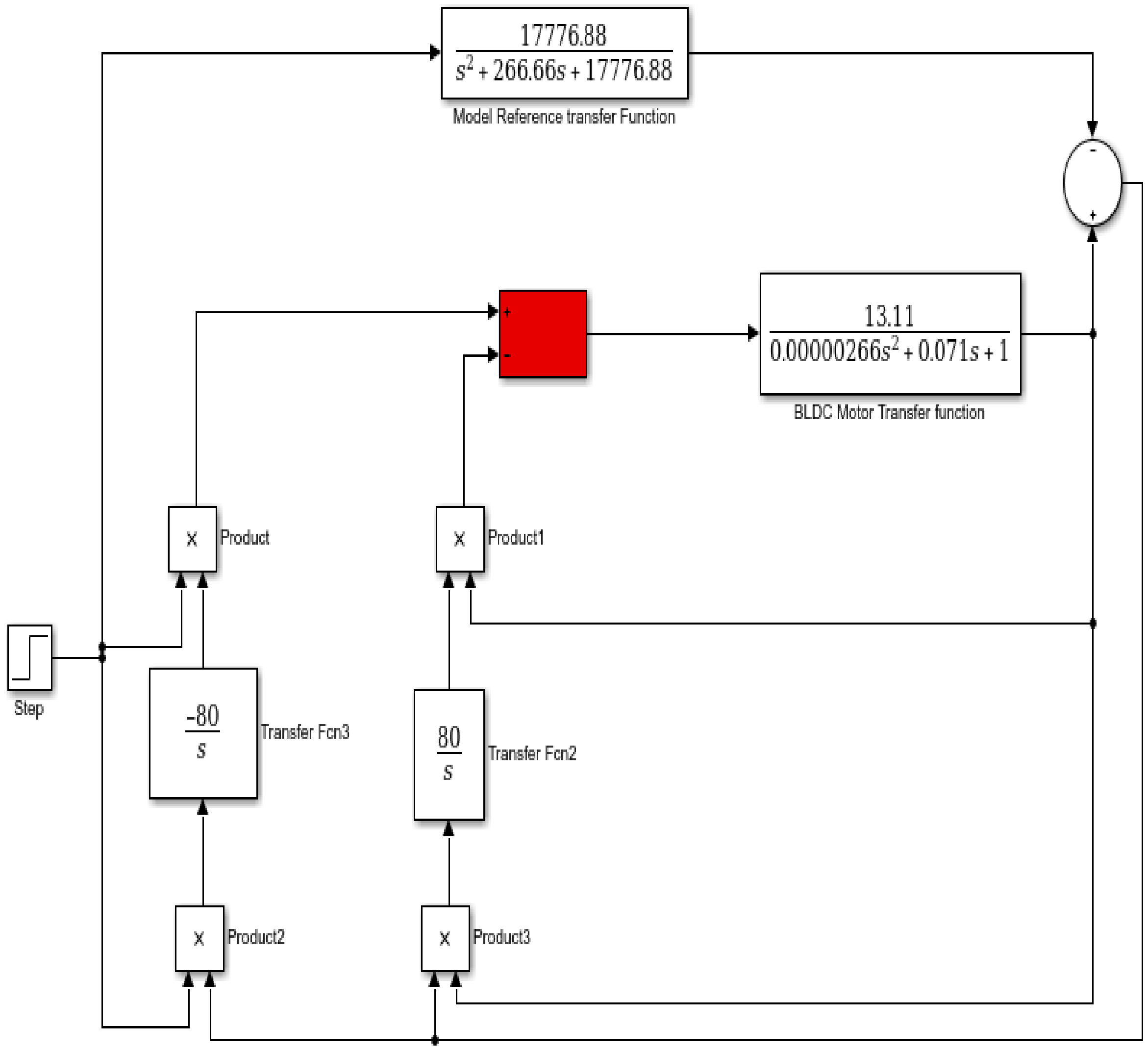

MRAC-Lyaponuv speed controller Simulink block for BLDC motor

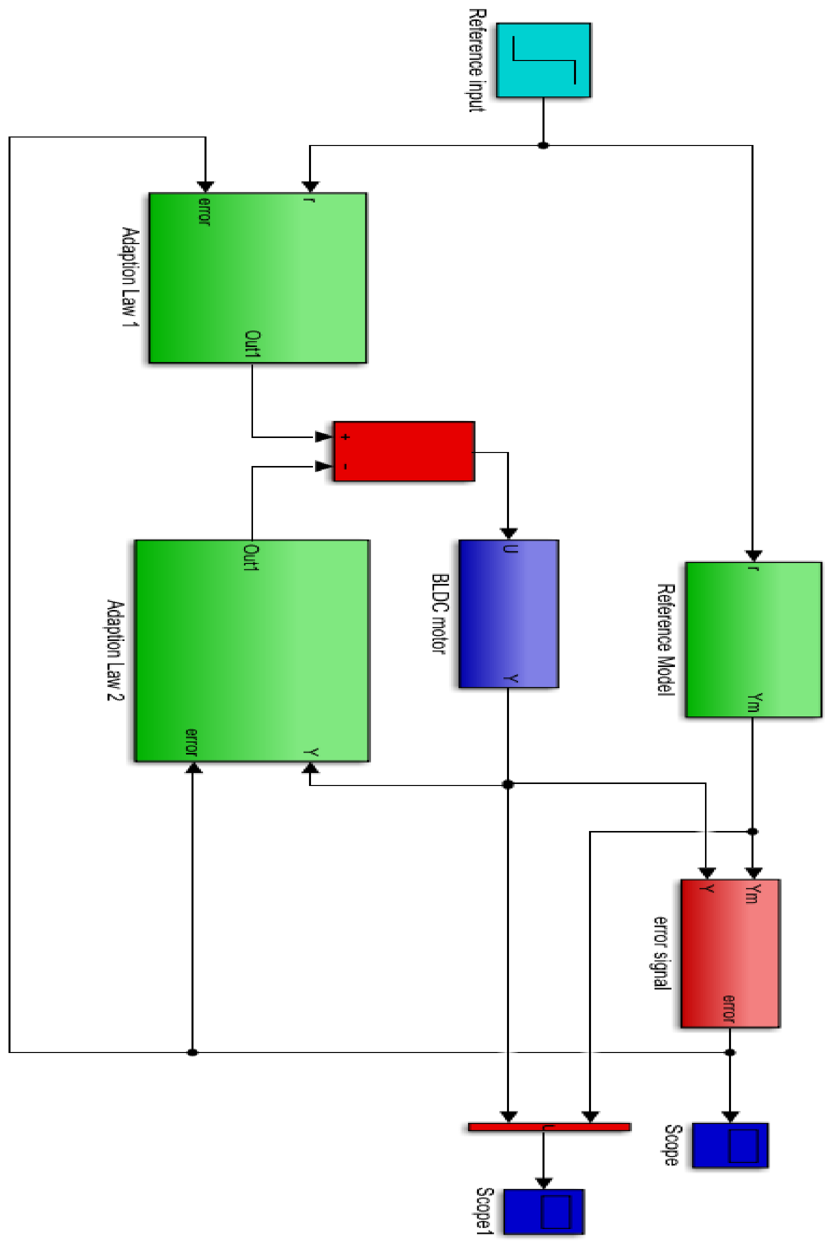

Conventional MRAC speed controller Simulink block for BLDC motor

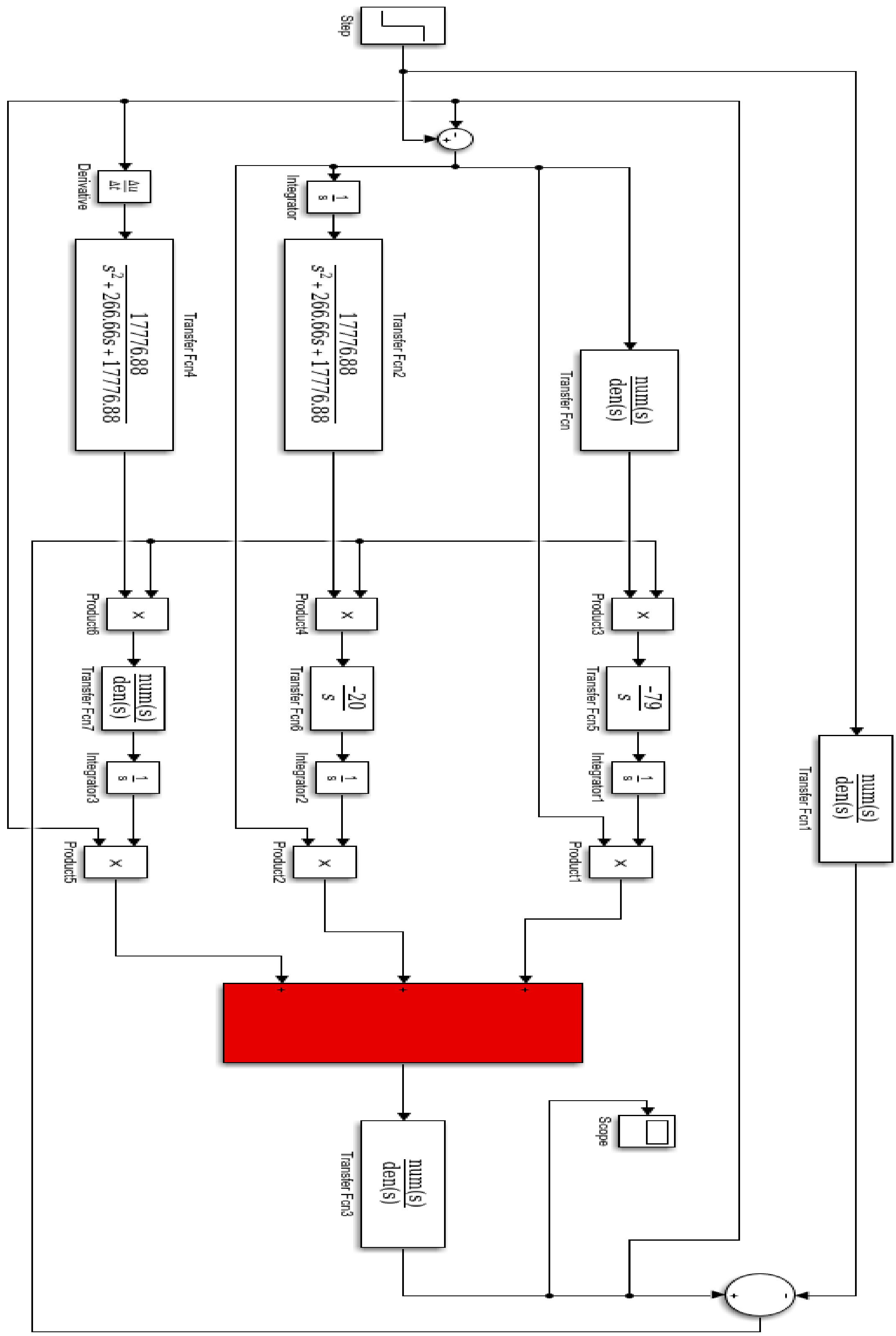

MRAC-PID speed controller Simulink block for BLDC motor

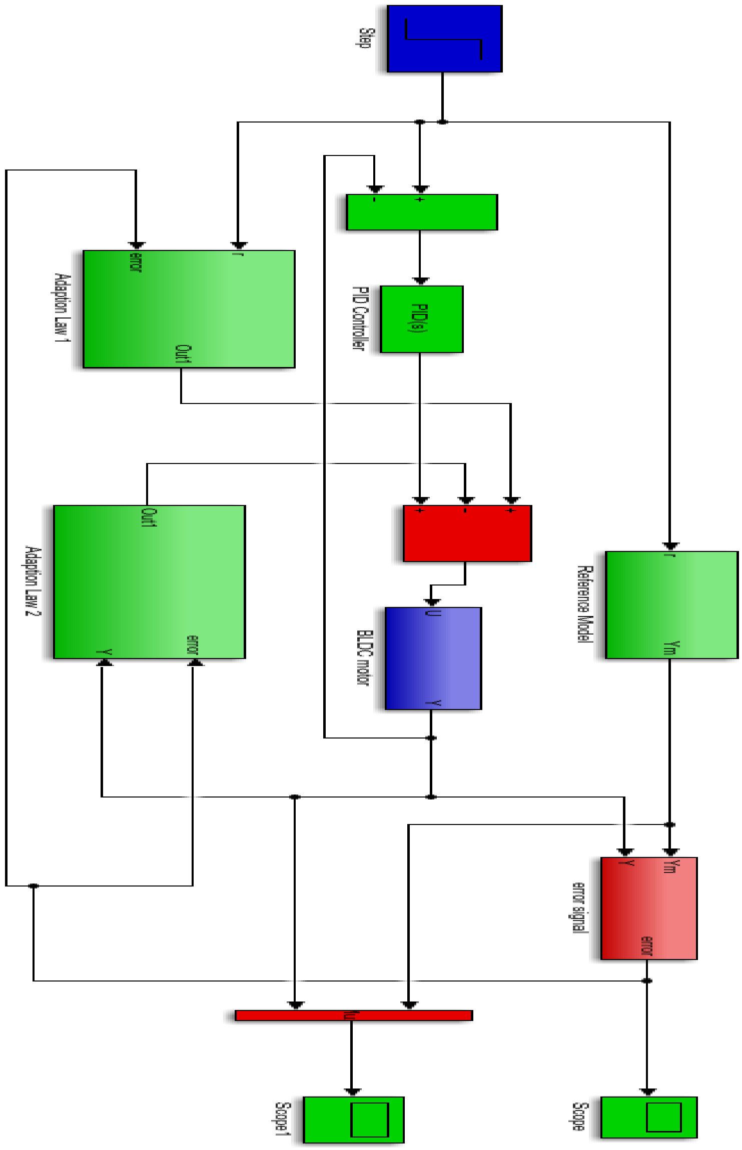

MRAC-PID speed controller Simulink block for both BLDC motor

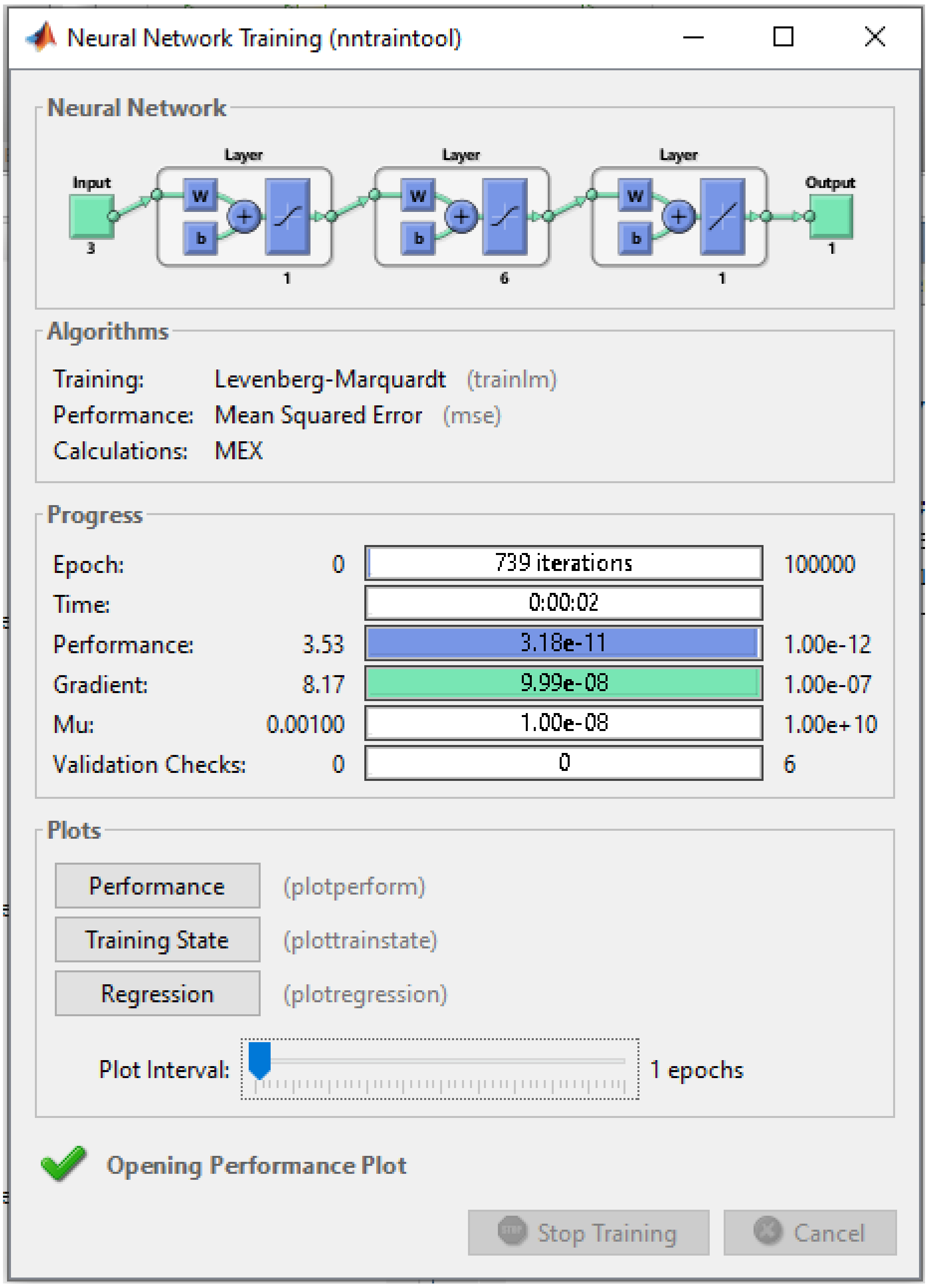

Neural Network training tool

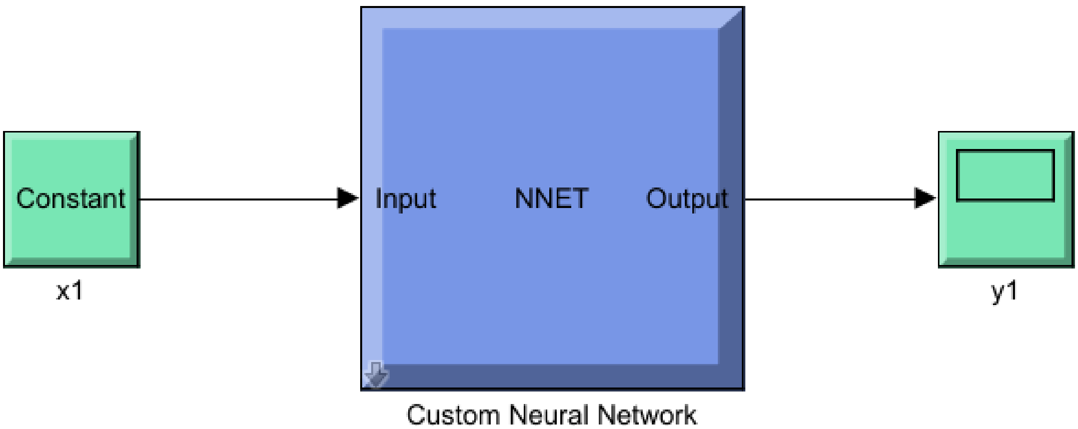

The Simulink block of the trained neural network structure

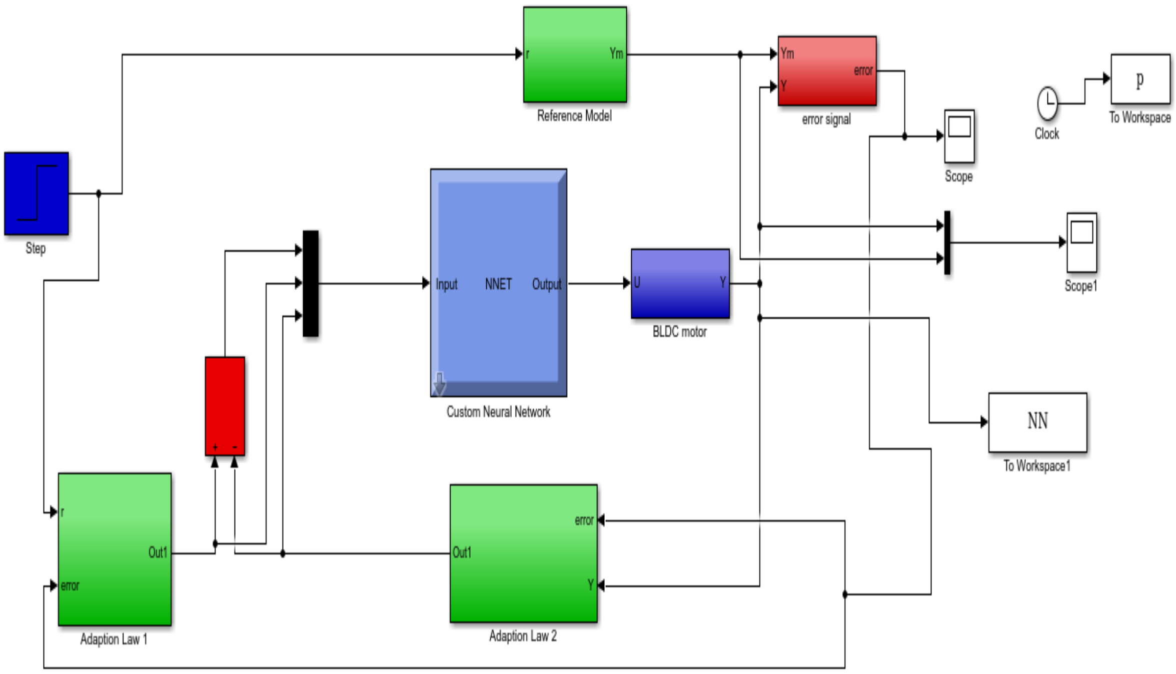

MRAC-NN speed controller Simulink block for both BLDC motor